ISSN 1849-0751 (On-line)
ISSN 0013-7448 (Print)
UDK 621.31

Journal of Energy

VOLUME 67 Number 2 | 2018 Special Issue

Journal of Energy

Scientific Professional Journal Of Energy, Electricity, Power Systems

Online ISSN 1849–0751, Print ISSN 0013–7448, VOL 66

Published by

HEP d.d., Ulica grada Vukovara 37, HR–10000 Zagreb

HRO CIGRÉ, Berislavićeva 6, HR–10000 Zagreb

Publishing Board

Robert Krklec, (president) HEP, Croatia,

Božidar Filipović–Grčić, (vicepresident), HRO CIGRÉ, Croatia

Editor–in–Chief

Goran Slipac, HEP, Croatia

Associate Editors

Helena Božić HEP, Croatia
Stjepan Car Green Energy Cooperation, Croatia
Tomislav Gelo University of Zagreb, Croatia
Davor Grgić University of Zagreb, Croatia
Mićo Klepo Croatian Energy Regulatory Agency, Croatia
Stevo Kolundžić Croatia
Vitomir Komen HEP, Croatia
Marija Šiško Kuliš HEP, Croatia
Dražen Lončar University of Zagreb, Croatia
Goran Majstrović Energy Institute Hrvoje Požar, Croatia
Tomislav Plavšić Croatian Transmission system Operator, Croatia
Dubravko Sabolić Croatian Transmission system Operator, Croatia
Mladen Zeljko Energy Institute Hrvoje Požar, Croatia

International Editorial Council

Anastasios Bakirtzis University of Thessaloniki, Greece
Eraldo Banovac J. J. Strossmayer University of Osijek, Croatia
Frano Barbir University of Split, Croatia
Tomislav Barić J. J. Strossmayer University of Osijek, Croatia
Frank Bezzina University of Malta
Srećko Bojić Power System Institute, Zagreb, Croatia
Tomislav Capuder University of Zagreb, Croatia
Ante Elez Končar-Generators and Motors, Croatia
Dubravko Franković University of Rijeka, Croatia
Hrvoje Glavaš J. J. Strossmayer University of Osijek, Croatia
Mevludin Glavić University of Liege, Belgium
Božidar Filipović Grčić University of Zagreb, Croatia
Dalibor Filipović Grčić Končar-Electrical Engineering Institute, Croatia
Josep M. Guerrero Aalborg Universitet, Aalborg East, Denmark
Juraj Havelka University of Zagreb, Croatia
Dirk Van Hertem KU Leuven, Faculty of Engineering, Belgium
Žarko Janić Siemens-Končar-Power Transformers, Croatia
Igor Kuzle University of Zagreb, Croatia
Niko Malbaša Ekonerg, Croatia
Matislav Majstrović University of Split, Croatia
Zlatko Maljković University of Zagreb, Croatia
Predrag Marić J. J. Strossmayer University of Osijek, Croatia
Viktor Milardić University of Zagreb, Croatia
Srete Nikolovski J. J. Strossmayer University of Osijek, Croatia
Damir Novosel Quanta Technology, Raleigh, USA
Hrvoje Pandžić University of Zagreb, Croatia
Milutin Pavlica Power System Institute, Zagreb, Croatia
Robert Sitar Končar-Electrical Engineering Institute, Croatia
Damir Sumina University of Zagreb, Croatia
Elis Sutlović University of Split, Croatia
Zdenko Šimić Joint Research Centre, Pette, The Netherlands
Damir Šljivac J. J. Strossmayer University of Osijek Croatia
Darko Tipurić University of Zagreb, Croatia
Bojan Trkulja University of Zagreb, Croatia
Nela Vlahinić Lenz University of Split, Croatia
Mario Vražić University of Zagreb, Croatia

EDITORIAL

Journal of Energy special issue: Papers from second regional CIGRE conference SEERC 2018 "Energy transition and innovations in electricity sector"

Welcome to this special issue, which is based on selected papers presented at second regional CIGRE conference SEERC 2018 "Energy transition and innovations in electricity sector", held in Kyiv, Ukraine, on June 12th–13th, 2018. The conference was organized by the Ukrainian National Committee of CIGRE.

SEERC (South Eastern European Region of CIGRE) is a regional association of the International Council on Large Electric Systems CIGRE, created for effort consolidation to develop the power industry of the South European countries. Among SEERC member-countries are: Austria, Bosnia and Herzegovina, Greece, Italy, Kosovo, Macedonia, Romania, Serbia, Slovakia, Slovenia, Turkey, Hungary, Ukraine, Croatia, Czech Republic, Montenegro.

The SEERC conference became a communication platform for a productive dialogue between representatives of power generating and power distributing companies, power equipment manufacturers, suppliers of services, developers of innovations and energy systems, international power engineers' community and for everyone, interested in the issues of forming and development of the market of electric energy.

The topics of the conference were related to receiving practical results in modernization and development of power industry in SEERC region. The conference discussed regional aspects of power energy market development, issues related to achieving a better stability of the power systems of the countries of south-east Europe, innovations in the power industry infrastructure of the countries of the region and other key issues.

In this special issue, 9 papers were accepted for publication in Journal of Energy after additional peer-review process. Authors of these papers are mostly members of the Croatian National Committee of CIGRE, so this special edition gives in some way a current review of the electro-energy projects and issues in the Croatian power system and in the SEERC region. We would like to thank the authors for their contributions and the reviewers who dedicated their valuable time in selecting and reviewing these papers. We hope this special issue will provide a brief insight into current issues of the SEERC region, as well as a pleasant and inspiring reading.

Guest Editors

Božidar Filipović-Grčić, PhD
Prof. Ivica Pavić
University of Zagreb, Croatia
Faculty of Electrical Engineering and Computing

Journal of Energy
VOLUME 67 Number 2 | 2018 Special Issue
journal homepage: http://journalofenergy.com/

Hydro Pumped Storage Power Plants perspectives in SEERC Region

T. Plavšić*, V. Valentić*, D. Franković**
***Hrvatski operator prijenosnog sustava d.o.o.**
****Tehnical University Rijeka**
Croatia

ABSTRACT

The paper is focusing to the hydro pumped storage power plants perspectives in SEERC region, investigating their present market position, that has clearly been jeopardized by low electricity market prices and small peak – off peak electricity market price differences. Lack of positive market signals could stop the development of new hydro pumped storage power plants projects in the region, and prevent the existing ones in achieving expected financial goals. Paper is analysing future power system operational needs in high renewable sources penetration environment, proposing a new perspectives for existing and new hydro pumped storage power plants in SEERC region.

KEYWORDS

hydro pumped storage, power system operation, renewable sources, flexibility, electricity market, energy policies, energy investments

1. INTRODUCTION

Present circumstances and situation in European countries regarding energy policies, energy investments and electricity market development are characterized by following. Recent trends in EU energy policies towards the reduction of greenhouse gas emissions and increase of the renewable energy sources (RES) share in overall energy mix are continuing to grow, with much higher requirements until 2030 comparing to 2020, and significantly higher requirements until 2050. EU energy policies have high demands towards energy sector but without a clear pathway how to achieve the set goals. Direct consequences of 2020 energy directives are already visible in the field of energy investments and electricity market.
From the EU data regarding the electricity generation installed capacity change during last fifteen years, it is crystal clear that dominant new technologies in EU energy sector today are wind and PV power plants. Gas power plants still have a high portion in overall installed capacity, but those days are already behind, because it is a known fact that some brand new gas power plants in Germany have been built and never put into the operation because of the lack of the competitiveness. Hydro power plants have a very small portion in overall EU

T. Plavšić, V. Valentić, D. Franković, Hydro Pumped Storage Power Plants perspectives in SEERC Region, Journal of Energy, vol. 67 Number 2 (2018), Special Issue, p. 3–12

electricity generation installed capacity change, while technologies like coal, fuel oil and even nuclear have a negative trend, are going out of operation.
The main answer for the above described EU energy investment trends lies in the electricity market prices. Observing the electricity market prices trends in last three to four years, there is a rather stable trend of constant drop in the prices due mostly to the large penetration of RES in western European countries. Further, negative electricity market prices are occuring more and more often, coinciding with periods of extremely high RES production.
The power system operation is becoming more unpredictable than ever before in its history, demanding for more flexibility sources, that could cope with the highly intermittent RES operation unpredictability. At the same time, because of the low market prices and lack of investments in classical energy technologies such as hydro and hydro pumped storage power plants (HPSPP), due to large scale RES penetration, power system operation is facing the flexibility shortage, demanding thus for new technology opportunities such as demand side response, battery storage systems or multi-energy systems. Still, those new technologies are far from being mature, and government policies should establish an adequate framework for enabling the investments in classical power production facilities for providing flexibility.
In the second section an overview of present hydro pumped storage power plants market position, considering actual circumstances and situation over European electricity markets, with special focus to SEERC region. Third section is analysing future power system operation needs in high RES penetration environment, while in fourth section possible perspectives for existing and new hydro pumped storage power plants in SEERC region are proposed.

2. OVERVIEW OF PRESENT HYDRO PUMPED STORAGE POWER PLANTS MARKET POSITION

A typical HPSPP station is presented in Figure 1. When in generating mode, the reversible pump-turbine feeds produced power to the electric power system. Conversely, the power from an external source (e.g. grid, other plant) powers the pumps, when in pumping/storage mode. Dividing HPSPP energy output (from generation) by the energy input (for pumping regime) provides the round-trip efficiency (RTE) of the HPSPP facility. Round trip efficiency takes values lower than 1 due to overall losses. In fact, efficiency factors are applied twice, both in pumping and generating mode, and the round-trip efficiency is calculated using equation (1):

$$RTE = \frac{E_{out}}{E_{in}} \ [-] \tag{1}$$

RTE includes both hydraulic and equipment-related losses (pump, turbine, generator, motor and transformer). Typical HPSPP systems' RTE range between 65 and 80%, depending on the technical characteristics of the equipment. Older stations reflect lower RTE, while modern systems achieve RTE up to 87% [1].

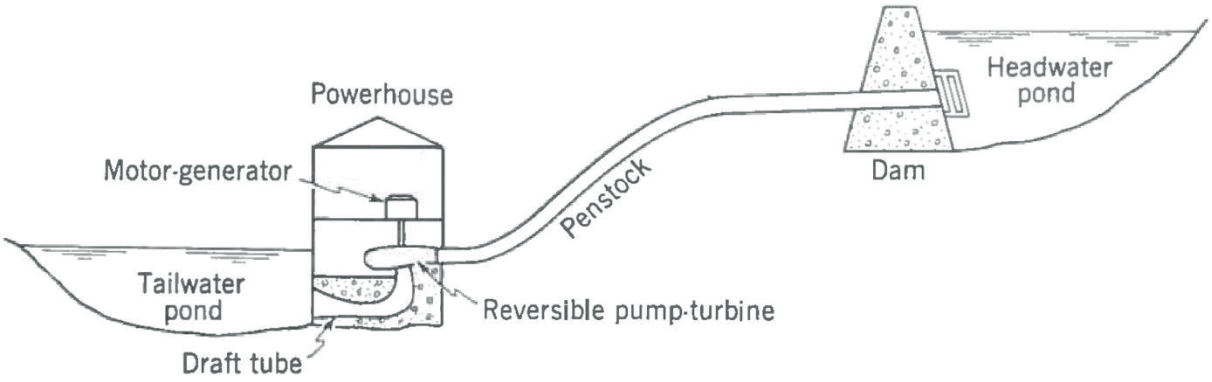

Figure 1. Pumped-hydro storage station

HPSPP systems, except for having advantageous characteristics of conventional hydropower, are readily available for peak power production with very short ramp-up time. Furthermore, in case of local or widespread black-outs HPSPP units can provide "black start" services.

HPSPP plants can generally be located far from streams and purely provide energy storage. This type of HPSPP plants are also known as pure HPSPP or "closed-loop HPSPP". In contrast, pump-back HPSPP (also known as "mixed" HPSPP) utilizes both stored water and natural inflows to produce electricity. Apart from pure and mixed HPSPP systems, ternary HPSPP systems are a prominent technology that offers the best answer for a very fast grid response, being carried out with the torque converter which allows fast change-over between turbine and pump mode. Full regulating capability exists in both modes of operation from 0% to 100% of the unit output. As two separate hydraulic machines, the rotational direction of the motor-generator can be the same in both operational modes. This results in considerable commercial value for the power plant's operation.

The levelized cost of electricity (LCOE) is widely used to define a characteristic cost of electricity generation. Construction costs of hydro pumped storage power plants can be shown by equation (1):

$$\mathrm{LCOE} = \frac{\mathrm{TCR}\cdot\mathrm{FCF}+\mathrm{FOM}}{\mathrm{CF}\cdot 8766\cdot \mathrm{P}} + \mathrm{VOM} \qquad (2)$$

where: LCOE levelized cost of electricity (€/MWh), TCR total captial requirement (€), FOM fixed operational and maintenance cost (€/MWh), CF capacity factor (fraction), P net power output (MW), VOM variable operational and maintenance costs (€/MWh), and 8766 (fraction) number of hours per year including leap years.
The total investment cost includes engineering, procurement and construction (EPC) costs. It also includes owner's costs regarding the development of the project, but excludes grid connection costs. The cost of capital depends on the interest rate or on the expected rate of return on investment (ROI), the time needed for building the power plant, investment payback period and repayment of the loan. The fixed operational and maintenance cost (FOM) includes spare parts and planned maintenance, overhauls, personnel and general and administrative costs. The weighted average cost of capital (WACC) is based on a 30 : 70 ratio of equity and bank loan respectively. The cost of equity is set at 10% and the price of the loan is based on a 20 year Euro loan with a variable interest rate based on 6-month EUR Euribor plus 120 basis points of risk premium. Since the value of Euribor changes daily, our cost of capital varies over time, but on average, our WACC is 4.47%. The capacity factor is multiplied by the total number of hours in a year, (i.e. 8.766, including leap years).

Estimated costs of construction of a hydro pumped storage power plants in Croatia, with nominal power of 100 MW and with a gross drop of 750 m, is 460,000.00 € / MW. The average production cost in large hydroelectric power plants has the following structure: plant staff about 1 c€/kWh, services about 3.25 c € / kWh and various deliveries is about 0.25 c € / kWh.

In modern power systems, HPSPP capacities constitute a balancing role as net generation and load plus losses must be continuously balanced, i.e. in real time, to maintain system stability and reliability. The benefits of HPSPP units were recognized early in the development of electric power systems, especially as systems became larger and more interconnected. Roughly 75% of the overall installed HPSPP capacity in Europe is concentrated in 8 countries, with more than half of this in 4 countries: Italy, Germany, France and Spain, [2].

With increasing demand variability, HPSPP capacities utilization also increases if other balancing power units are unavailable. Usually a certain number of gas turbines perform this role in existing power systems. The extent of HPSPP plants and gas turbines usage for balancing purposes reveals the mechanisms of electricity generation portfolios managing in different European countries. The most relevant factors that influence generation portfolio management are related to ownership of the various power units, production unit efficiency, structure relation between the day-ahead market and dispatching market (monopolistic, oligopolistic markets), price setting mechanisms (marginal and priority producers), carbon pricing.

Development of HPSPP capacities is very sensitive to their utilization rate. Actually, the decreasing electricity market prices (sometimes even negative prices in the day-ahead markets are observed), stagnation of demand and new policy regimes (RES targets for 2020, 2030 and RES incentives) introduced considerable uncertainties and setbacks in future market developments not only regarding HPSPP technology but also all other power technologies. Actually, in the light of increasing share of intermittent renewable sources in modern electric power systems, one could expect that flexible HPSPP capacities would be utilized more extensively. However, when examining the HPSPP utilization rates a wide spectrum of operation levels is observed: in some countries both capacities and utilization rates increased, while in others even the existing capacities are left idle or used less than before.

Throughout Europe, the average capacity of a HPSPP plant is about 300 MW. On average, European HPSPP plants are older than 30 years and 60% of them were built between 1970. and 1990., [3]. The first large development of HPSPP capacities, occurred between 1970. and 1990. In fact, HPSPP systems were developed to utilize and store the minimum technical output of coal-fired stations as well as the night production of nuclear power plants in light loading conditions, and later on to deliver electricity in times of peak load. By the end of the 1980s only a few new HPSPP plants were constructed in Europe. Between 1990. and 2010., only 15 HPSPP plants, with a total capacity of 5.6 GW, were built in Europe.

While the need of HPSPP capacities to utilize nuclear output in EU has decreased, HPSPP importance is maintained. The increased share of intermittent RES in the energy mix should favoure HPSPP, because its technical characteristics can potentially enable higher penetration of RES (energy from wind turbines night operation used for water pumping, and curtailment minimisation). The electricity prices in Western Europe were facing a constant drop until 2016., as shown in Figure 2., as well as price difference between peak and off-peak electricity market prices [4], what was directly threatening HPSPP market position. There has been some

rise due to the scarcity situation in winter 2017. Occasional occurences of negative electricity market prices could be beneficiary to HPSPP owners, but this is still not a permanent condition on which one could base its investment economic feasibility.

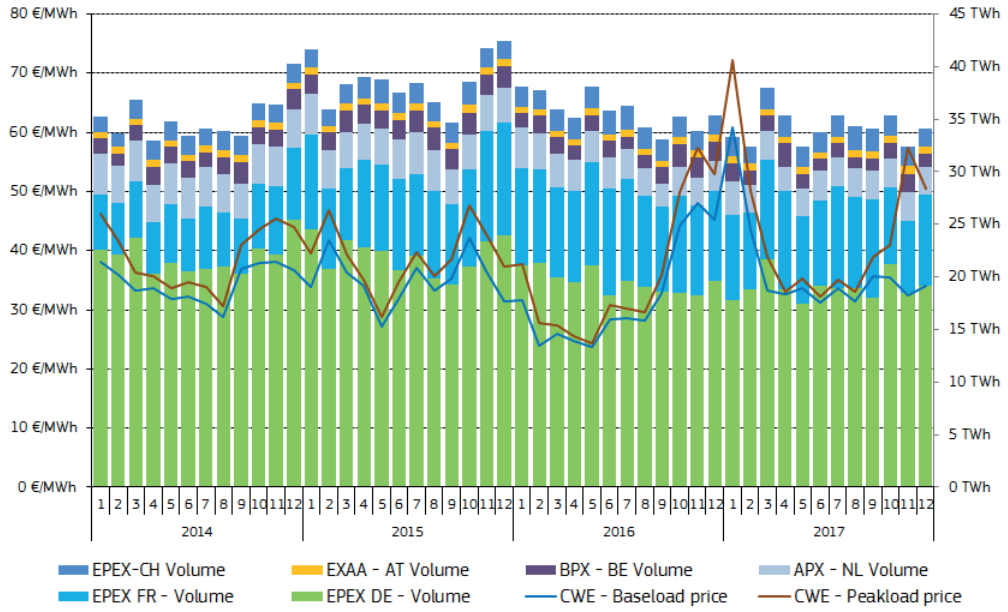

Figure 2. Monthly exchange traded volumes of day-ahead contracts and monthly average prices in Central Western Europe, source Platts, EPEX

After a long period, the market for HPSPP capacities is once again on a rising slope. In the next 10 years, more HPSPP plants will be constructed in Europe than previously in any other decade. There are plans for installing nearly 60 plants with an overall installed capacity of about 27 GW. This represents roughly 50% of the existing plants capacity and an investment of almost €26 billion. Most of the largest new plants will be constructed in countries with large penetration of wind and solar energy resources or in countries with appropriate topographical conditions (like Switzerland or Austria), [3].

In Eastern Europe the approach to HPSPP capacities is different than that in the Western European countries. Renewable wind and solar power play only a minor role. New HPSPP capacities are constructed in countries with low renewable sources e.g. Romania, Lithuania, Latvia, Estonia, Slovenia and Hungary, where HPSPP plants are mainly needed to utilize electricity from fossil and nuclear power plants. This development has been seen in the Western European countries in the period of 1970s to 1980s. The advanced economies in Poland and the Czech Republic have already undergone this phase, therefore no new HPSPP capacities are planned in these countries, [3]. Maybe the fastest and most dynamic growing market is Romania. Romanian HPSPP capacities are small, despite the favourable natural preconditions for hydropower plants. The need for new HPSPP capacities in Romania is affected by electric energy production from large fossil and nuclear power plants. Central Easte European electricity market prices [4], Figure 3., are still not so influenced by RES integration as it is a case in Western European countries.

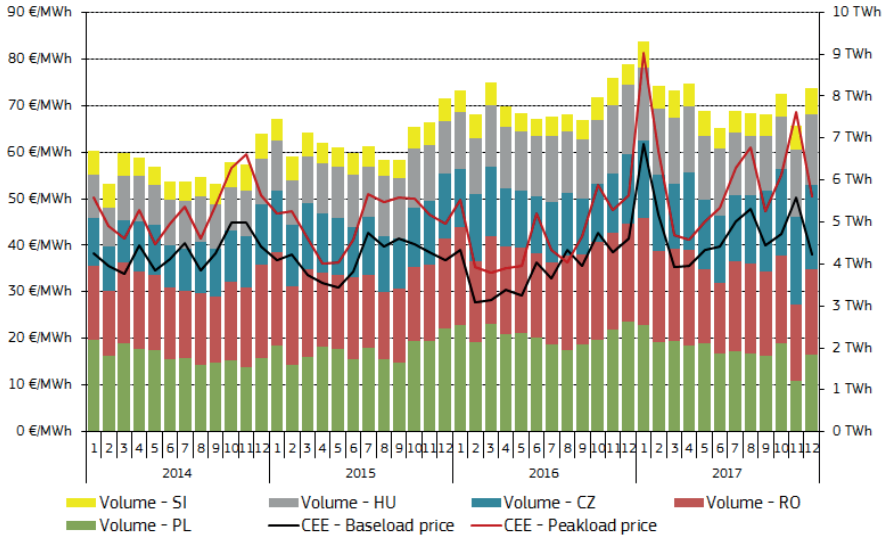

Figure 3. Monthly electricity exchange traded volumes and average day-ahead prices in Central Eastern Europe, Source: Regional power exchanges, Central and Eastern Europe (CEE)

3. POWER SYSTEM OPERATIONAL NEEDS FOR INTERMITTENT RENEWABLE ENERGY SOURCES INTEGRATION

Intermittent RES are bringing high uncertainity into the power system operation. As the generation from such kind of energy sources is in the same time hardly predictable in the day-ahead operational planning process, their operation can cause severe variations in the control area balance. Therefore, more control reserves for balancing the system are required for the secure power system operation, both in upward and downward direction.

Minimum and maximum load are important parameters considering the RES integration in certain country / control area. Those figures compared against average total RES production roughly show percentage of load expected to be covered by RES production. For the topic analysed in this article, percentage of minimum load covered by RES production is of special interest. Minimum load period occurs during night hours, and for countries with high wind power penetration, it very often coincides with periods of high wind power plants production. If there is a shortage of downward control capacities it usually leads to the curtailment of wind energy production, and thus extensive financial compensation to wind power plant owners and for redispatch.

According to [5] in European countries with large wind penetration ratio the wind curtailment is growing rapidly, both in absolute values and curtailment ratio. In Germany, the total wind generation has almost doubled from 48.883 GWh in 2011., to 87.975 GWh in 2015., while in the same period wind curtailment has grown seven times, from 410 GWh to 3.060 GWh, and with wind curtailment ratio growth from 0,8% to 3,5%. At the same time, this has caused extreme costs to the German transmission system operators. Only Tennet's total redispatch costs in Germany reached almost €1 billion in 2017.

Italy has almost similar situation, with total wind generation of 19.913 GWh in 2015. and with wind curtailment of 119 GWh. Wind curtailment ratio in Italy has droped, from 1,1% in 2013. to 0,6% in 2015., although the wind penetration ratio has risen from 5,3% in 2013. to 7,4% in 2015. Those reduction rates had happened mostly because of infrastructure upgrades linking the southern and northern Italian regions, where most of the congestions have taken place in the past, demanding for the curtailment of wind generation in southern part of Italy. Also, battery storage facilities have been put in operation in in southern part of Italy, helping the relieve of congestions.

Wind curtailment can be treated as a waste of energy, similar to the accumulation overflow in the periods of extreme hydrology. But, in the contrary to the extreme hydrology periods, which can appear at the most few times a year, the wind energy surpus can appear rather often, causing constantly repeated disturbances to normal power system operation.
It would be ideal if there would be enough storage capacities to safely store those energy surpluses and use it later, in the periods of energy shortage. This could be a double benefit for the power system operation, but also a clear benefit from the economical point of view. As the RES will continue to grow in European, but also non-European SEERC countries, the need for flexibility will be more urgent, specially need for storage capabilities.
RES integration figures in SEERC countries are quite different in integration dynamics from country to country, as well as in total amount and percentage of totally installed generation. Table 1. gives a comparison of installed generating capacity in SEERC countries, specially focusing on intermittent RES (wind, solar). Minimum and maximum loads are also compared.
Observing the RES share in totally installed generation, seven SEERC countries are significantly more developed than others. Three of them, Greece, Italy and Romania, have more than 20% of RES share in totally installed generation. Austria has a significant RES share of 15,6 %, but also very high total amount of 3841 MW of installed RES generation. Turkey and Czech Republic have RES share around 10 %, but again very high total amount of installed RES generation. Than comes Ukraine with more than 900 MW, and Croatia and Hungary with more than 600 MW of installed RES generation, and moderate RES integration figures. Third group of countries consists of Slovenia, Slovakia and Macedonia, with rather low RES share, but with tendency of further development. Fourth and last group of countries are at the beginning stage of RES integration.

Table 1. Comparison of installed generating capacity in SEERC countries

Country	TPP [MW]	HPP [MW]	Wind [MW]	Solar [MW]	TOTAL RES [MW]	TOTAL GENERATION [MW]	RES [%]	Maximum Load [MW]	Minimum Load [MW]
Austria	7059	13656	2489	732	3841	24646	15,6	11728	4664
Bosnia and Herzegovina	1876	2096	0	0	0	3972	0,0	2142	868
Croatia	2005	2112	489	48	613	4730	13,0	2869	1155
Czech Republic	10735	2259	277	2027	1982	20188	9,8	10512	4446
Greece	12520	3393	2092	2605	4984	20897	23,9	9207	3314
Hungary	5611	57	328	49	681	8236	8,3	6437	2994
Italy	68867	26527	9416	19288	29384	133255	22,1	56103	18664
Kosovo	1200	72,2	0	0,6	29,82	1293	2,3	1160	240
Macedonia	1157	676	36	17	57	1890	3,0	1457	487
Montenegro	220	660	0	0	0	880	0,0	576	174
Romania	8185	6405	2965	1301	4384	20274	21,6	8752	3785
Serbia	5594	3015	0	0	0	8609	0,0	6958	2414
Slovakia	2476	2537	3	530	142	7829	1,8	4360	2285
Slovenia	1379	1296	3	270	150	3816	3,9	2144	929
Turkey	43923	26681	5751	832,5	7894	78497	10,1	44341	17796
Ukraine	27800	6200	439	458	961	55331	1,7	23898	11203
SEERC	200607	97642	24288	28158	55102,14	394343	13,97	N/A	N/A

* RES without large HPP

4. HYDRO PUMPED STORAGE POWER PLANTS PERSPECTIVES IN SEERC REGION

Large-scale RES integration development in EU and non-EU SEERC countries will urge for higher system flexibility and energy storage possibilities. Some of the countries already have energy storage facilities, mostly hydro pumped storage power plants. Energy storage facilities in SEERC countries [6] are listed in Table 2.

Table 2. Energy storage facilities in SEERC countries

Country	Total Number	Technology Type	Rated Power (kW)
Austria	18	Pumped Hydro Storage	4680000
	1	Electro-chemical	64
Bosnia and Herzegovina	1	Pumped Hydro Storage	420000
Croatia	1	Pumped Hydro Storage	276000
Czech Republic	3	Pumped Hydro Storage	1145000
	1	Flywheel	70000
	2	Electro-chemical	40
Greece	4	Pumped Hydro Storage	1429000
	1	Electro-chemical	800
Hungary	1	Electro-chemical	500
Italy	19	Pumped Hydro Storage	7642700
	31	Electro-chemical	56178
	2	Thermal Storage	5120
	1	Hydrogen Storage	1200
Romania	1	Pumped Hydro Storage	53000
	1	Flywheel	300
Slovenia	1	Pumped Hydro Storage	185000
	1	Electro-chemical	10
Serbia	1	Pumped Hydro Storage	614000
Ukraina	3	Pumped Hydro Storage	3173000

HPSPP have a number of advantages comparing to the new energy storage technologies like battery storage systems for example. HPSPP storage capabilities are much larger, having thus the posibillity to store large amounts of energy from RES. From the economical perspective HPSPP's main advantage is peak energy production and arbitrage between peak and off-peak energy, but at the same time disadvantage are very high investment costs. Still, HPSPPs have significantly longer life cycle than battery storage systems.

HPSPP can contribute to the frequency control, but also to the system balancing and congestion relieve. Besides the system flexibility, HPSPP can also contribute to the voltage and reactive power control what is not possible for the battery systems, unless there is a combination of battery system and FACTS installed.

From the ecological perspective HPSPP's advantage comparing to the battery systems is again long life cycle, where there is no need to often replace old equipment and thus produce large amounts of waste, having issues with the waste disposal. Battery systems therefore have much higher environmental impact than HPSPPs, specially those battery systems that use nickel and cobalt, like lithium-ion batteries.

European Commission has approved six electricity capacity mechanisms so far, to ensure security of supply in Belgium, France, Germany, Greece, Italy and Poland, Figure 4. Taking into account all that was elaborated above, authors propose to establish a special kind of capacity mechanisms in SEERC, but also other countries, that would support the operation of existing and new HPSPPs, enabling that way further RES integration, and fulfillment of the ambitious EU climate goals. In further research authors will focus to the detailed elaboration of the proposed HPSPP capacity mechanism.

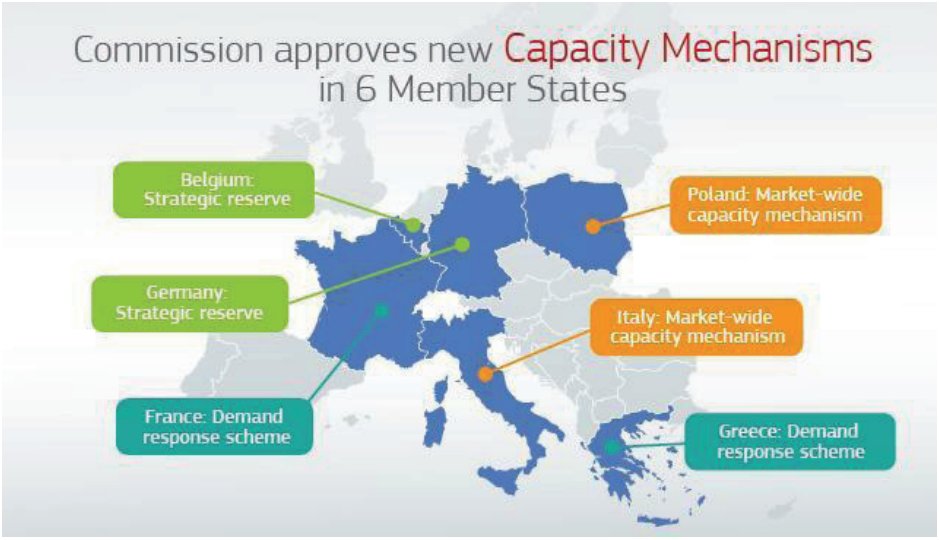

Figure 4. EU approved capacity mechanisms

5. CONCLUSION

Installed capacity of new RES is constantly increasing worldwide since more than 20 years, and projections foresee a continuous growth at the horizon 2040. European Union itself targets a 20% share of electricity generation by renewable energies in 2020, where wind and solar power are expected to represent the main contribution. However, these two sources of energy are known for being highly volatile and therefore, their integration in the existing power networks constitutes a challenging task. This requires development of adequate primary, secondary and tertiary production reserves and massive storage capacities where pumped storage power plants, regardless of HPSPP type should play a significant role. Because of the uncertain HPSPP future market position and economic feasibility, authors propose the establishment of a HPSPP operation support scheme through a capacity mechanism for HPSPP.

LITERATURE

[1] M. Manwaring, D. Mursch, K. Tilford Challenges and opportunities for new pumped storage development, technical report, National Hydropower Association (2012)
[2] https://ceeesa.es.anl.gov/projects/psh/ANL_DIS-13_07_Modeling_Ternary_Units.pdf
[3] https://www.hydroworld.com/articles/print/volume-19/issue-3/articles/new-development/renaissance-for-pumped-storage-in-europe.html

[4] Quarterly report on European electricity markets, DG Energy,Volume 10, issue 4, fourth quarter of 2017.
[5] WindEurope views on curtailment of wind power and its links to priority dispatch, WindEurope, June 2016., https://windeurope.org/wp-content/uploads/files/policy/position-papers/WindEurope-Priority-Dispatch-and-Curtailment.pdf
[6] "DOE Global Energy Storage Database." [Online]. Available: http://www.energystorageexchange.org/projects/data_visualization. [Accessed: 07-Feb-2018].

Journal of Energy

VOLUME 67 Number 2 | 2018 Special Issue

journal homepage: http://journalofenergy.com/

Harmonic Performance Analysis of Static Var Compensator Connected to the Power Transmission Network

[a]Ivana Damjanović, [a]Frano Tomašević, [a]Ivica Pavić, [a*]Božidar Filipović-Grčić, [b]Alan Župan

[a]University of Zagreb, Faculty of Electrical Engineering and Computing, Croatia

[b]Croatian Transmission System Operator Ltd., Zagreb, Croatia

SUMMARY

The static var compensator (SVC) is a device which is designed to compensate reactive power, increase voltage stability and to reduce voltage fluctuations. Thyristor controlled reactors (TCRs) are composed of reactors in series with bidirectional pair of thyristors. Current through reactors can be continuously controlled by changing the firing angle of thyristor valves, thus the inductive power can be easily controlled. Typical applications of TCRs in AC systems are voltage stabilization and temporary overvoltage reduction, stability improvement, damping of power oscillations and load balancing.

In this paper, harmonic performance analysis of SVC equipped with TCRs is presented. SVCs utilizing TCRs generate harmonic currents and therefore it is necessary to determine the effect of harmonics generated by the SVC on the power system and its elements. This includes interaction of the SVC with the system, the SVC performance under balanced and unbalanced operating conditions and finally, evaluation of countermeasures such as installation of harmonic filters. In order to carry out these analysis, it is necessary to determine harmonic characteristics of the network at the point of SVC connection, existing levels of harmonics, and to know appropriate standards regarding acceptable harmonic levels in the power system. Since harmonic distortions in the system are caused by the interaction between SVC and the system, all system contingencies which may affect system's frequency response should be evaluated. Detailed power system model should be considered to make sure that parallel resonance points of system do not directly coincide with characteristic harmonics from the SVC. Harmonics generated by SVCs are largely dependent on the operating point within the SVC characteristic. A conservative approach is to use the maximum values of harmonics generated within the spectrum irrespective of the operating point. The results of harmonic performance analysis are important for appropriate design of SVC. Harmonic performance analysis related to SVC application which are presented in this paper include the determination of: frequency response of the transmission network impedance required for the specification and design of filters; the effects of SVC generated harmonics on the power system; the overall filter requirements and countermeasures to reduce harmonics to acceptable levels.

KEYWORDS

Static Var Compensator (SVC), thyristor-controlled reactors, harmonic performance study, filter design, frequency response of the network.

1. FUNDAMENTALS OF POWER SYSTEM HARMONICS

1.1. Harmonic Sources

Harmonic sources cause harmonic distortion by injecting the current of a given harmonic spectra into the system. Causes of harmonics may be divided into two groups: power electronics devices and devices with nonlinear voltage and current relationship. Examples of the harmonic sources from the first group are SVC and TCR, while the second group includes nonlinear devices such as arc furnaces and saturated transformers.

TCRs are composed of reactors in series with bidirectional pair of thyristors which continuously control amount of absorbed reactive energy by changing the firing angle. The structure of TCR and its waveform are in Figure 1.1.

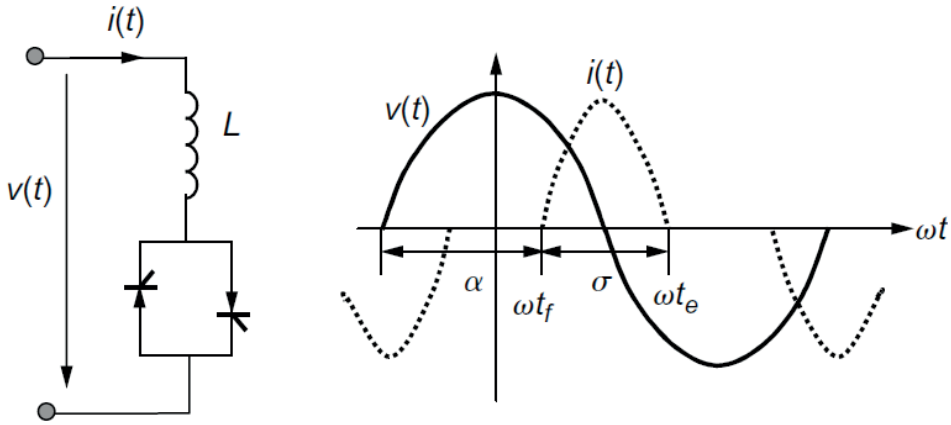

Figure 1.1 Thyristor controlled reactor and its current and voltage waveforms [1]

The thyristor control angle α at the TCR is typically between 90° and 180° and is defined from the zero crossing of the voltage appearing across its terminals. At the firing angle 90°, thyristors leak the full sinusoidal current to the TCR, while at 180° the current reduces to zero. Between these limits of the control angle, there are current waveform distortions which are equal in the positive and negative half-cycles, causing only odd-order harmonics. Multiple different harmonics are generated at same firing angle, and the typical amplitude values of a given harmonic in relation to the rated current depending on firing angle are shown in Figure 1.2. The TCR, modeled in this paper, has an anti-parallel-connected thyristor pair for each phase as shown in Figure 1.1, connected in delta giving a 6-pulse unit. Assuming that the reactors in each branch are identical and that all thyristors fire with equal firing angles, SVC generates only odd harmonics while zero sequence triplen harmonics remain trapped inside delta, thus reducing the harmonic injection into the power system. On the preliminary consideration it can be deduced that the TCR will produce harmonics of the order $6p \pm 1$ where $p = 0, 1, 2, 3 \ldots$ (5^{th}, 7^{th}, 11^{th}, 13^{th} ... harmonic). The most significant influence on power quality have 5^{th} and 7^{th} harmonic because their amplitudes are the most dominant.

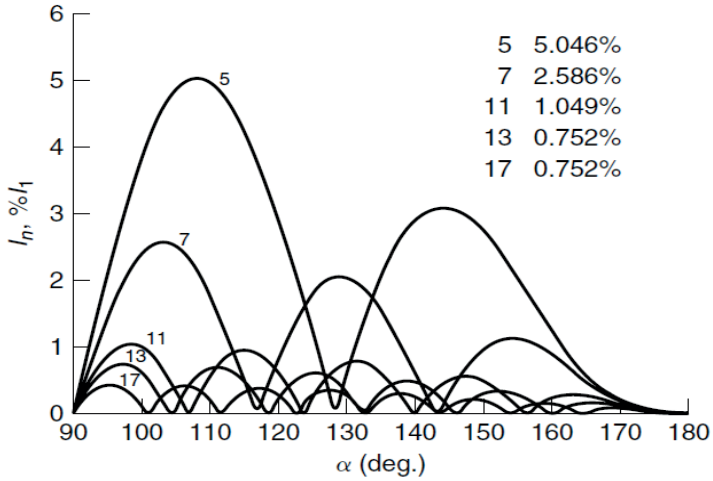

Figure 1.2 Current harmonics of TCR depending of thyristor firing angle [2]

1.2. Standardization of Harmonic Levels

Total harmonic distortion (THD) and individual harmonic distortion (IHD) are widely used power quality indicators. According to literature [3], these factors for voltage distortion are defined as:

$$IHD_n = \frac{U_n}{U_1} * 100\%, \tag{1}$$

$$THD = \frac{U_H}{U_1} * 100\%, \tag{2}$$

$$U_H = \sqrt{\left(U_2^2 + U_3^2 + U_4^2 + U_5^2 + U_5^2 + U_6^2 + \ldots + U_n^2\right)}, \tag{3}$$

where n is harmonic order. Equations (1), (2) and (3) also apply to the calculation of current distortion.

Concerning voltage harmonic distortion, IEEE 519 standard [4] defines limits shown in Table I as a function of the system voltage level. The recommended limits apply only at the point of common coupling (PCC) and should not be applied to either individual pieces of equipment or at locations within a user's facility. In most cases, harmonic voltages and currents at these locations could be found to be significantly greater than the limits recommended at the PCC due to the lack of diversity, cancellation, and other phenomena that tend to reduce combined effects of multiple harmonic sources to levels below their algebraic summation.

Table I Individual and total voltage harmonic distortion limits [4]

Bus voltage *U* at PCC	**IHD (%)**	**THD (%)**
$U \leq 1.0$ kV	5.0	8.0
1 kV < $U \leq 69$ kV	3.0	5.0
69 kV < $U \leq 161$ kV	1.5	2.5
161 kV < U	1.0	1.5

According to the Croatian grid code, voltage THD in normal operating conditions caused by either generator or user connection at the withdrawal and injection point shall typically amount to at most:

- 1.5% at 400 kV and 220 kV levels;
- 3.0% at 110 kV level.

The above given values refer to the 95% of the 10-minute averages of effective voltage values for the period of one week.

1.3. Harmonic Analysis

Power system harmonic analysis includes network frequency response analysis and harmonic power flow analysis and is used for system planning, equipment design, etc. Frequency response characteristic of a network helps in verifying whether resonance conditions exist and how to mitigate them. Frequency scan is generally determined at network locations where nonlinear loads, capacitor banks, or harmonic filters are connected. A harmonic power flow calculation gives an insight into the harmonic voltages and currents of the observed system operating point, which allows to check whether the distortions are within the defined limits.

2. HARMONIC FILTERING TECHNIQUES

Harmonic filters are used to prevent adverse effects of harmonics and can generally be classified into passive and active filters. Their basic difference stands on whether they provide filtering action within a selected bandwidth (passive) or as a result of a real-time monitoring process (active). Hybrid filters are a combination of the two mentioned groups.
Passive filters are most commonly used and can be designed as single-tuned or band-pass [5]. Single-tuned filters represent a low impedance for the harmonic frequency that needs to be filtered out, while the band-pass devices filter harmonics of a given frequency bandwidth.

2.1. Single-tuned filters

The most commonly used filter type is single-tuned, which is a series combination of a capacitance and an inductance whose values are determined in a way that their combination achieves serial resonance at tuned frequency. The interaction of the filter and the source impedance results in a parallel resonance. If multiple single-tuned filters are used, it is necessary to take into account that each filter branch provides a certain amount of reactive compensation. In this case, a parallel resonant frequency exists for every individual passive filter.

2.2. IEEE 18 standard

Filter capacitors are designed to operate continuously at or below their rated voltage. Recommended operation values for filter capacitors are defined in IEEE 18 standard [6]. Maximum limits shown in Table II for the operation of shunt capacitors in the power system including current, reactive power, and voltage across the capacitor units are basic for filter design.

Table II Maximum operating limits for shunt capacitors

***Q* (kvar)**	135% of rated reactive power
Voltage (rms)	110% of rated rms voltage
Voltage (peak)	120% of rated peak voltage, including harmonics, but excluding transients
Current (rms)	135% of nominal rms current based on rated reactive power and rated voltage

2.3. Methodology for design of tuned harmonic filters

Determining the technical characteristics of the filter is an iterative procedure in which the initial presumed nominal filter values (rated power and rated voltage) are checked according to the limits from Table II. It is necessary to know harmonic distortions created by the device for which the filter is dimensioned and existing distortions of current and voltage in the network.

SVC substation considered in this paper consist of two TCR branches with total reactive power 250 Mar connected to the 220 kV transmission network via transformer 242/26 kV. TCR branches produce current harmonics as shown in Figure 1.2. Filters for 5^{th} and 7^{th} harmonic are designed assuming that harmonics in the network are generated only by SVC operation.

2.3.1. Verifying filter technical characteristics according to IEEE 18 standard

After a few iterations, required technical characteristics (rated voltage and reactive power) of the observed filters are determined in a way to meet the limits given in [6]. Selected rated voltage and reactive power of filter for 5^{th} harmonic are 27 kV / 50Mvar and for 7^{th} harmonic filter 27 kV / 20 Mvar. The examined system is shown in Figure 2.1.

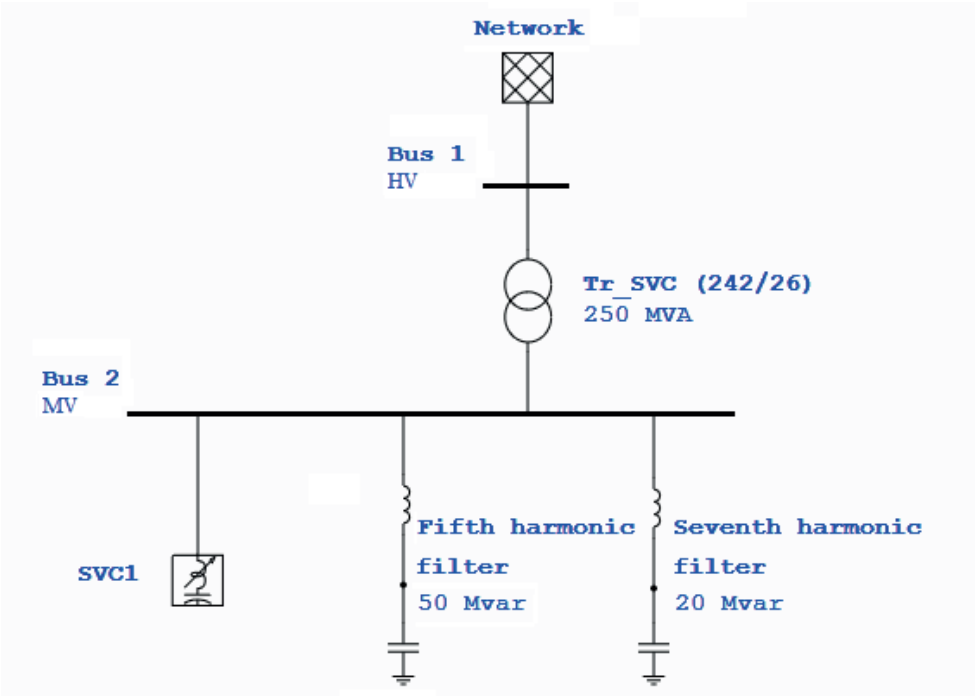

Figure 2.1 Equivalent scheme of system for analyzing SVC and filters interaction with the network

3. NETWORK FREQUENCY RESPONSE

Once the filter parameters are selected according to [6], it is necessary to check the parallel resonant conditions between filter branches and the inductive reactance of the network. If the parallel resonant frequency coincides with a characteristic harmonic present at network, resonant overvoltages are produced and this may cause insulation damage or failure of high voltage equipment. Using ETAP software, frequency scan of network is determined at the point of SVC connection to check the parallel resonant frequencies.

3.1. Parallel resonance

Parallel resonance is a result of interaction between capacitive and inductive parallel parts of network characterized by large impedance peak at frequency slightly below tuned filter frequency. A parallel resonance is to be established at a frequency:

$$f_{res} = \frac{1}{2\pi\sqrt{(L_s + L)C}} \tag{4}$$

where:
L and C are filter elements
L_s is source inductance.

3.2. Parallel resonance in the simplified network

Parallel resonant frequency would experience a shift whenever changes in the source inductance or in the filter elements occurs. Due to that, it is necessary to check parallel resonance for wider range of network operating conditions. Minimum and maximum short circuit current at bus 1 in network from Figure 2.1 are 10 kA and 20 kA, based on which the worst-case network impedance is calculated.

Frequency scan gives impedance amplitude and angle depending on frequency for the observed bus in the network. Results for bus 2 are shown in Figure 3.1 and Figure 3.2. From Figure 3.1, frequency response has four resonant frequencies in range 50-600 Hz, at which impedance angle is equal to 0°.

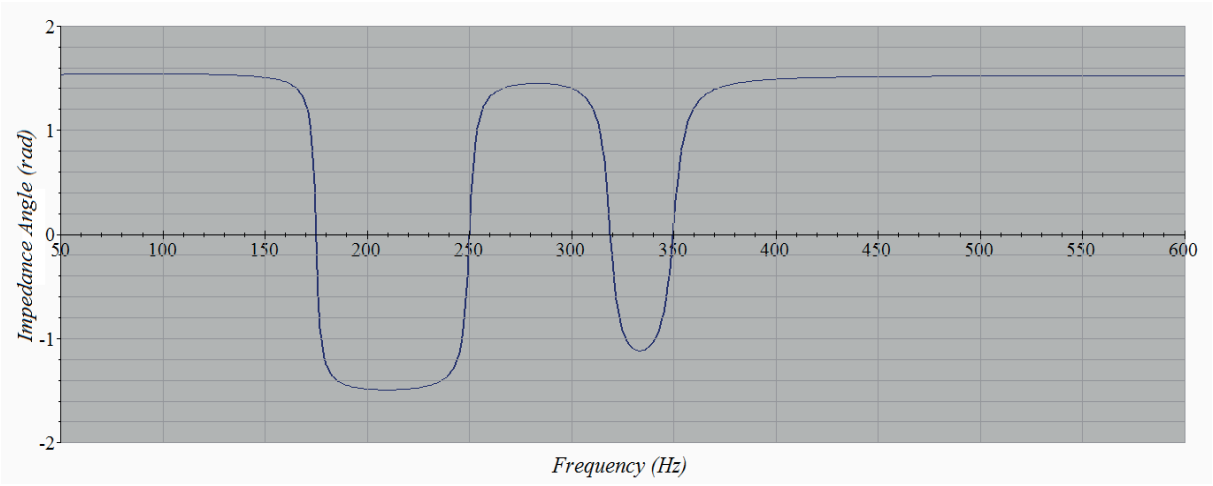

Figure 3.1 Impedance angle in dependence of frequency at point of SVC connection

Two peaks of impedance amplitude shown in Figure 3.2 correspond to parallel resonance between filter branches and network. Impedance amplitude is equal to 0 Ω at fifth and seventh harmonic frequencies which corresponds to series resonance, since filters are tuned at that frequencies.

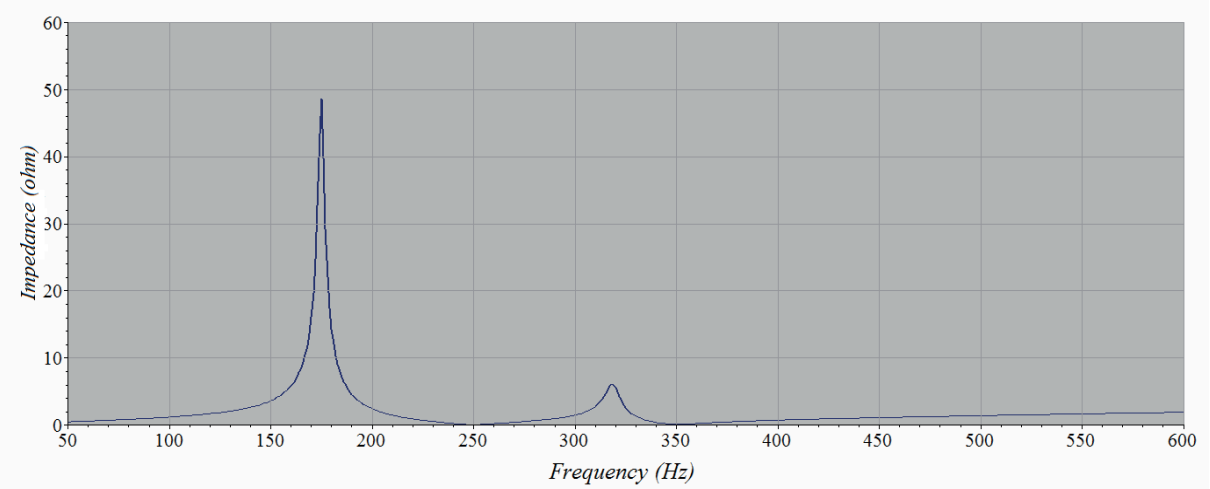

Figure 3.2 Impedance amplitude in dependence of frequency at point of SVC connection

Frequency scan results for minimum and maximum short circuit current are shown in Table III. Results show that higher short circuit current gives lower impedance magnitude at parallel resonant frequency.

Table III Resonant frequencies and impedance magnitudes at these frequencies

$I_{SC} = 20\ kA$			$I_{SC} = 10\ kA$		
Bus	**Impedance magnitude**	**Resonant frequency**	**Bus**	**Impedance magnitude**	**Resonant frequency**
Bus 2	48.51 Ω	175 Hz	Bus 2	55.68 Ω	168 Hz
Bus 2	6.1 Ω	318 Hz	Bus 2	6.42 Ω	317 Hz

3.3. Frequency scan in the real transmission network

In the previous chapter, short circuit impedance is used as a simplified representation of network. It was shown that filter branches lead to new resonant frequencies appearing. For more detail network frequency scan, so as more accurate assessment of filter influence on resonant conditions, it is necessary consider a more realistic model of transmission network.

Frequency scan at bus 1 is determined before and after filter connection at SVC substation considering real network model. Results of impedance magnitude in dependence of frequency are shown in Figure 3.3 and Figure 3.4.

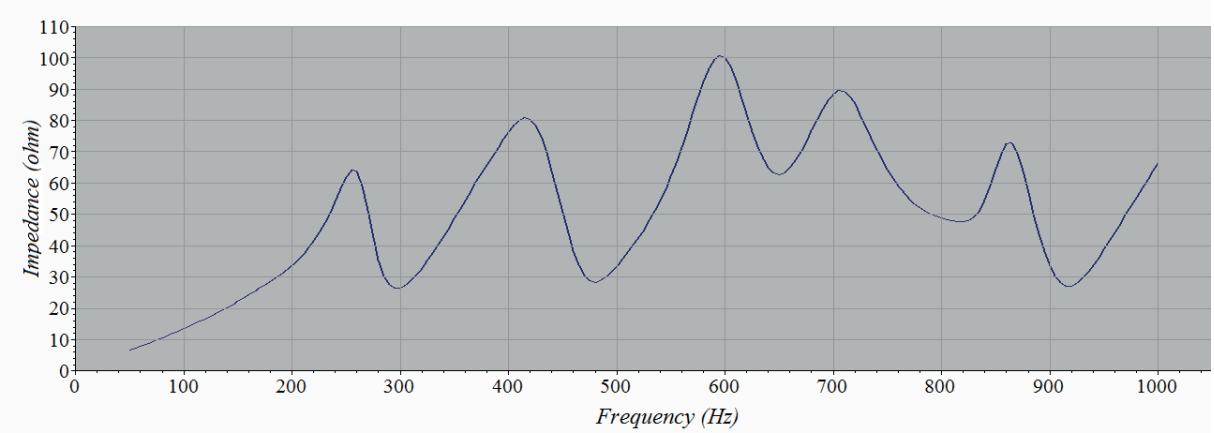

Figure 3.3 Impedance magnitude in dependence of frequency at bus 1 for real transmission network model

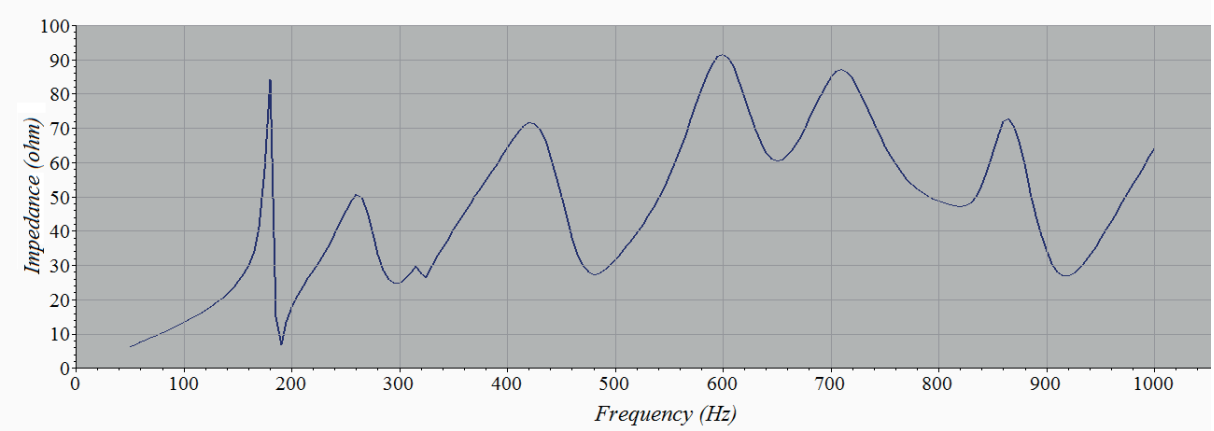

Figure 3.4 Impedance magnitude in dependence of frequency at bus 1 for real transmission network model with SVC and filters connected at bus 2

New parallel resonant frequencies after SVC and associated filters connection can be read off from above graphical results. Resonant frequencies and impedance magnitudes at bus 1 are given in Table IV.

Table IV Resonant frequencies and impedance magnitudes at bus 1 for model with real transmission network

Z [Ω]	f [Hz]
84.12	180.00
50.65	260.00
29.72	315.00
71.57	420.00
91.44	600.00
87.08	710.00
72.85	865.00

Real transmission network model in comparison to the simplified short circuit impedance model used in chapter 3.2 doesn't have great impact on resonant frequencies whilst higher impedance magnitudes at resonant frequencies can be noticed in the case of real network model.

4. HARMONIC POWER FLOW ANALYSIS

Depending on the network model complexity, harmonic analysis can be classified into balanced and unbalanced method. Assuming linear network model and linear harmonic sources, single-phase harmonic analysis is sufficient, and calculation applies the superposition principle so that harmonic sources are separately injected into each node of power system where harmonic distortions are created. Unbalanced harmonic sources require three-phase harmonic power flow calculation.

4.1. Harmonic characteristic of network

There can be multiple harmonic sources in the network, each contributing to harmonic distortion. It is necessary to check whether current harmonic distortions in the network for observed operating point are within defined limits.

Existing harmonic sources in the network can be modeled in ETAP software according to known, measured values of harmonic spectra. Current and voltage harmonic source models are available. Each harmonic component that observed source produces should be defined in percentage of nominal amplitude at fundamental frequency with associated phase angle.

4.2. Effect of harmonics generated by the SVC

In this section, voltage harmonic distortions of SVC, as the only harmonic source in the network, are presented. SVC is modeled as harmonic source according to previously described harmonic spectrum shown in Figure 1.2. Results of harmonic analysis, regarding total and individual harmonic distortions at observed buses are shown in Table V.

Table V Impact of SVC on voltage harmonic distortion

Bus 1 (20 kV)			**Bus 2 (220 kV)**		
THD = 6.92 %			THD = 1.27 %		
Harmonic order	**Frequency (Hz)**	**IHD (%)**	**Harmonic order**	**Frequency (Hz)**	**IHD (%)**
5	250	5.56	5	250	1.23
7	350	3.56	7	350	0.49
11	550	2.28	11	550	0.27
13	650	1.79	13	650	0.20
17	850	2.30	17	850	0.20

4.3. Impact of filters on voltage harmonic distortion

Harmonic load flow after connecting the fifth and seventh harmonic filter with above selected parameters, lead to reduction of total and individual harmonic distortions within defined limits. Results of harmonic analysis in case of SVC with connected filters are presented in Table VI.

Table VI Impact of filters on voltage harmonic distortion caused by SVC operation

Bus 1 (20 kV)			Bus 2 (220 kV)		
THD = 1.33 %			THD = 0.16 %		
Harmonic order	**Frequency (Hz)**	**IHD (%)**	**Harmonic order**	**Frequency (Hz)**	**IHD (%)**
5	250	0.13	5	250	0.03
7	350	0.15	7	350	0.02
11	550	0.83	11	550	0.11
13	650	0.74	13	650	0.09
17	850	1.01	17	850	0.09

5. CONCLUSION

The harmonic propagation of a SVC connected to a high-voltage transmission network has been analyzed in this paper. In order to reduce the negative influence of SVC operation on power quality, filters for fifth and seventh harmonic are selected due to their major impact in harmonic content from harmonics generated at the SVC terminals.

A method to obtain the filter parameters is presented. Once iterative process of filter parameters selection fulfills IEEE 18 standard it is necessary to carry out harmonic analysis. Harmonic analysis include frequency scan and harmonic load flow analysis whereby harmonic resonant existence and harmonic distortions in the network are analyzed. Connection of selected filter branches lead to appearance of two new parallel resonant frequencies at PCC. Frequency scan for real network model as result gives more accurate impedance amplitude at resonant frequencies in comparison to simplified network representation by short circuit impedance. Of special importance is to check that filter connection does not cause resonant points at harmonic frequencies, which frequency scan confirmed. Harmonic load flow analysis showed that IHD and THD are lower and within defined limits when using filters.

As conclusion, it can be highlighted that analysis method presented in this paper can be extended to any scenario and it is a useful tool for filter parameters determination and harmonic propagation analysis of power electronic devices connected to the transmission network.

REFERENCES

[1] A. Gómez-Expósito, A. J. Conejo and C. Canizares, Electric Energy Systems Analysis and Operation, Boca Raton: CRC Press, 2009.

[2] R. M. Mathur and R. K. Varma, Thyristor-based FACTS Controllers for Electrical Transmission System, New York: John Wiley & Sons, Inc. Publication, 2002.

[3] C. Sankaran, Power Quality, New York: CRC Press LLC, 2002.

[4] IEEE Std 519, IEEE Recommended Practice and Requirements for Harmonic Control in Electric Power Systems, New York, 2014.

[5] F. De La Rosa, Harmonics and power system, Boca Raton: CRC Press, 2006.

[6] IEEE Std 18, IEEE Standard for Shunt Power Capacitors, New York: IEEE, 2012.

Journal of Energy

VOLUME 67 Number 2 | 2018

journal homepage: http://journalofenergy.com/

Automatic Generation Control Application for Transmission and Generation Centres

K. VRDOLJAK*, B. KOPIĆ, M. GEC, J. KRSTULOVIĆ OPARA, S. SEKULIĆ
Končar - Power Plant and Electric Traction Engineering Inc.
Croatia

SUMMARY

Recently, a new Emergency Control Centre for Albanian Transmission System Operator (TSO), which includes Supervisory control and data acquisition (SCADA) and Automatic Generation Control (AGC) applications, has been commissioned. Nowadays, an AGC application is being prepared for the biggest generation company in Croatia, as part of control centre for hydropower plants within western part of Croatia. Both of these implementations use the same AGC application, which is presented in this paper.

Although AGC for TSO and AGC for Generation Centre (GC) have many similarities, their main goals are different. AGC for TSO must mainly regulate system's frequency and area's active power interchange to their desired values, using only power plants engaged in load-frequency control (LFC). However, AGC for GC must ensure that power production of each power unit not engaged in LFC tracks its planned value, while also ensuring that centre's share in LFC is being respected.

Albeit the AGC is standalone application, in both afore-mentioned implementations it is affiliated with SCADA application, from which it obtains all required input measurements and indications and to which it delivers calculated setpoints. Additionally, all AGC pictures are integrated into SCADA pictures as well, in order to simplify operation and monitoring functionalities.

AGC for Albanian TSO controls active power generation of six hydro power plants engaged in LFC. AGC for GC West in Croatia controls active power generation of ten hydro power plants. In both implementations, communication with remote objects is done using IEC 60870-5-104 communication protocol, while communication with other control centres is done using ICCP communication protocol. Power production plans are sent to AGC either from Market Management Systems (in TSO case) or from scheduling and optimization application (in GC case).

KEYWORDS

Automatic Generation Control, Load-frequency control, Emergency Control Centre, Generation Centre, Transmission System Operator, SCADA.

1. INTRODUCTION

Since the beginning of 2018, a new Emergency Control Centre (ECC) for OST, Albanian Transmission System Operator (TSO), has been in operation. Besides, by the end of 2018, an Automatic Generation Control (AGC) application will be implemented in Generation Centre (GC) West of Croatian biggest generation company, HEP Generation.

For these two implementations the same AGC application is used, PROZA HAT AGC.

2. AGC HIERARCHY

PROZA HAT AGC is an application that can be used both, for AGC at the highest level (in dispatching centre of master TSO) or at lower level (in dispatching centre of slave TSO or generation centre for several power plants). AGC levels are shown in Figure 1.

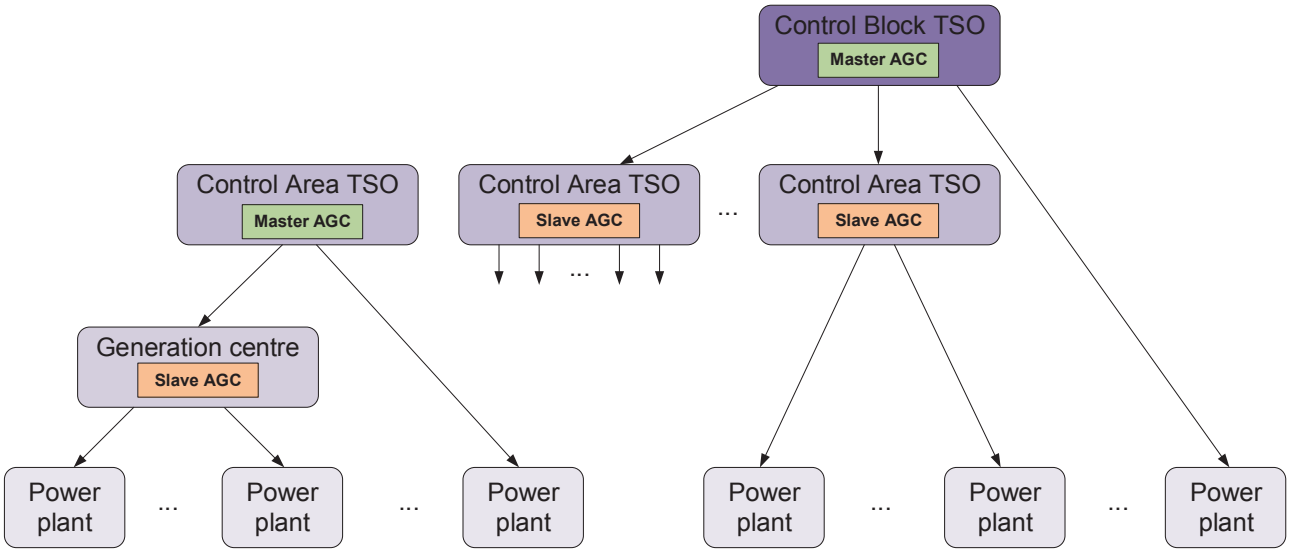

Figure 1: AGC application hierarchy

Master AGC in TSO centre is independent of any other AGC/TSO and it is in charge of conducting load-frequency control (LFC) in its control area or for the entire control block (see Figure 1). At this level, TSO usually has two redundant centres: Main (or National) Control Centre (MCC or NCC) and Emergency Control Centre (ECC). Slave AGC in TSO's centre or in GC receives its total share in LFC from the master AGC, which it has to redistribute to its AGC-units engaged in LFC. Besides, within GC implementation, automatic plan tracking is usually used for AGC-units not engaged in LFC. Generally, AGC-unit can be power unit, power plant or a group of power plants, depending on the implementation.

3. PROZA HAT AGC APPLICATION

PROZA HAT AGC application consist of several modules, which are shown in Figure 2. Whether a module is used or not in an AGC implementation, depends on the AGC's hierarchical role (master AGC or slave AGC). Master AGC uses all modules shown in Figure 2, with input measurements and indications arriving from SCADA and input plans from MMS system. Slave AGC uses only *Units* module, while *Preprocessing* module is not obligatory. In this case, inputs to *Units* module are: total power change from master AGC, production plan from scheduling application and raw (or pre-processed) measurements of actual powers from SCADA.

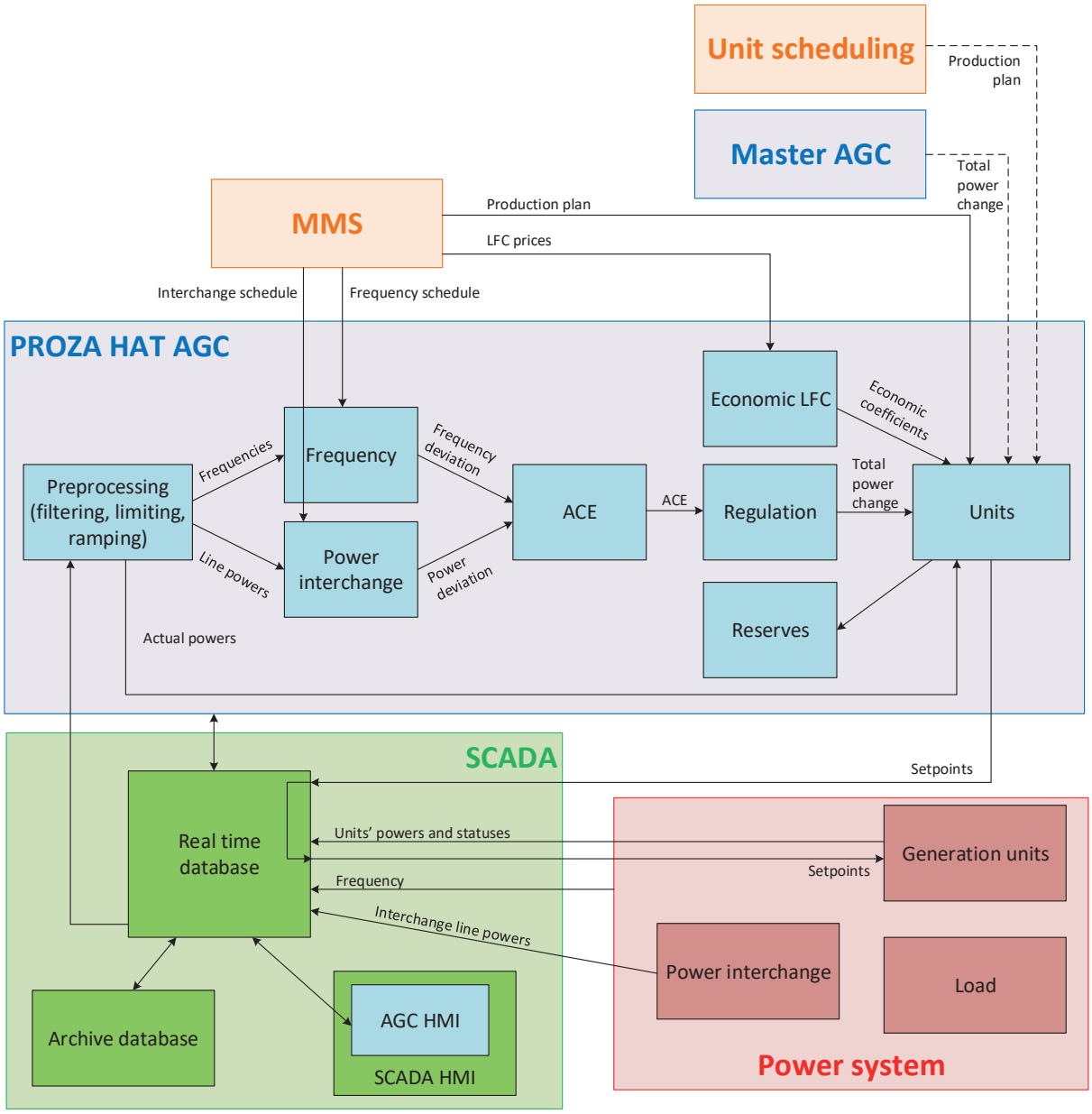

Figure 2: PROZA HAT AGC application modules

3.1 PROZA HAT AGC's integration with SCADA

Although PROZA HAT AGC is a standalone application, in its current version it should be associated with an operating SCADA application to obtain its full functionalities regarding communication, visualisation, archiving and control.

From SCADA's real time database PROZA HAT AGC obtains all required input measurements and indications, which are gathered using SCADA's communication with remote objects. To SCADA, it delivers calculated active power setpoints, which SCADA forwards to AGC-units. PROZA HAT AGC's communication with SCADA is done through software communication gateway.

If input data cannot be obtained from inherent SCADA system, PROZA HAT AGC has its own IEC 60870-5-104 and TASE.2 communication drivers, which can also be used for exchanging information with remote objects in the power system.

All measurement data, obtained from SCADA, can be pre-processed before its usage in AGC

algorithm. During pre-processing, functions of limiting, ramping, filtering or dead zone can be applied to unlimited number of raw measurement inputs.

Additionally, PROZA HAT AGC doesn't require its own HMI, since all AGC pictures can be drawn and integrated into related SCADA. This manner ensures that monitoring and control functionalities are grouped at one place and thereby simplified for operator's usage.

SCADA system also serves for archiving AGC data. For those purposes, all AGC data required for reporting or archiving purposes must be sent from AGC to SCADA.

PROZA HAT AGC has no limitations regarding the SCADA system it need to connects with. If chosen SCADA application doesn't support connection with external applications through existing driver or software gateway, a communication between SCADA and PROZA HAT AGC using Inter-Control Centre Communications Protocol (ICCP) can be established for data exchange purposes.

3.2 AGC for Transmission System Operator purpose

AGC is a function that TSO of a power system uses to control production of generating units in LFC in order to keep system's frequency and interchange with neighboring areas at their desired values and production of generating units not in LFC to track area's production plan.

PROZA HAT AGC functionalities that are used for implementation for TSO are:

- data pre-processing
- control area/control block support
- priorities of measurement sources
- calculation of area control error from frequency and interchange deviations
- PI regulation algorithm
- AGC prices included in total power distribution to AGC-units
- merit order list in selection of AGC-units
- sending planned or manual setpoints
- monitoring of system reserves
- simulation of anticipated AGC-unit's response

Within AGC algorithm, firstly frequency and total active power interchange deviations are calculated. Each input measurement can be included or excluded from AGC algorithm. The deviations are afterwards used to calculate area control error (ACE) signal. A proportional-integral (PI) regulator is used to calculate total desired active power of all AGC-units engaged in LFC in order to drive ACE to zero MW value.

Total power change is optimally (from TSO's perspective) distributed to all power units engaged in LFC. If LFC market prices are present for the TSO, then minimum total price can be used as optimal criteria for the distribution of powers. Otherwise, the distribution can be done based on regulating ranges or on manually defined participation factors.

Secondary and tertiary reserves are calculated for all power units, power plants and the whole system. System reserves are monitored against their desired values.

AGC in master TSO can also regulate AGC-units not engaged in LFC. The can be regulated to manually set active power value or to its value obtained from the plan from Market Management System (MMS).

3.3 AGC for Generation Centre purpose

AGC for GC must mainly ensure that power production of AGC-units not engaged in LFC tracks desired plan, while also ensuring that centre's share in LFC is being regulated to received value through AGC-units engaged in LFC.

PROZA HAT AGC functionalities that are used for implementation for GC are reduced to:

- data pre-processing
- planned or manual setpoints
- merit order list in selection of AGC-units
- monitoring of system reserves
- simulation of anticipated AGC-unit's response

Power production plans are sent to AGC from units' scheduling application. Those plans should be calculated optimally based on defined/chosen criteria.

4. IMPLEMENTATIONS OF PROZA HAT AGC

4.1 Emergency Control Centre in Albania

Transmission System Operator in Albania is Operatori i Sistemit të Transmetimit (OST Sh.a.). OST had a NCC, but due to ENTSO-e requirements they also put into operation ECC in the beginning of 2018. ECC in Albania includes SCADA and AGC applications [1].

SCADA system in ECC is connected with 24 remote objects (transformer stations, HPPs or both). AGC for Albanian TSO controls active power generation of six hydro power plants (HPPs) engaged in LFC. Those are: HPP Fierza, HPP Koman, HPP Vau Dejes, HPP Fangu, HPP Banja and HPP Moglica. All remote object and their interconnected lines are shown in Figure 3.

PROZA HAT AGC in Albanian ECC is implemented in redundant configuration on two SCADA/AGC servers. It is connected with SCADA system PROZA NET, also in redundant configuration. Two additional servers are used for archive database.

AGC's communications with HPPs is done through PROZA NET using IEC 60870-5-104 communication protocol. In each HPP, an additional communication gateway, named LKKU, is installed between ECC and local control system. It is used as network interface for communication between HPP and ECC and also for blocking unauthorised commands from ECC. Input data that AGC receives from HPPs are actual active power measurements and AGC-unit's statuses.

AGC's communications with transformer stations (TS) is also done through PROZA NET using IEC 60870-5-104 communication protocol and through LKKU gateway. Input data that AGC receives from each border TS are actual interchange power measurements for all interconnection lines.

AGC's communication with NCC is done using ICCP (TASE.2) communication protocol. The data that is being exchanged between the centres is used for authority handling, since at the time only one centre can be allowed to send SCADA commands and AGC setpoints. However, centres can monitor OST's system simultaneously. Other data that is received from NCC are alternative measurements of interchange power for interconnection lines between Albania and Greece and Albania and Montenegro. AGC sends to SCADA system calculated setpoints of AGC-units, for forwarding to AGC-units.

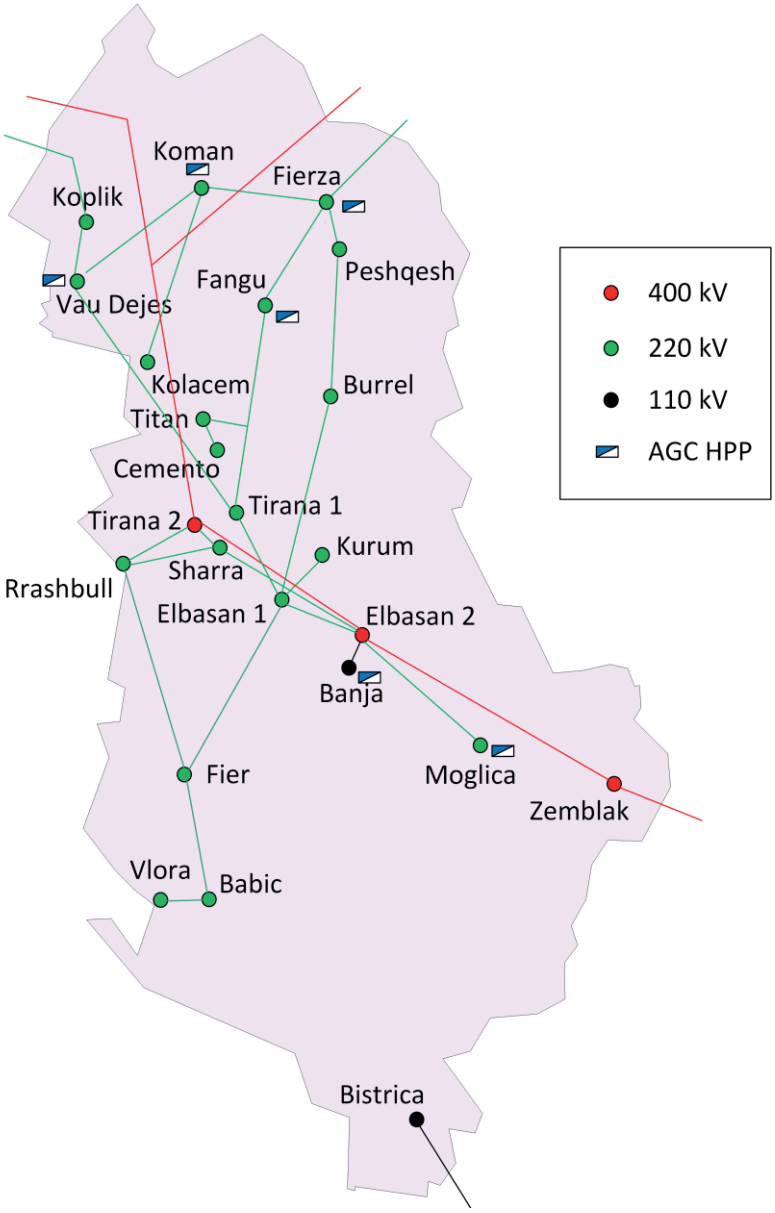

Figure 3: Remote objects within ECC in Albania

AGC's communication with neighbour control area of Kosovo is also done using ICCP communication protocol. In block operation mode, ECC exchanges with KOSTT (TSO in Kosovo) all data required for block control. In the block, OST is the block leader.

AGC in ECC receives AGC-unit's regulation limits and Albania's interchange schedule from OST's MMS system in form of standardized XML file format. After data from XML files are imported to PROZA HAT AGC, a CSV file is created as an interface for data visualization and manual interventions. In case plans are not available or they are corrupt, manually entered values can be used instead.

AGC pictures are divided into two categories: for operators and for administrator. Authority and allowable action through pictures is defined with user's role. Example AGC pictures of ECC system are shown in Figure 4.

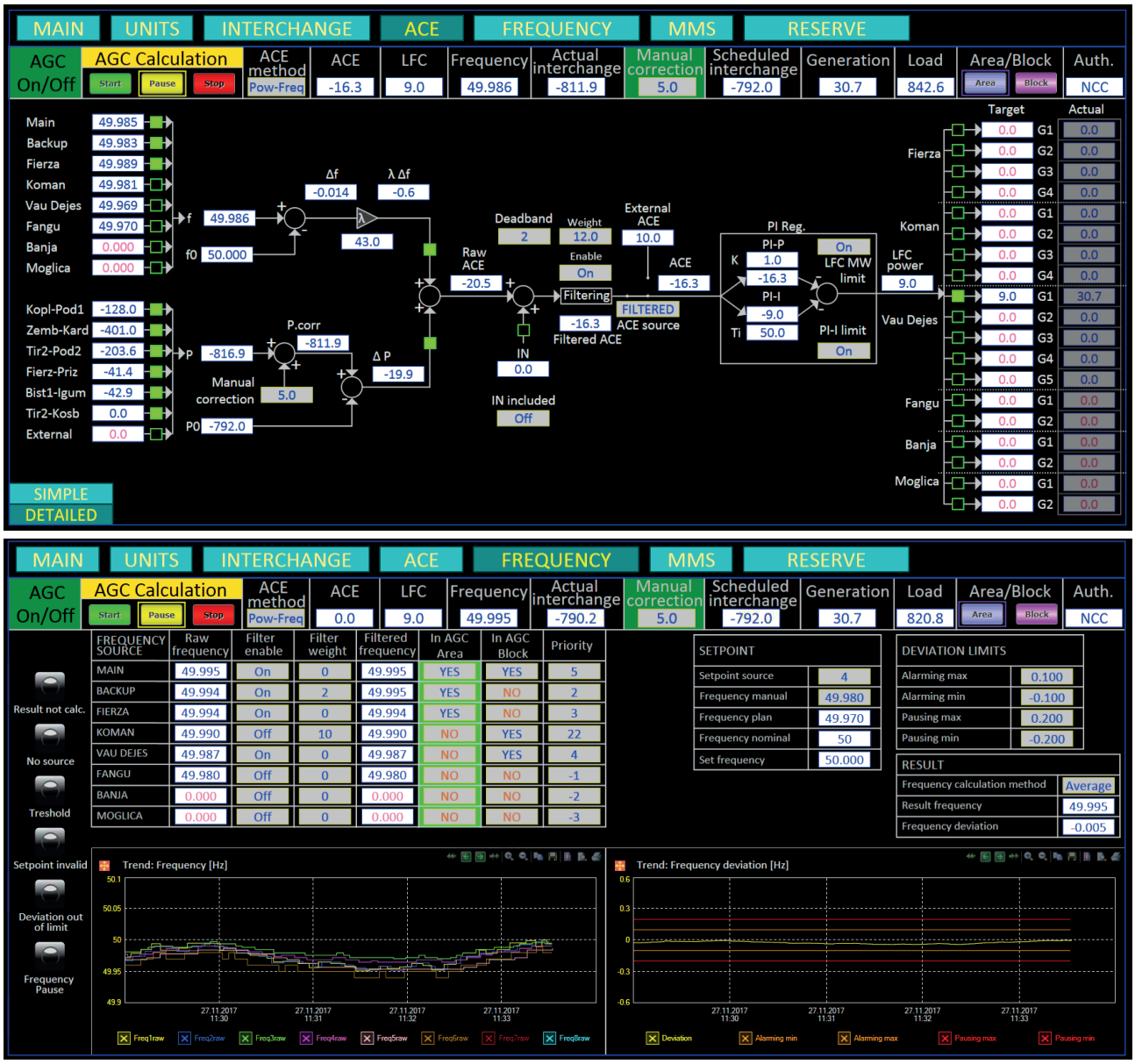

Figure 4: Example AGC pictures in ECC in Albania

4.2 Generation Centre West in Croatia

GC West in Croatia servers as monitoring and control centre for all (ten) hydropower plants of HEP Generation company in western part of Croatia, Hydro West [2]. Some of them are pump-storage (PSHPP) and some are just pump (PHPP) power plants. They are all located on four independent river catchments. All objects within area of Hydro West are shown in Figure 5.

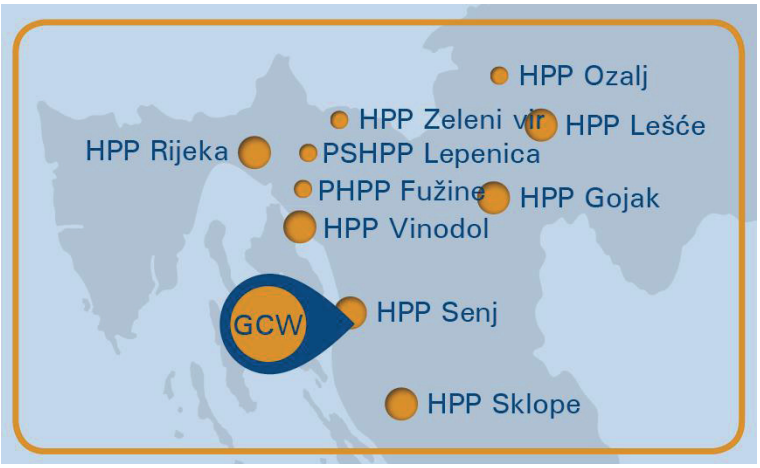

Figure 5: Remote objects within GC West in Croatia

In Hydro West only HPPs Senj and Vinodol are engaged in LFC in Croatia. So far, they have been receiving setpoints from Croatian TSO's NCC (or ECC), but in the future it will be possible to insert GC West into control path between NCC/ECC and HPPs. In NCC/ECC, GC West will be modelled as a single AGC-unit, while all distribution of its share in LFC to HPPs of Hydro West will be done within AGC application in GC West.

Additionally, AGC for GC West in Croatia must ensure that all power units not engaged in LFC follow defined plans that are provided to GC West by an external company, HEP Trade. Since in Croatian power system those plans are given for each power unit, in GC West's AGC power units are modelled as AGC-units (instead of power plants in Albanian ECC).

AGC in GC West will be set in redundant configuration, on two SCADA/AGC servers. SCADA system in GC West will also be PROZA NET.

AGC in GC West will only communicate with HPPs in Hydro West area and with Croatian's TSO NCC/ECC. AGC's communications with HPPs will be done using IEC 60870-5-104 communication protocol. In each HPP, a separate programmable logic controller (PLC) is in charge of LFC functionality and it will receive setpoints from GC West. Input data that AGC will receive from HPP are actual active power measurements and statuses of AGC-units. Communication between AGC in GC West and HPP within Hydro West will not be direct, but will go through GC West's SCADA application.

AGC's communication with NCC/ECC will be done using IEC 60870-5-104 and ICCP communication protocols. The data that will be exchanged between the centres will be used for authority handling, since in migration period only one centre will be allowed to send AGC setpoints towards HPPs. AGC in GC West will forward to NCC/ECC all required data gathered from HPPs but also information about plans for units not engaged in LFC.

NCC/ECC in Croatian TSO will either consider power plants as AGC-units or the whole Hydro West area as a single AGC-unit. Since AGC-unit in Hydro West's AGC is power unit, GC West will be in charge of distribution of signal(s) received from NCC/ECC to its power units engaged in LFC.

For power units not engaged in LFC, AGC in GC West will receive units' planned power schedule from external application Hydro Scheduling. Communication between these two applications will be done through GC's archive database. In case plans will not be available or will be corrupt, it will be possible to use manually entered values.

Example AGC pictures for GC West are shown in Figure 6.

Figure 6: Example AGC pictures in GC West in Croatia

GC West will be put into operation by the end of 2018.

Besides GC West, there are two mode GC centres in Croatia: GC South [3] and GC North [4], which were put in operation in 2013 and 2016, respectively. The both have PROZA NET SCADA system, while AGC is only implemented in GC South, but in reduced scope, since there is only one power plant in LFC.

5. CONCLUSIONS

A combination of PROZA HAT AGC application and PROZA NET SCADA application has proven to be highly reliable and very flexible solution for both, AGC in TSO's control centre and AGC in generation centre. The basic application's structure and functionality in both types of centre remains the same, only the selection of required modules and their parameters are adjusted according to implementation requirements. The AGC application can also connect to various external application and systems on higher or lower level of regulation and successfully exchange data with them.

REFERENCES

[1] K. Vrdoljak, M. Zrno, I. Krajnović, I. Pikula, A. Paci, R. Dhimo "Implementation of Emergency Control Center of Transmission System Operator in Albania" (13th HRO CIGRÉ Session, November 2017, Croatia)

[2] K. Vrdoljak, B. Horvat, V. Mustapić, B. Pavlović, M. Dabro, M. Kačić, G. Gašparović, A. Prpić "Overview of Applications and Functions at Generation Center West" (13th HRO CIGRÉ Session, November 2017, Croatia) (in Croatian).

[3] B. Horvat, A. Martinić, M. Dabro, T. Blažević "The Cetina river catchment control centre: combining commercial and tailor-made solutions" (The International Journal on Hydropower and Dams, Issue Six, 2012)

[4] K. Vrdoljak, B. Horvat, I. Strnad, Ž. Štefan "Integration of applications for revitalization of a remote control centre, Hydro North" (HYDRO 2015 - Advancing policy and practice, Bordeaux, 2015)

Journal of Energy

VOLUME 67 Number 2 | 2018 Special Issue

journal homepage: http://journalofenergy.com/

Power system static and dynamic security studies for the 1st phase of Crete Island Interconnection

J. KABOURIS(*), [1], M. KARYSTIANOS[1], B. NOMIKOS[1], G. TSOURAKIS[2], J. MANTZARIS[2], N. SAKELLARIDIS[2],E. VOUMVOULAKIS[2]

[1] Independent Power Transmission Operator (IPTO) S.A.

[2]Hellenic Electricity Distribution Network Operator (HEDNO) S.A.

Greece

SUMMARY

The island of Crete is currently served by an autonomous electrical system being fed by oil-fired (Heavy fuel or light Diesel oil) thermal power plants and renewables (wind and PVs). The peak load and annual electric energy consumption are approximately 600 MW and 3 TWh respectively; wind and photovoltaic parks contribute approximately 20% of the electricity needs of the island. Due to the expensive fuel used, the Cretan power system has very high electric energy generation cost compared to the Greek mainland. On the other side the limited size of the system poses severe limitations to the penetration of renewable energy sources, not allowing to further exploit the high wind and solar potential of the island.

According to the Ten Year Network Development Plan (TYNDP) of the Greek TSO (Independent Power Transmission Operator S.A. IPTO S.A.), the interconnection of Crete to the mainland Transmission System of Greece will be realized through two links: A 150 kV HVAC link between the Peloponnese and the Crete (Phase I) and a HVDC link connecting the metropolitan area of Athens with Crete (Phase II). The total length of submarine and underground cable of the HVAC link will be approximately 174km; it is at the limits of the AC technology and the longest and deepest worldwide at 150 kV level.

A number of studies have been conducted by a joint group of IPTO and Hellenic Electricity Distribution Network Operator (HEDNO) for the design of this interconnection. This paper presents briefly the power system static and dynamic studies conducted for the design of the AC link and its operation. Firstly, the paper presents the main results of the static security study regarding the calculation of the maximum power transfer capability of the link and the selection of the reactive power compensation scheme of the cable. Results from dynamic security analysis studies are also presented. The small-signal stability analysis concludes that a new (intra-area) electromechanical oscillation is introduced to the National System after the interconnection. The damping of the electromechanical oscillations is sufficient; however the operation of power system stabilizers at power plants located both at the mainland and at Crete power system can increase significantly the damping of important oscillation modes. Finally with respect to the risk of loss of synchronism after a significant disturbance in the system of Crete, such as a three-phase fault ("transient stability")- enough safety margin is estimated by means of Critical Clearing Time calculations.

KEYWORDS

HVAC submarine cable, Interconnection, Crete, Static and Dynamic Security

1. INTRODUCTION

The island of Crete is currently served by an autonomous electrical system being fed by oil-fired (Heavy fuel or light Diesel oil) thermal power plants and variable RES installations (Renewable Energy Sources, mainly wind and PVs). Currently wind power plants and photovoltaic installations generate approximately 20% of electric energy. The peak load and annual electric energy consumption are approximately 600 MW and 3 TWh respectively. Due to the expensive fuel used, the Cretan power system has very high electric energy generation cost compared to the Greek mainland. On the other side the limited size of the system poses severe limitations to the penetration of renewable energy sources, not allowing to further exploit the high wind and solar potential of the island.

According to the Ten Year Network Development Plan (TYNDP) of the Independent Power Transmission Operator (IPTO) of Greece, the interconnection of Crete to the mainland Transmission System of Greece will be realized in two phases: A 150 kV HVAC link between the South East (SE) Peloponnese and the North West (NW) Crete (Phase I) and an HVDC link connecting the metropolitan area of Athens with Crete (Phase II). The double-circuit 2x200 MVA AC link will be an integral part of the 150 kV network of the Hellenic Transmission System connecting the existing substations of Molaoi (Peloponnese) and Chania (Crete).

The AC Interconnector of Crete is a project in the international forefront, due to the high length of the continuous cable part, which reaches approximately 174 km. In fact, during the last years, apart from the tendency towards HVDC interconnections, a trend for long HVAC cables can be also observed (e.g. the Mallorca-Ibiza interconnection of 126 km at 132 kV [1]). Beyond certain distance, the HVDC option is more cost-effective, however the exact distance is case dependent [2]. Besides, the experience from operational HVDC interconnections shows that in some cases costs had been underestimated [3]. Currently, the longest AC cable interconnection is the (single-circuit) 163 km 100 kV AC cable interconnection of the Martin Linge oil and gas platform with a design power of 55 MW [4].

A number of studies have been conducted by IPTO for the design of the interconnection. This paper presents briefly the power system security studies conducted for the design of main AC link parameters and its operation (i.e. before the realization of Phase II of the interconnection) by a working group of IPTO and HEDNO (Hellenic Electricity Distribution Network Operator, responsible also for the transmission systems of non-interconnected islands of Greece).

2. DESIGN CRITERIA

The most important aspects of the interconnection design can be summarized as follows:

- The power system of Crete is very small compared to the Hellenic Interconnected System, (which is part of the Continental Europe synchronous area).
- Environmental EU Directives impose important limitations on the operation of conventional power plants after 2020 and, thus, an imperative issue of security of supply emerges for the island of Crete.
- The interconnection is one of the most cost effective options for further exploitation of the important renewable energy potential of Crete. There is currently an important penetration of renewables in the power system of Crete (approx. 20% of annual electric energy supply).
- The high total length of the interconnection cable.

The main design criteria were:

- Economic optimization: The most cost-effective assurance of the security of supply of Crete was a main design objective.
- Power system reliability: Another important design objective was improving the reliability of the power system of Crete which is currently lower than the reliability of the Hellenic Interconnected System, due to its autonomous operation.
- Avoidance of complexity: Another objective of the project design was to avoid complex procedures real operation so that it will be fully exploited.
- Minimization of new transmission projects at Peloponnese and Crete.
- Operations automation and minimization of manual operations by the Control Center: It is foreseen to upgrade the Control Center of Crete in order to accommodate automated operations for the control of the interconnection. At the same time, the project was designed in a way to minimize the necessary manual operations for the interconnection control by the personnel of the Control Center of Crete.
- Equipment redundancy.

3. DESCRIPTION OF INTERCONNECTION SET-UP

The interconnection routing is depicted in Fig. 1. The interconnector between Crete and Peloponnese shall be implemented by using two 150 kV AC circuits; the thermal limit of each circuit is 200 MVA.

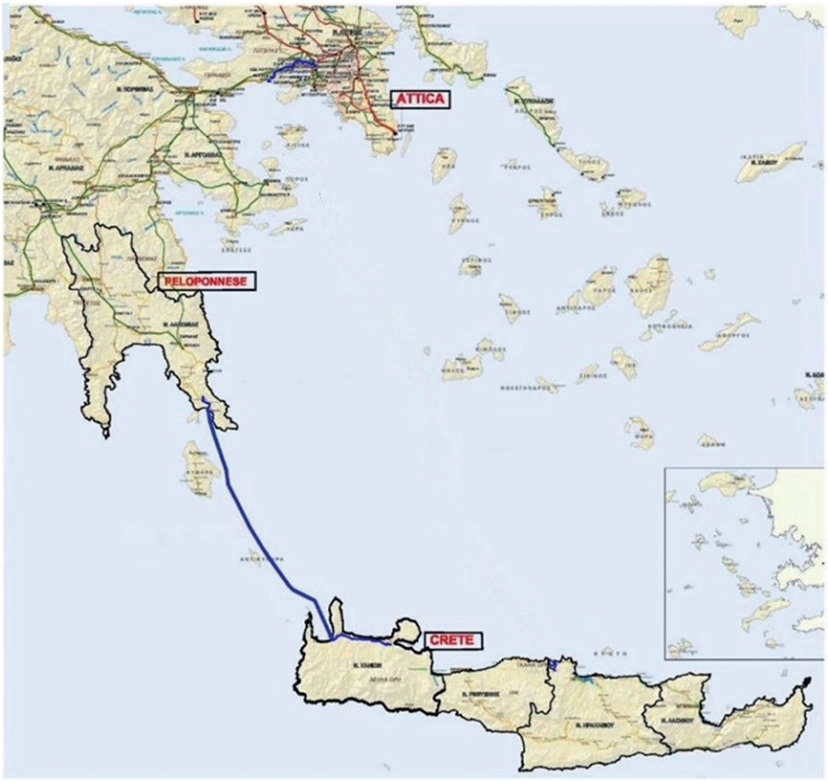

Figure 1. Interconnector routing

The lenth of each submarine cable is 132 kmconnecting the two landing points in SE Peloponnese and NW Crete. In addition, two underground double circuit cables connect:

- The new terminal station of SE Peloponnese to the sea shore (next to Neapoli) (10 km)
- The landing point in NW Crete (34 km) to the existing Chania I substation.

The total length of continuous underground and submarine cables will be thus 176 km, as the cable reactive power compensation will be installed at the Chania substation in Crete and at the terminal station in Peloponnese.

The new 150kV terminal station in SE Peloponnese will be constructed using GIS technology. It will be connected to the existing Molaoi 150kV substation at SE Peloponnese with an overhead double circuit line of 24 km (using ACSS conductors of the Grosbeak type with increased thermal rating) plus a 4 km double circuit cable part (at the Molaoi substation side).

4. STATIC SECURITY ANALYSIS

Static security analysis has been performed in order to investigate the following issues and relevant critical figures:

- Maximum power transfer capability of the cable interconnection and identification of the operational limitation of power transfer taking into account the cable loading limits under transient and steady-state conditions.
- Selection of appropriate compensation type and dimensioning.
- Investigation of necessity for installation of dynamic compensation (SVC/STATCOM), its dimensioning and placement.
- Identification of the must-run conventional units (if any) to operate in Crete independently of the load level for static security reasons.

Identification of these figures is a problem of high complexity. This is further aggravated due to the high level of variable RES installations, as it requires more detailed representation of the distributed generation (up to MV level) and multiple scenarios for various combinations of load and RES generation levels. For this reason, it was decided to separate the system into three sub-systems, which were initially examined separately: The Hellenic Interconnected

System, the links and the system of Crete. Possible limitations (e.g. operational constraints) and issues were identified for each subsystem and finally the proposed solutions were verified using an integrated complete model. More specifically the static security studies were conducted for the following subsystems:

- Hellenic interconnected system with interconnector
- Power system of Crete with interconnector
- Standalone interconnector to identify the permissible operation range.

The design of the interconnection is based on the typical power system security criteria, such as the N-1 criterion. In this respect, the complete loss of the interconnector (N-2 contingency) is considered only for the design and installation of a Special Protection Scheme, which will lead to partial load shedding to ensure normal operation of the power system. The examined contingencies are the following:

- Loss of a transmission element (N-1 in mainland, N-1 in Crete, loss of one cable system)
- Loss of a generator
- Loss of a compensation device (e.g. reactor)
- Open-end of the cable link due to the trip of circuit breaker either at the SE Peloponnese terminal substation or at the Chania substation (Crete).

Furthermore, prior to the static security analysis a preliminary analysis of the interconnected operation of the system was conducted. More specific a detailed day by day Unit Commitment and Economic Dispatch simulation for a period of one year and a time step of one hour was performed in order to investigate the impact of certain operational parameters to the variable cost of the power system. A number of cases was considered with regard to the operational parameters under study, as described below:

- Power Transfer Maximum Setpoint (4 cases):
  - 150 MW, 160 MW, 170 MW ,180 MW
- Local Units Spinning Reserve Required (3 cases):
  - 20 MW, 30 MW ,40 MW
- Must-Run Units (2 cases):
  - 2 Must-Run Units, 3 Must-Run Units

The combination of the above cases provides 24 scenarios each of which has been simulated in detail. The analysis of the simulation results indicates that there is no significant variation with regard to the annual operating cost among the scenarios. According to the simulation results in all cases-scenarios, spinning reserve provided by local units is maintained well above 40 MW and more than 3 generating units are in operation for the most part of the year, even if this is not required by the constraints.

The hourly results of the simulation of the system have been further processed in order to get a minute granularity, both under normal operation of the system and assuming the outage of the largest power unit. The residual load ramp and the generation trip disturbance is undertaken by the interconnection and local units according to their reserve levels and ramp –up and ramp-down technical limits. It will be required to minimize the number of minutes during which the interconnection exceeds its transfer capacity limit as it will be defined by the static analysis.

Taking the above considerations into account, it is recommended to operate the system under the following constraints:

- Power Transfer Maximum Setpoint $\leq$ 150 MW
- Spinning reserve by local units $\geq$ 30 MW
- Must-Run Units = 3

With regard to the must run units, it is recommended to use 2Atherinolakos power plant units due to their low cost and 1 unit at Linoperamata power plant.

4.1 Power System of Crete

The current transmission system of Crete is depicted in Fig. 2, together with some planned reinforcements. There are three thermal power plants at the west (Chania), center (Linoperamata) and east (Atherinolakkos) of the island.

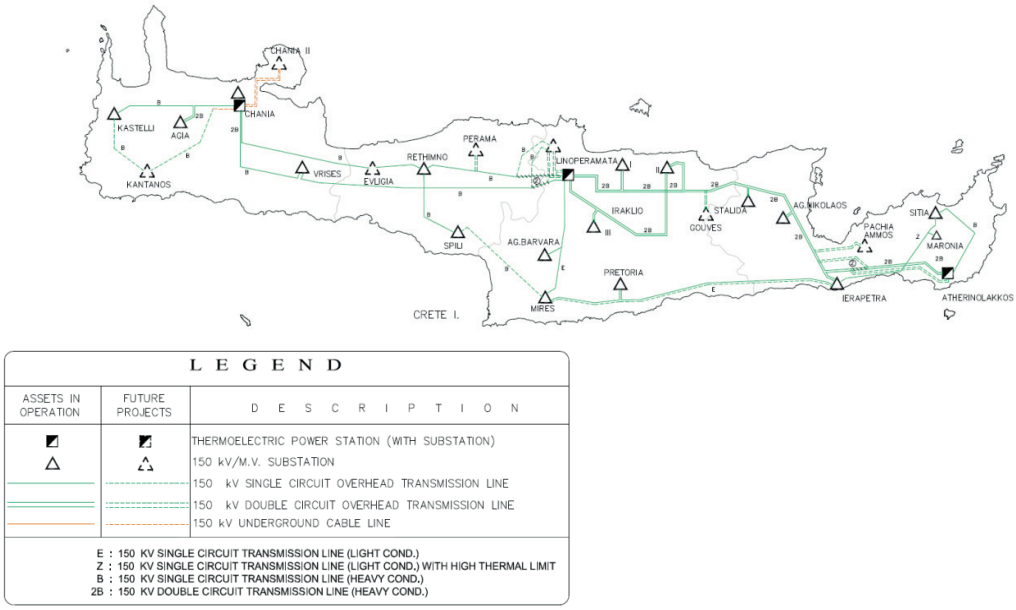

Figure 2. Transmission system of Crete

The main scenarios examined referred to year 2020, taking into account the planned evolutions in both the transmission and the generation system of Crete. The examined system model under investigation includes the power system of Crete (Fig. 3) together with the interconnection SE Peloponnese - Chania (Fig. 2). The Hellenic Interconnected System is modelled as a Thevenin equivalent at SE Peloponnese.

The snapshots analyzed correspond to 4 load levels (including minimum and maximum), 5 RES generation levels and 2 voltage levels at SE Peloponnese. Ten scenarios were finally selected to be analyzed in details representing extreme and intermediate operational conditions of the power system of Crete after the AC interconnection with Peloponnese. The main result of the analysis is that a serious lack of voltage control can emerge as the power import through the interconnector displaces local conventional generation with voltage control capabilities. Therefore, dynamic reactive compensation (SVC or STATCOM) needs to be installed.

4.2 Interconnector range of operation

In order to calculate the maximum power transfer through the AC interconnector, a model of its cable systems based on two-port networks has been used to identify the interconnector permissible range of operation. The analysis is based also on studies for similar interconnections [5-8], as well as the methodology proposed in [9] by the CIGRE Working Group on technical performance issues related to the application of long HVAC cables.

In specific, the interconnector was modeled by a series of two-port networks according to Fig. 3.

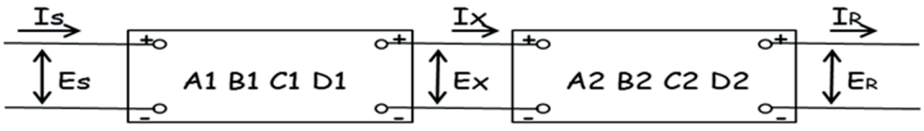

Figure 3. Series connection of two two-port generic networks

Each two-port network represents an equipment element of the interconnector, i.e. the overhead line, the compensation reactors at each side of the cable part, the underground and submarine cables modeled in multiple parts. For the modeling of the lines and cables, the distributed parameters model was used. Therefore, the following holds for each two-port network representing a line or cable part:

$$\begin{bmatrix} \widetilde{E}_s \\ \widetilde{I}_s \end{bmatrix} = \begin{bmatrix} \cosh \gamma l & Z_C \sinh \gamma l \\ \dfrac{\sinh \gamma l}{Z_C} & \cosh \gamma l \end{bmatrix} \cdot \begin{bmatrix} \widetilde{E}_R \\ \widetilde{I}_R \end{bmatrix}$$

where

$$\gamma = \sqrt{zy} = \sqrt{(R + j\omega L) \cdot (G + j\omega C)}$$

A simplified one-line diagram of the interconnector model developed is shown in Fig. 4.

Figure 4. Interconnector model

This is a multi-parameter model depending on the following:

- Reactive power compensation at each side (QS, QR)
- Cable ampacity (Imax)
- Voltage operation range at Chania substation (Vmax, Vmin)
- Maximum voltage along the Interconnector (Vmax)
- Short-circuit level at Molaoi substation at SE Peloponnese
- Thevenin equivalent voltage (Es)
- Angle difference

Introducing the necessary parameters, the calculation of the operational ranges can be demonstrated in P-Q diagrams as shown in Fig. 5, where P and Q are the active and reactive power received at Crete (Chania substation). In Fig. 6 the following limits are depicted:

- Maximum current at sending point ("Imax MOLAOI")
- Maximum current at receiving end ("Imax XANIA")
- Maximum voltage at 150kV bus of Chania substation ("Vmax XANIA")
- Minimum voltage at 150kV bus of Chania substation ("Vmin XANIA ")
- Maximum voltage along the Interconnector ("Vmax CABLE")
- Maximum angle difference ("Angle LINK"). An indicative limit of 25 degrees is assumed whilerotor angle stability was examined by means of a dynamic security study.

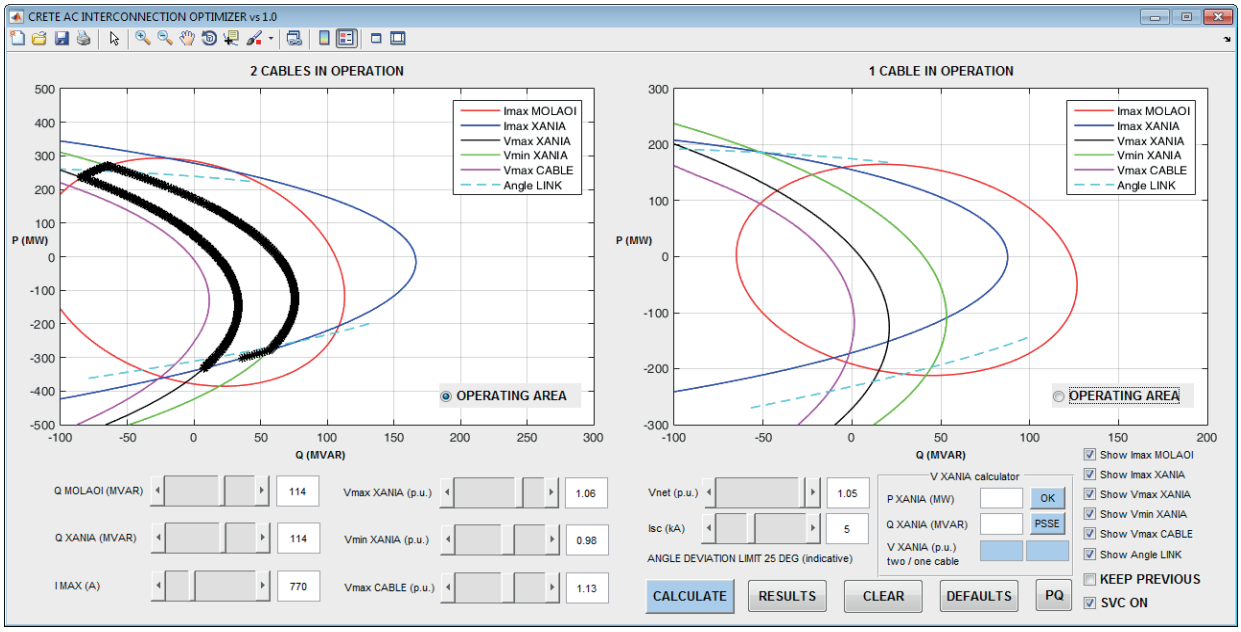

Figure 5. Calculation of AC Interconnector operational range

The area defined by all the above mentioned limits is the root locus of the permissible operational range. Next, the P-Q pairs that correspond to the power flows of the examined operation points of the power system of Crete were drawn on the P-Q plane. The capability of the static and dynamic reactive compensation is selected so that the points fall into the permissible root locus as shown in Fig. 6.

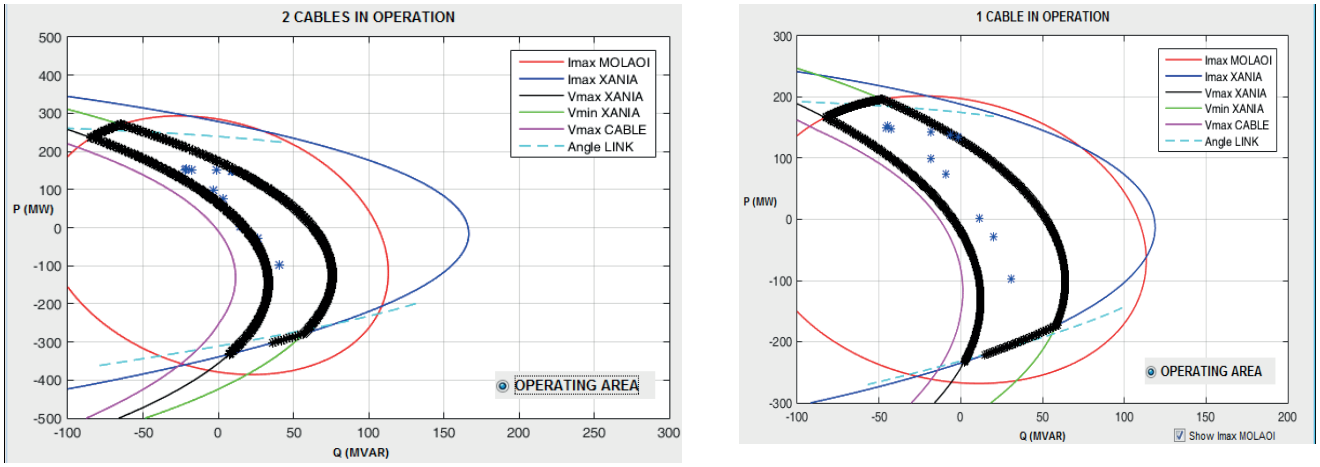

Figure 6. Operating loci of AC link with P,Q points representing Crete system load conditions

4.3 Static security analysis conclusions

According to the analysis the main limiting factors regarding maximum transfer capacity comes from:

- Thermal limits of underground and submarine cables.
- Voltage operational limits in High Voltage level (150 kV) in Crete power system
- Angular differences between the conventional generating units in mainland and Crete power system, which operate under synchronizing conditions.

Based on the above the main conclusions from the static security analysis of the Interconnector are the following:

- Each circuit of the cable interconnection will be compensated by 96% with installation of 6 independent reactor units (non-variable), 38 MVAr each, per circuit, equally distributed at the two Interconnector ends.
- The necessary capability of the dynamic reactive compensation (SVC or STATCOM) is ±60 MVAr with optimal placement at Linoperamata substation or closeby.
- The maximum power transfer due to static security limitations is 180 MW (after the Interconnector losses) with main limitation factor the voltage levels at the power system of Crete and the angle difference.
- It is possible to transfer at least 100 MW from Crete to the Hellenic Interconnected System.

5. DYNAMIC SECURITY ANALYSIS

Based on the results of the static security analysis, a dynamic security analysis was performed focusing on maximum load conditions with and without high RES generation. In both cases, high import of power from the Interconnector to Crete (150 or 180 MW) is assumed. A complete dynamic model of the Hellenic Interconnected System and Crete is used, including the EHV systems of SE Europe (Balkan Peninsula). The rest of the Continental Europe synchronous zone is represented with a Thevenin equivalent. In both scenarios high power import to the Hellenic System is assumed as shown in Fig. 7.

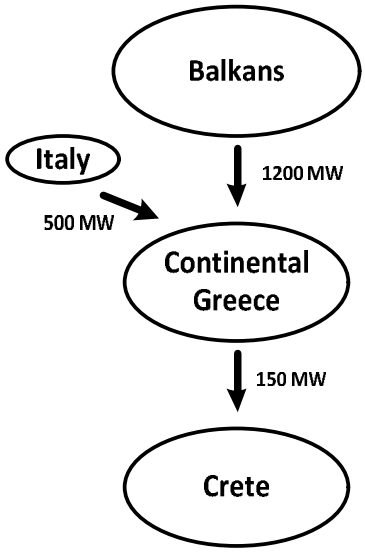

Figure 7. Power imports to Greece and transfer to Crete

5.1 Small-signal stability

The small-signal stability study (modal analysis) identified the emergence of a new intra-area electromechanical oscillation mode of relatively low frequency and damping between the synchronous generators of Crete and the Hellenic Interconnected System (Peloponnese mainly). The frequency of the new mode was calculated 0.8 Hz approximately under maximum load conditions and its damping at least 5%, which can be considered satisfactory. The synchronous generators of Crete also participate in two already existing intra-area modes (with frequency of 0.7 - 0.8 Hz), which results to a very small reduction of their frequency and damping. Their participation to the inter-area oscillation modes of the Hellenic System is negligible. Results of the modal analysis are summarized in Table I for the case without RES contribution, with and without the interconnection of Crete.

Table I. Main electromechanical oscillation modes under maximum load conditions (no RES) with and without AC interconnection of Crete

	With Interconnection				Without Interconnection			
Mode	**Real**	**Imag.**	**Damping (%)**	**Freq. (Hz)**	**Real**	**Imag.**	**Damping (%)**	**Freq. (Hz)**
Intra-area "Crete"	-0.263	5.020	5.2	0.799				
Intra-area "Central GR"	-0.251	4.874	5.2	0.776	-0.286	4.931	5.8	0.785
Intra-area "South GR"	-0.137	4.501	3.1	0.716	-0.168	4.559	3.7	0.725
Interarea "GR"	-0.106	3.508	3.0	0.558	-0.092	3.650	2.5	0.581
Interarea "SE Europe"	-0.260	1.706	15.1	0.272	-0.249	1.741	14.2	0.277

It is also concluded that:

- After the AC interconnection of Crete, the operation of the power system stabilizers installed at large synchronous generators becomes even more important, in particular at the Megalopoli power plant in Peloponnese. It is noteworthy that increasing the oscillations damping reduces the possibility of resonance,

taking into account that the frequency of the new intra-area oscillation mode is at the same frequency range (0.7 - 0.8 Hz) with already existing intra-area modes, which involve some generators in common.

- Activation of the power system stabilizers of the synchronous generators at Atherinolakkos power plant of Crete is expected to provide important damping to the new intra-area oscillation mode, as well as to the other two intra-area models.

The case with the lowest damping was without RES generation and assuming no stabilizers are active, remaining however above the 5% limit. Just the activation of the stabilizers of the largest generator in Megalopoli power plant increases the damping significantly. In the case with RES contribution, the frequency of the Crete intra-area mode is increased as fewer synchronous generators are in operation in Crete. The damping is also increased.

5.2 Dynamic security assessment

The dynamic security assessment consists of time-domain simulations of critical disturbances for the two examined scenarios assuming initial import of 180 MW to Crete from the Interconnector. Solid three-phase faults are simulated regarding clearing after 100 ms. The main conclusions of this study can be summarized as follows:

- In case of a three-phase fault at one Interconnector circuit, close to Chania substation, which is cleared by opening the circuit with a time delay of the order of 100 ms, it is possible that an important part of wind power is lost, because some old wind power plants in Crete are not equipped with Low Voltage Ride-Through (LVRT) capability. This would result to an import of possibly more than 220 MW via the remaining Interconnector circuit, and, thus, unacceptably low voltages in Crete.
- Similarly, in case of loss of a large conventional generator (e.g. at Atherinolakkos station) after a severe fault, it is possible that an additional loss of important amounts of wind power generation also occurs. This could result to a very high import of power from the Interconnector (e.g. 300 MW) and, thus, to marginally secure or even insecure voltage levels.

As a conclusion, a Special Protection Scheme should be adequately designed in order to operate in case events such as the above mentioned actually emerge, e.g. by monitoring voltage at Chania, current and power through the Interconnector, etc. In addition, the load shedding should (be able to) take place in various substations (e.g. Chania, Iraklio). As a proof-of-concept example, Fig. 8 shows the voltage at Chania HV bus in case after a solid three-phase fault which is cleared by opening of one Interconnector circuit in two cases:

- Without SPS: The active power transfer through the remaining circuit is close to 250 MW. The voltage at Chania does not recover above 90% which is the emergency low voltage limit.
- With SPS: It is assumed that load shedding takes place at Chania. The active power transfer through the remaining Interconnector circuit is limited to approximately 225 MW and the voltage recovers above 90%. In order to limit the power transfer to 180 MW, loads from other substations need to be shed as well.

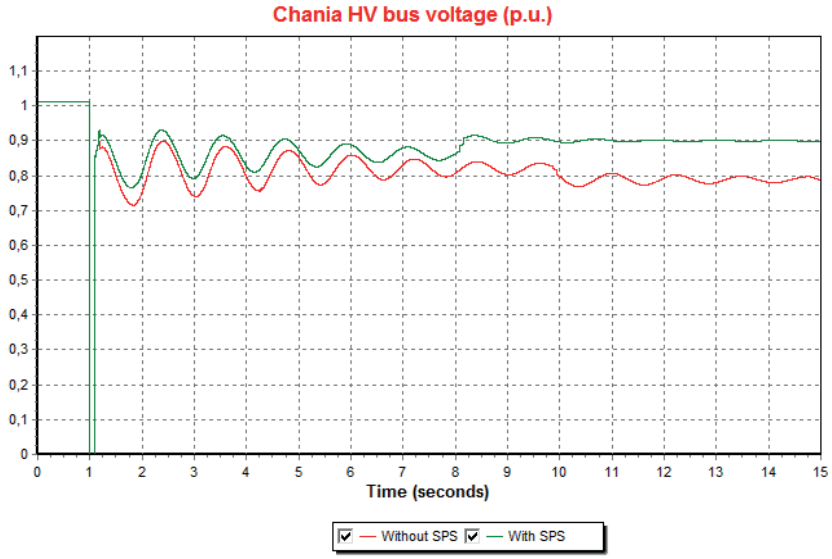

Figure 8. Voltage at Chania HV bus and active power to Chania with and without Special Protection Scheme

5.3 Transient stability

The dynamic security analysis did not detect any loss of synchronism issues. In order to assess a security margin with

respect to transient stability (large-disturbance rotor-angle stability), the critical clearing time of solid three-phase fault at the transmission system of Crete was calculated for a worst-case scenario with high load conditions, all synchronous generators of Crete in operation at maximum output and an export of approximately 150 MW from Crete through the Interconnector. As the lowest critical clearing time found was 200 ms, it can be concluded that there is an adequate margin with respect to transient stability, taking into account that adverse assumptions were used (e.g. solid three-phase fault) and typical fault clearing times are close to 100 ms. An example of a fault at Chania, cleared with opening of one Interconnector circuit, is shown in Fig. 9 for the marginally stable and marginally unstable cases. It can be seen that in the unstable case all generators of Crete lose synchronism with respect to the generator in Megalopoli (Peloponnese).

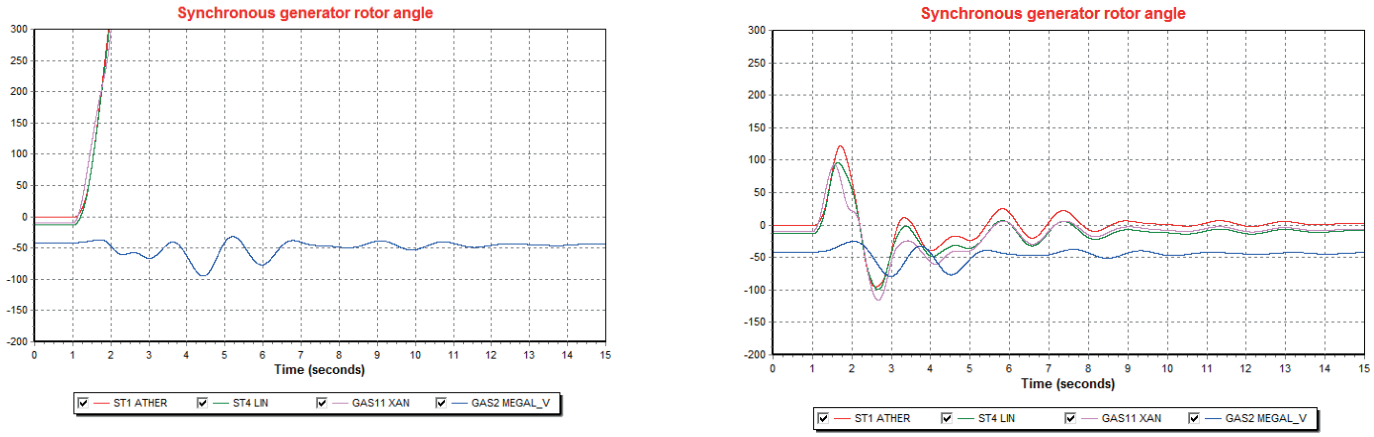

Figure 9. Synchronous generator rotor angles in marginally unstable and stable cases

6. CONCLUSIONS

According to the Ten Year Network Development Plan (TYNDP) of the Independent Power Transmission Operator (IPTO) of Greece, the interconnection of Crete to the mainland Transmission System of Greece will be realized in two phases: A 150 kV HVAC link between the SE Peloponnese and the NW Crete (Phase I) and a HVDC link connecting the metropolitan area of Athens with Crete (Phase II).

The AC Interconnector of Crete is a project with certain characteristics that place it in the international forefront of cable interconnections, such as the high length of the continuous cable part which reaches approximately 174 km. In this paper power system security studies conducted for the design of AC link parameters and its operation (i.e. before the realization of Phase II of the interconnection) were presented.

The main conclusions of the static security analysis can be summarized as follows:

- In order to achieve adequate voltage control at the power system of Crete after the AC interconnection, it is necessary to install a dynamic reactive compensation device such as an SVC or STATCOM close to the electrical center of Crete.
- Each Interconnector cable circuit will be compensated at approximately 96% by installation of 6 independent reactors (non-controllable), equally distributed at both ends of the Interconnector.
- The maximum power transfer through the Interconnector, as defined by static security limitations is 180 MW. Main limiting factors are the voltages of Crete power system and the angle difference. Possible transient overloading of the cables does not constitute a limiting factor for static security.

From the dynamic security analysis, the following conclusions were drawn:

- The AC interconnection of Crete practically eliminates the frequency stability issues currently faced due to its autonomous operation.
- The 180 MW maximum power transfer limit is not decreased due to dynamic security constraints. However, the installation of a Special Protection Scheme is deemed necessary, not only for the extreme case of total loss of the Interconnector (N-2 contingency), but also for ensuring that the power transfer through the Interconnector is not excessively increased in case of critical disturbances so that the system security is not jeopardised
- The small-signal stability analysis identified changes in the inter-area and intra-area electromechanical oscillation modes in the mainland system after the interconnection of Crete with the AC link.
- With respect to the risk of loss of synchronism right after a significant disturbance in the system of Crete, such as a three-phase fault (“transient stability”), an adequate safety margin is estimated by means of Critical Clearing Time calculations.

REFERENCES

[1] L. Colla, L.V. Lombardo, N. Kuljaka, E. Zaccone"Submarine projects in the Mediterranean Sea. Technology developments and future challenges"(First South East European Regional CIGRE Conference, Portoroz 2016)

[2] D. Elliott, K. R. W. Bell, S. J. Finney, R. Adapa, C. Brozio, J. Yu, K. Hussain "A Comparison of AC and HVDC Options for the Connection of Offshore Wind Generation in Great Britain" (IEEE Trans. on Power Delivery, Vol. 31, No. 2, Apr 2016)

[3] T. K. Vrana, O. Mo "Optimal Operation Voltage for Maximal Power Transfer Capability on Very Long HVAC Cables" (13th Deep Sea Offshore Wind R&D Conference, EERA DeepWind'2016, Trondheim, January 2016)

[4] T. Skaanoey, U. Kerin, N. Van Luijk, E. Thibaut "AC Subsea Power Transmission Architectures, Design And Challenges, The Martin Linge Case." (Offshore Technology Conference, May 1 2017)

[5] S. Lauria, F. Palone "Optimal Operation of Long Inhomogeneous AC Cable Lines: The Malta-Sicily Interconnector" (IEEE Transactions on Power Delivery, Vol. 29, No. 3, June 2014)

[6] F. M. Gatta, A. Geri, S. Lauria, M. Maccioni "Steady-state operating conditions of very long EHV AC cable lines" (Electric Power System Research, vol. 81, n.7, pp. 1525-1533, July 2011)

[7] S. Lauria, F. M. Gatta, and L. Colla "Shunt compensation of EHV Cables and Mixed Overhead-Cable Lines" (Proc. 2007 IEEE Lausanne Power Tech Conf., paper n. 562, Lausanne, July 2007)

[8] S. Lauria, F. Palone "Operating envelopes of the Malta-Sicily 245 kV – 50 Hz cable" (2nd IEEE ENERGYCON Conference & Exhibition, 2012)

[9] Working Group C4.502 CIGRE. "Power System Technical Performance Issues Related to the Application of Long HVAC Cables" (Tech. Brochure 556, October 2013)

[10] J. Kabouris, K. Tsirekis, A. Georgopoulos, I. Aravanis, "The Interconnection of the Cycladic Islands: A Major Innovative Transmission Project for the Greek EPS, 1st CEERC, Portoroz, Slovenia, 2016.

Journal of Energy

VOLUME 67 Number 2 | 2018 Special Issue

journal homepage: http://journalofenergy.com/

Lightning caused overvoltages on power transformers recorded by on-line transient overvoltage monitoring system

[a]Samir Keitoue, [a]Ivan Murat, *[b]Božidar Filipović-Grčić, [c]Alan Župan,
[b]Ivana Damjanović, [b]Ivica Pavić
[a]Končar - Electrical Engineering Institute Inc., Zagreb, Croatia
[b]University of Zagreb, Faculty of Electrical Engineering and Computing, Croatia
[c]Croatian Transmission System Operator Ltd., Kupska 4, 10000 Zagreb, Croatia

SUMMARY

Transient overvoltages generated by lightning strikes or switching operations represent a significant risk to bushings and windings of power transformers. They cause stress on the insulation system and can, over time, cause dielectric failure and damage to power transformers. Many transformer failures are reported as dielectric failures and they are not necessarily linked to any particular event when they occur but may be the result of prior damage from transient overvoltage events. Lightning and switching overvoltage waveforms appearing at transformer terminals in real operating conditions may significantly differ from standard impulse voltage waveforms used during laboratory testing. The number and amplitudes of overvoltages which stress the insulation depend on various parameters such as the lightning strike density in the considered area, since it determines how often the transformer is stressed by lightning overvoltages. Since the overvoltage amplitudes at transformer terminals are usually unknown, an on-line overvoltage transient recorder can be used with the ability to sample, analyse and store transients in real-time.

In this paper, an on-line transient overvoltage monitoring system (TOMS) for power transformers is presented that is capable to continuously record in real-time various kinds of transient overvoltages such as lightning or switching overvoltages. Special attention is paid to lightning caused transient overvoltages recorded at the terminals of 150 MVA power transformer. Recorded waveforms originating from lightning strikes to overhead lines are correlated with data from the lightning location system (LLS) and supervisory control and data acquisition (SCADA) system. Collected data about overvoltage stresses can be used as the basis for the assessment of the transformer insulation condition, estimation of health index and for analysis of various kinds of events such as faults or equipment failures.

KEYWORDS

On-line transient overvoltage monitoring system, power transformers, lightning overvoltages, lightning location system.

1. INTRODUCTION

Power transformers are one of the key and most valuable components in a power system. Equipping them with an on-line monitoring system is essential for information gathering, condition assessment, better management and decision making. The worldwide transformer reliability survey conducted by CIGRE WG A2.37 and published in [1], collected and analysed 964 major failures which occurred in the period 1996 to 2010, within a total population of 167,459 transformer-years, contributed by 58 utilities from 21 countries. The results point out the main causes of transformer failures, including the reasons with most severe results such as fire or explosion. Fig. 1 shows the failure location analysis according to transformer application in units with voltages 100 kV and above, respectively. The number of failures classified as 'unknown' location was 17%, and these 'unknown' cases were not considered in the analysis. The failure mode analysis [2] according to application is shown in Fig.1. Windings, tap changer and bushing related failures were the major contributors followed by lead exit insulation related failures irrespective of application or manufacturing period. The failure mode analysis [2] according to application is shown in Fig. 2. Dielectric mode failures were the most prominent, followed by mechanical and electrical type failures, for substation transformers, whereas generator step-up transformers had higher contributions of thermal and dielectric mode failures.

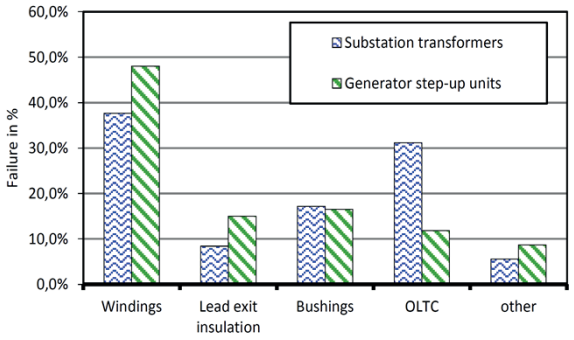

Figure 1. Failure location of substation transformers (536 failures) and generator step-up units (127 failures)

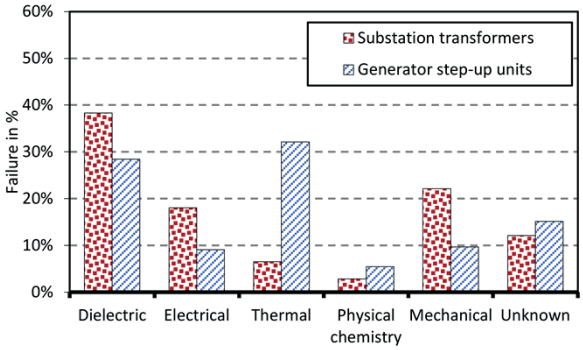

Figure 2. Failure mode analysis of substation transformers (799 failures) and generator step-up units (165 failures)

As can be seen from the survey results, dielectric mode failures were the most prominent, followed by mechanical and electrical type failures, for substation transformers, whereas generator step-up transformers had higher contributions of thermal and dielectric mode failures. Analysis showed that HV bushings significantly contribute to large failures, which means that operators should place large focus on bushing monitoring. Thus, the need for bushing diagnostic and monitoring system has risen.

At present, the performances of oil paper insulation systems of power transformers under switching and lightning overvoltages can be evaluated by testing in HV laboratory with standard lightning and switching impulse voltage waveforms, in accordance with the IEC standard [3]. In actual conditions, however, the waveforms of transient overvoltages that appear on the terminals of power transformer can be extremely complex due to the numerous factors such as the location of surge arresters, the topology of the network, etc. [4-6]. Front and tail time of such overvoltages may be shorter or longer than the standard one defined by IEC standard, and the wave shapes may be very different from the unidirectional double exponentials used in laboratory conditions and may even be bidirectional [7]. Results presented in [8] indicate that transformer winding's response to certain oscillatory voltages can be worse than that under any form of aperiodic voltages, whether lightning impulse, chopped lightning impulse or steep front - long tailed switching surge. It was shown that terminal excitation at

Samir Keitoue, Ivan Murat, Božidar Filipović-Grčić, Alan Župan, Ivana Damjanović, Ivica Pavić, Lightning caused overvoltages on power transformers recorded by on-line transient overvoltage monitoring system, Journal of Energy, vol. 67 Number 2 (2018), Special Issue, p. 44–53

frequencies coinciding with any one of the winding's natural frequencies may lead to large voltage amplification inside a transformer and can cause severe stresses on insulation. For the above described reason, there is a need to study the characteristics of the transient overvoltages in the field. Transient overvoltages where suspect to be the reason for a number of insulation breakdowns in the last decades, so their monitoring with true waveform recording is of high importance. Actual measurements can also be used to study the interaction between the power transformer and the grid.

In this paper, an on-line TOMS for power transformers and shunt reactors is presented. Overvoltages are measured on the outside measurement terminal of bushing. The focus of the paper is on the analysis of transient overvoltages caused by lightning strikes recorded at the terminals of power transformer with rated power 150 MVA and rated voltages 220/110 kV located near thermal power plant. To determine the cause of the recorded transient overvoltages, data from TOMS are correlated with data from the LLS and from the SCADA system. Collected data about number, peak and duration of recorded transient overvoltages can be used as the basis for the assessment of the transformer insulation condition and estimation of health index. Data recorded by TOMS are also of significant importance since the insulation system of power transformer and other equipment in the substation can be damaged by lightning of switching overvoltages.

2. ON-LINE TRANSIENT OVERVOLTAGE MONITORING SYSTEM

Overvoltages in power network can be caused by lightning strikes to overhead transmission lines, circuit breaker switching operations and faults. Power transformers can be exposed to such transient overvoltages during the operation. Transient overvoltages with steep wave front have an impact on dielectric stresses of the insulation of first few winding turns. The number and amplitudes of overvoltages which stress the insulation depend on various parameters such as the lightning strike density in the considered area, since it determines how often the transformer is stressed by lightning overvoltages. Since the overvoltage amplitudes at transformer terminals are usually unknown, an on-line overvoltage transient recorder is used with the ability to sample, analyze and store transients in real-time. Collected data can be used as the basis for the assessment of the transformer insulation condition, especially if combined with other transformer data such as dissolved gas analysis (DGA). This fact was the driving force for upgrading the existing (TMS) transformer monitoring system [9], [10] with TOMS. Overvoltages, as well as voltages, are measured on a measuring tap of corresponding bushing. The connection with the measuring tap shown in Fig. 3 (a) is accomplished with a specially designed adaptor while the link between the adaptor and impedance matching circuit is carried out with a coaxial cable. TOMS installed on a 150 MVA power transformer is shown in Fig. 3 (b) [11], [12].

Measurement of transients needs to be triggered by an external signal. Since only one of the eight input channels of the overvoltage acquisition module can be used as a trigger, the trigger can be set only for one phase at a time. It is necessary to provide an additional signal that is used as a trigger for data acquisition. This signal shall trigger data acquisition if overvoltage occurs in any of the phases. While overvoltages are acquired occasionally, voltages need to be measured continuously in order to detect changes of bushing capacitance. To accomplish this, continuous voltage measurement is performed with an additional analogue input module. The measuring range of the overvoltage acquisition module is ±15 V. In order to extend the overvoltage detection range to approx. $5 \cdot \hat{U}_{\mathrm{fn}}$ (where $\hat{U}_{\mathrm{fn}}$ equals to the peak value of the nominal phase voltage), it is necessary to dimension the capacitors of the matching circuit in a way that for the nominal voltage, the amplitude of the signal entering overvoltage acquisition module equals approximately 3 V. At the same time, the module used to continuously sample voltage signal has a measuring range of ±60 V. In order to optimally utilize

both measuring ranges i.e. vertical resolution of both acquisition modules, signal conditioning was done in two stages as shown in Fig. 4.

(a) (b)

Figure 3. (a) Connection to measurement terminal of bushing; (b) Transient overvoltage monitoring system (Končar TMS+) installed on power transformer

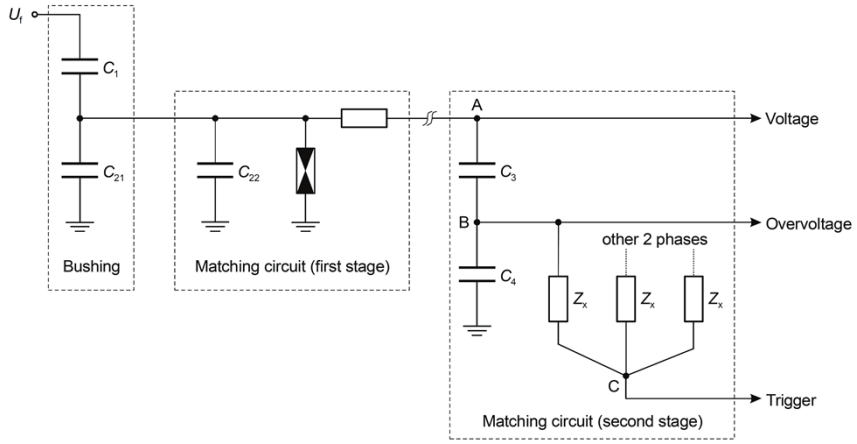

Figure 4. Scheme of matching circuit

Besides signal conditioning, the second stage of matching circuit also implements solution for the triggering of overvoltage acquisition. The following was considered during design:

- Capacitance of C_3 and C_4 needs to be selected to ensure that the potential of the node B is approximately 3 V when nominal voltage value $\hat{U}_{\text{fn}}$ is applied.
- Capacitance of C_3 and C_4 must not influence significantly on the potential of the node A, i.e. total capacitance of C_3 and C_4 connected into series must be negligible in comparison to the capacitance of C_2 ($C_2 = C_{21} + C_{22}$). The input impedance of the voltage measuring module is 1 MΩ and it does not change the potential of the node A much.
- Impedance of the condenser C_4 must be negligible at the lowest frequency (in this case system frequency of 50 Hz) to the input impedance of overvoltage module which is 1 MΩ.

The potential of the node C is used to trigger data acquisition when overvoltages occur. It is equal to 0 V as long as all the impedances Z_X are equal and the system voltage of all three phases balanced. In case of unbalance of three-phase system voltages, like it is the case when overvoltages occur, the potential of node C will not be equal to 0 V. In this way data acquisition

will also be triggered in case of a voltage disturbance in electrical grid (transients) which not necessarily have the amplitude higher than the nominal voltage. After completion of the design of the Končar TMS+ prototype and successful testing in the high voltage laboratory of Končar Electrical Engineering Institute, a project was started to install the system on in-service power transformers. TOMS is installed in the substation which is managed by the Croatian transmission system operator. Voltages are measured at 220 kV and 110 kV side of 150 MVA autotransformer AT1 with a vector group (Yna0d5). The brief layout of the 110/220 kV substation which is connected to thermal power plant is shown in Fig. 5.

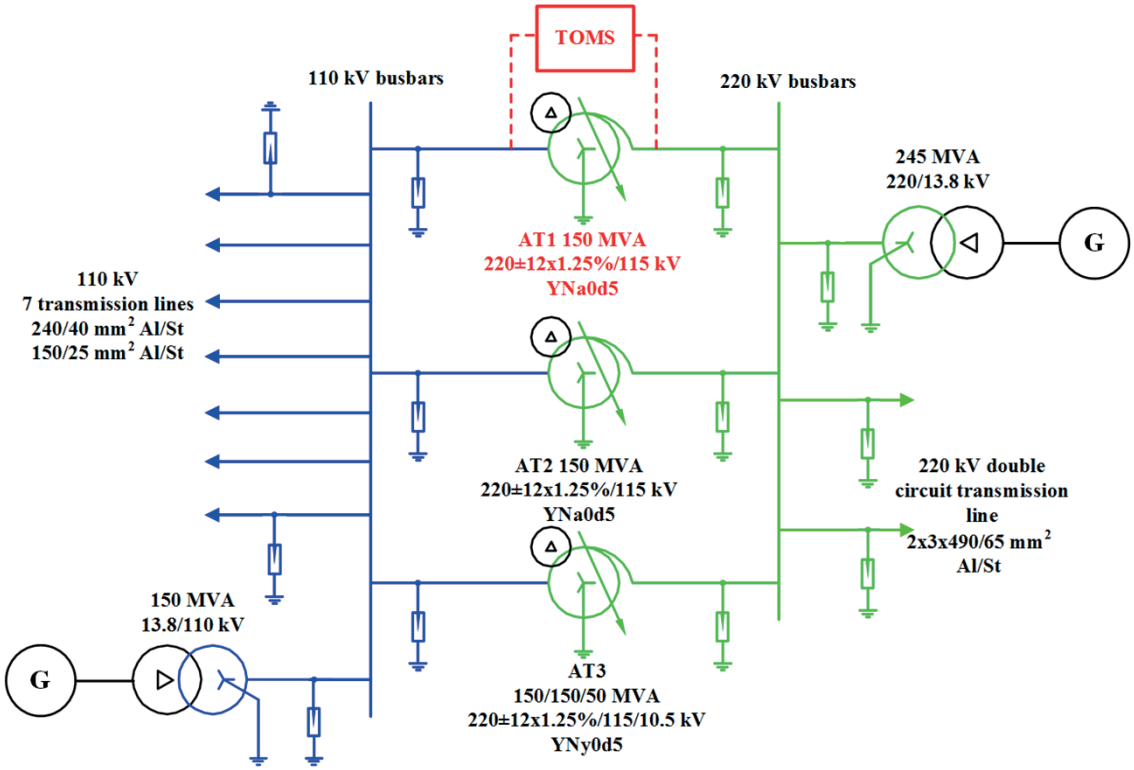

Figure 5. Layout of 110/220 kV substation connected to thermal power plant

This substation consists of three 150 MVA autotransformers, 7 transmission lines connected to 110 kV busbars and 1 double-circuit transmission line connected to 220 kV busbars. Generators located in thermal power plant are connected to 110 kV busbars via 150 MVA power transformer and to 220 kV busbars via 245 MVA power transformer. Surge arresters are installed in all transformer and transmission line bays (surge arresters with rated voltage U_r=198 kV are installed at 220 kV level and with U_r=108 kV at 110 kV level). All transmission lines are equipped with a single shield wire. Substation and connected transmission lines are situated in the area with relatively high lightning activity. Transmission lines are crossing over the rocky terrain with relatively high soil resistivity, some of them passing through mountainous area with relatively high tower grounding resistance. Therefore, flashovers on transmission lines often occur due to lightning strikes, leading to short circuit and automatic reclosing of circuit breakers located in transmission line bays.

3. LIGHTNING LOCATION SYSTEM

At the end of 2008, a LLS was established as part of the LINET network, covering a wide area of the Croatian territory. LINET is a modern LLS with a network of more than 125 sensors covering most of Europe. LLS measures the VLF/LF frequency spectrum of electromagnetic waves which lightning strikes emit. The measurement of magnetic flux is carried out through

highly sensitive sensors which are arranged across the area with spacing of around 150 to 250 km. Since the electromagnetic emission of the lightning spreads at the speed of light, it reaches the sensors at different points in time. Although the difference is in the order of micro-seconds, the exact calculation of the original emission location of the lightning strike is possible. The data measured by every single sensor is transmitted to a central server. The exact geographical position for all the lightning strikes measured is calculated and stored in a database. This measurement method is also known as the "time-of-arrival" method. Application of LLS in power system control of Croatian transmission system operator enables lightning activity tracking and time-spatial correlation with incidences (faults, automatic re-closures, outages) registered by the relay protection system [12].

4. TRANSIENT OVERVOLTAGES RECORDED ON 150 MVA POWER TRANSFORMER

Several cases of recorded transient overvoltages are analysed in more detail to determine the possible cause of each event.

4.1. Case 1 - lightning strike to 220 kV transmission line causing insulator flashover in one phase

Transients recorded by TOMS are shown in Fig 6. The recorded transients were time-correlated with a lightning strike which was detected by LLS. Lightning strike with current amplitude -184 kA occurred on the 220 kV transmission line route, at a distance of 62.4 km from the substation. At the same time, SCADA system detected single phase to ground fault in phase B at the 220 kV transmission line, following the single-pole auto-reclosure of circuit breaker in the line bay. Therefore, recorded transient overvoltages were most probably caused by lightning strike to transmission line which caused single phase to ground fault.

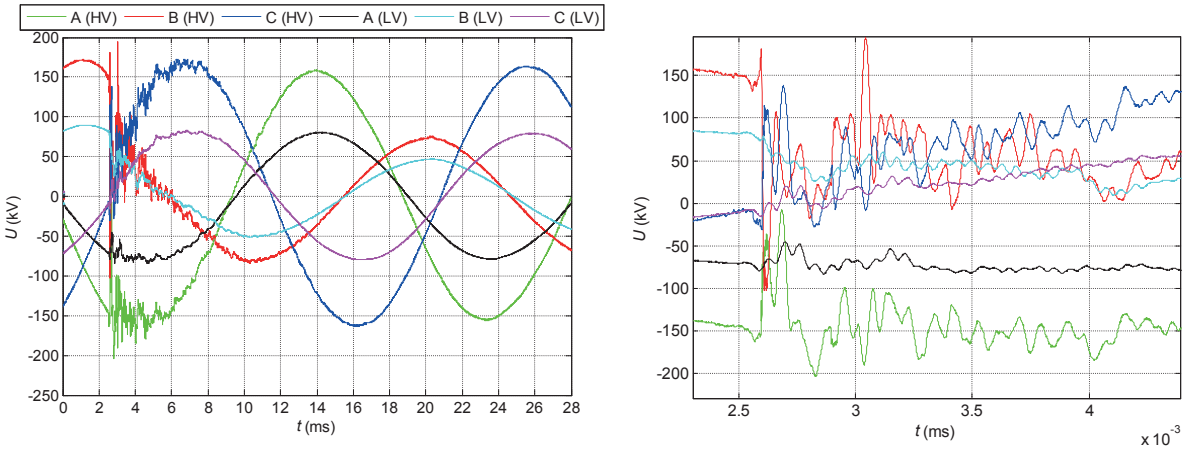

a) b)

Figure 6. (a) Transients recorded by TOMS in case of lightning strike to 220 kV transmission line (b) zoomed part of transients after flashover in phase B (HV)

4.2. Case 2 - lightning strike to 110 kV transmission line causing insulator flashover in one phase

Another event that was recorded by TOMS is shown in Fig 7. Second event (Fig. 7 b) occurred 113 ms after the first event (Fig. 7 a), and third event (Fig. 7 c) occurred 174 ms after the second event. Recorded transients were time-correlated with a lightning flash consisting of five subsequent lightning strikes which were detected by LLS. Parameters of multiple lightning strikes are given in Table I. Three lightning strikes marked in Table I were selected as the ones that probably caused recorded transients.

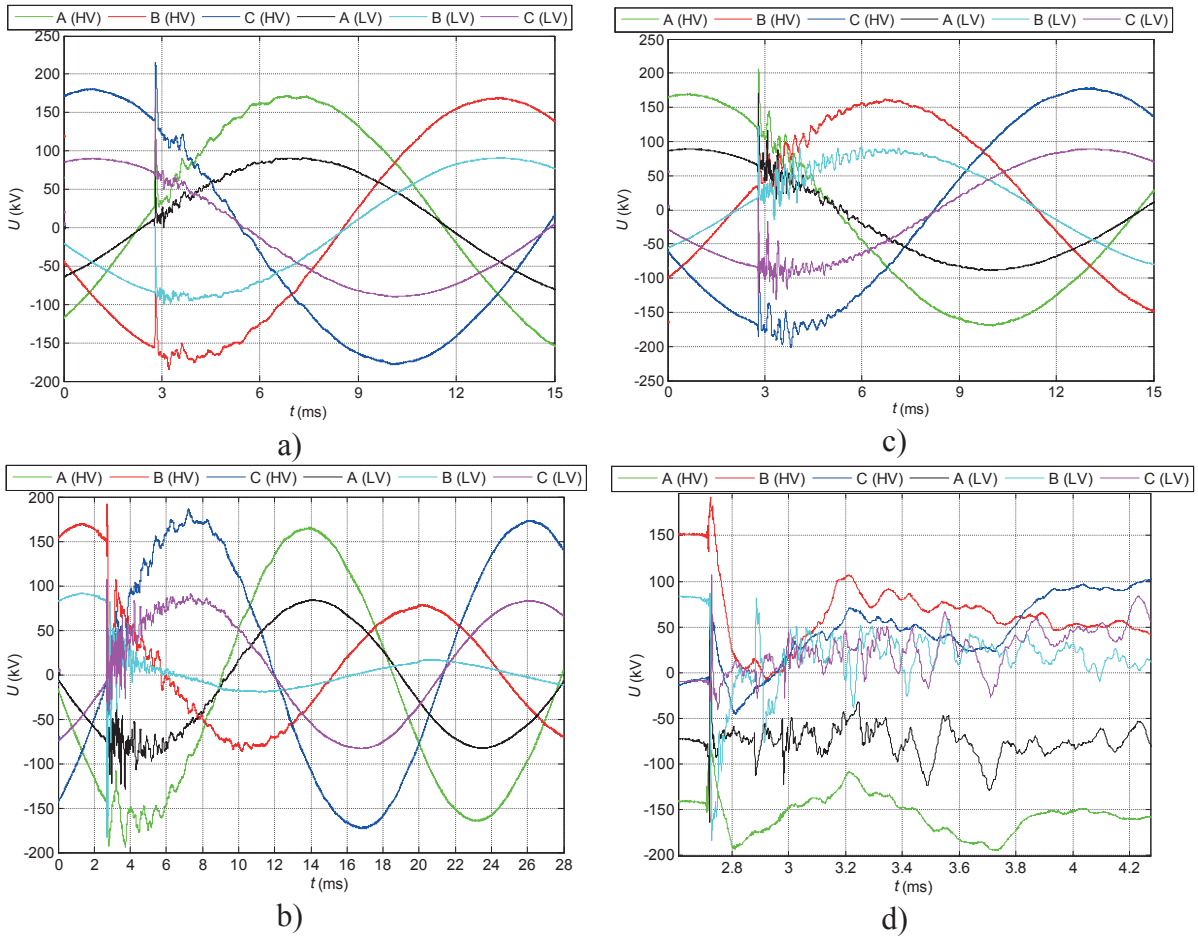

Figure 7. Transients recorded by TOMS in case of multiple lightning strikes to 110 kV transmission lines: (a) first recorded lightning overvoltage; (b) second recorded event which caused flashover in phase B (LV); (c) third recorded lightning overvoltage; (d) zoomed part of transients shown in (b) after flashover in phase B (LV)

Table I. Parameters of multiple lightning strikes detected by LLS

Lightning strike number	Time h:min:sec.milisec	Lightning current amplitude	Time difference between subsequent lightning strikes Δt
1	**22:05:21.701**	**-12.9 kA**	**-**
2	**22:05:21.814**	**-30.8 kA**	**113 ms**
3	22:05:21.886	-23.8 kA	72 ms
4	**22:05:21.988**	**-39.5 kA**	**102 ms**
5	22:05:22.098	-21.9 kA	110 ms

This was done by matching the time difference between the successive lightning strikes detected by LLS with the time difference between the events recorded by TOMS. Lightning strike occurred on the corridor of 110 kV transmission lines, at distance of 1.1 km from the substation. At the same time, SCADA system detected single phase to ground fault in phase B at the 110 kV transmission line, following by the single-pole auto-reclosure of circuit breaker in the line bay. Therefore, recorded transient overvoltages were most probably caused by multiple lightning strike in corridor of 110 kV transmission lines, which caused insulator flashover of the struck tower and consequently single phase to ground fault i.e. short-line fault in the vicinity of substation.

4.3. Case 3 - lightning strike to 110 kV transmission line causing insulator flashover in all phases

Transients recorded by TOMS are shown in Fig 8.

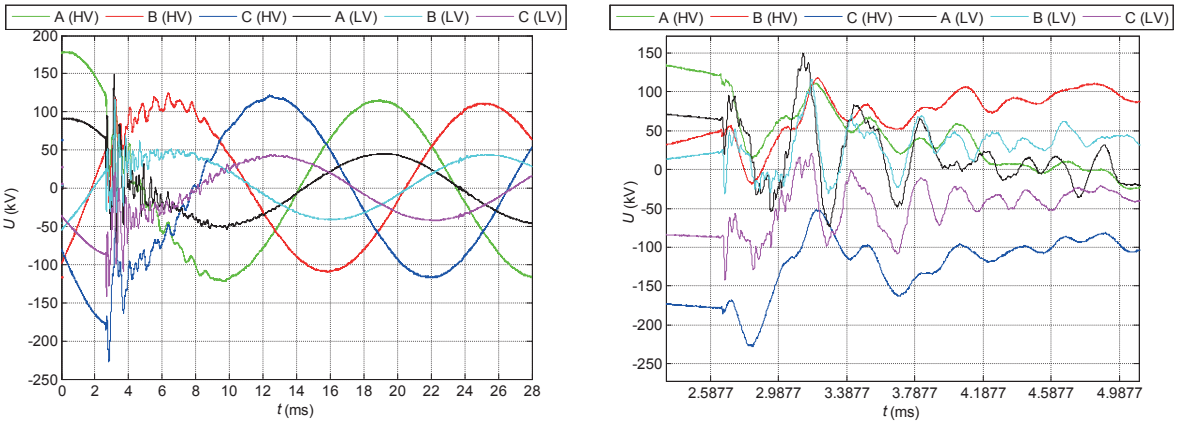

a) b)

Figure 8. (a) Transients recorded by TOMS in case of multiple lightning strike to 110 kV transmission line (b) zoomed part of transients after flashover in phases A, B and C (HV)

Recorded transients were time-correlated with a lightning flash consisting of three subsequent lightning strikes which were detected by LLS. Parameters of multiple lightning strikes are given in Table II.

Table II. Parameters of multiple lightning strikes detected by LLS

Lightning strike number	Time h:min:sec.milisec	Lightning current amplitude	Time difference between subsequent lightning strikes Δt
1	19:11:22.804	6.9 kA	-
2	**19:11:22.809**	**-24.7 kA**	**5 ms**
3	19:11:22.834	-9.1 kA	25 ms

Lightning strike with current amplitude -24.7 kA marked in Table II was selected as the one that probably caused recorded transients. Lightning strike occurred in the corridor of 110 kV transmission line, at distance of 9.7 km from the substation. At the same time, SCADA system detected three single phase to ground faults at 110 kV transmission line, following by the three-pole auto-reclosure of circuit breaker in the line bay. Therefore, recorded transient overvoltages were most probably caused by multiple lightning strike to 110 kV transmission line, which caused insulator flashover in all phases of the struck tower and consequently simultaneous three single phase to ground faults.

4.4. Case 4 - lightning strike to 220 kV transmission line causing insulator flashover in two phases

Transients recorded by TOMS are shown in Fig 9. Recorded transients were time-correlated with a lightning flash consisting of two subsequent lightning strikes which were detected by LLS. Parameters of lightning strikes are given in Table III. Lightning strike with current amplitude -169 kA marked in Table III was selected as the one that probably caused recorded transients.

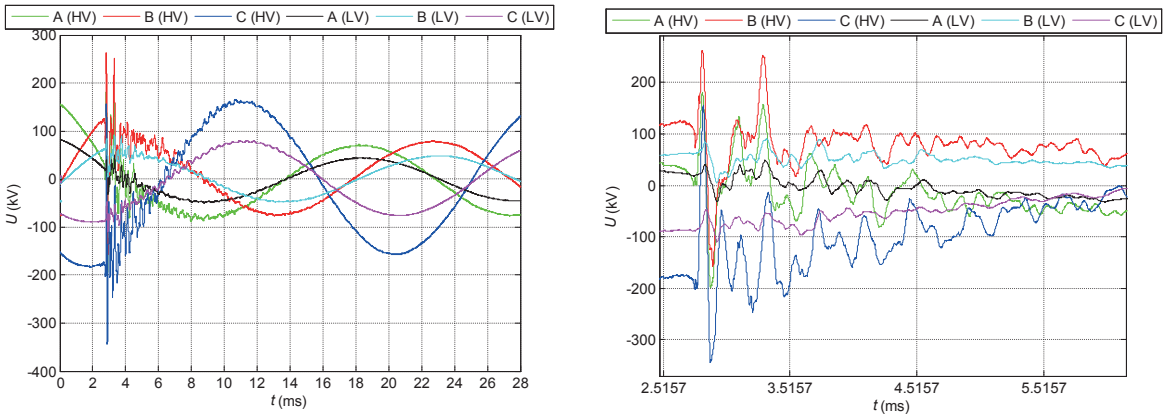

Figure 9. (a) Transients recorded by TOMS in case of lightning strike to 220 kV transmission line (b) zoomed part of transients after flashover in phases A and B (HV)

Table III. Parameters of multiple lightning strikes detected by LLS

Lightning strike number	Time h:min:sec.milisec	Lightning current amplitude	Time difference between subsequent lightning strikes Δt
1	20:03:55.864	56.3 kA	-
2	**20.03.55.865**	**-169 kA**	**1 ms**

Lightning strike occurred in the corridor of double-circuit 220 kV transmission line, at distance of 41.6 km from the substation. At the same time, SCADA system detected two simultaneous single phase to ground faults at one circuit of 220 kV transmission line, following by the auto-reclosure operation of circuit breaker in the line bay. Therefore, recorded transient overvoltages were most probably caused by lightning strike to 220 kV transmission line, which caused insulator flashover in two phases of the struck tower and consequently simultaneous two single phase to ground faults.

5. CONCLUSION

In this paper, an on-line TOMS for power transformers is presented that is capable to continuously record in real-time various kinds of transient overvoltages such as lightning or switching overvoltages. TOMS was used for recording lightning caused transient overvoltages at the terminals of 150 MVA power transformer located in 220/110 kV substation. Recorded waveforms originating from lightning strikes to overhead lines are correlated with data from the LLS and SCADA system. Four events recorded by TOMS were analysed to determine the possible cause of transient overvoltages appearing on the power transformer's terminals. Results show excellent time and spatial correlation between data from TOMS, LLS and SCADA system. According to the correlation between data from these systems, recorded events were most probably caused by lightning strikes to 110 kV and 220 kV overhead lines. Lightning strikes caused flashovers on the insulator strings of transmission line towers. Relay protections system successfully detected these faults and auto-reclosure of circuit breaker occurred.

In the future work, an analysis will be conducted focusing on the characteristics of recorded overvoltage waveforms, i.e. frequency and amplitude. Statistical analysis on time parameters of transient overvoltages will be performed, based on a large number of recorded events to obtain statistical distributions. Collected data about overvoltage stresses can be used as the basis for the assessment of the transformer insulation condition and estimation of health index.

ACKNOWLEDGEMENTS

This work has been supported in part by the Croatian Science Foundation under the project "Development of advanced high voltage systems by application of new information and communication technologies" (DAHVAT).

REFERENCES

[1] CIGRÉ WG A2.37, "Transformer Reliability Survey", technical brochure no. 642, Paris, 2015.
[2] S. Tenbohlen, J. Jagers, F. Vahidi, "Standardized survey of transformer reliability: On behalf of CIGRE WG A2.37", International Symposium on Electrical Insulating Materials (ISEIM), pp. 593-596, Toyohashi, 2017.
[3] IEC 60060-1, "High voltage test techniques - Part I: General definitions and test requirements", 2010.
[4] S. Okabe, J. Takami, "Evaluation of breakdown characteristics of oil-immersed transformers under non-standard lightning impulse waveforms - method for converting non-standard lightning impulse waveforms into standard lightning impulse waveforms", IEEE Trans. Dielectr. Electr. Insul., vol. 15, no. 5, pp. 1288-1296, 2007.
[5] S. Okabe, "Evaluation of breakdown characteristics of oil-immersed transformers under non-standard lightning impulse waveforms - definition of non-standard lightning impulse waveforms and insulation characteristics for waveforms including pulses", IEEE Trans. Dielectr. Electr. Insul., vol. 14, no.1, pp. 146-155, 2007.
[6] S. Okabe, T. Tsuboi, J. Takami, "Evaluation of K-factor based on insulation characteristics under non-standard lightning impulse waveforms", IEEE Trans. Dielectr. Electr. Insul., vol. 16, no.4, pp. 1124-1126, 2009.
[7] P. Sun, W. Sima, M. Yang, X. Lan, J. Wu, "Study on Voltage-number Characteristics of Transformer Insulation under Transformer Invading Non-standard Lightning Impulses", IEEE Transactions on Dielectrics and Electrical Insulation, vol. 22, no. 6, December 2015.
[8] P. Mitra, A. De, A. Chakrabarty, "Investigation on the voltage stresses developed on transformer insulation under non-standard terminal excitations", TENCON - IEEE Region 10 Conference, pp. 1-5, Singapore, 2009.
[9] S. Keitoue, R. Gardijan, "Transformer Monitoring System – Important Component of Smart Grid", ITCE, Teheran, 2014.
[10] T. Jaković, I. Murat, F. Klarić, S. Keitoue, "Transformer Fleet Monitoring", 4th International CIGRE Colloquium "Transformer Research and Asset Management", Pula, Croatia, 2017.
[11] S. Keitoue, A. Keller, R. Gardijan, "Transient overvoltage on-line monitoring system for power transformers", International Colloquium Transformer Research and Asset Management, Cavtat, Croatia, November 12 – 14, 2009.
[12] B. Filipović-Grčić, B. Franc, I. Uglešić, I. Pavić, S. Keitoue, I. Murat, I. Ivanković, "Monitoring of transient overvoltages on the power transformers and shunt reactors – field experience in the Croatian power transmission system", Procedia Engineering, vol. 202, pp. 29-42, 2017.

Journal of Energy
VOLUME 67 Number 2 | 2018 Special Issue
journal homepage: http://journalofenergy.com/

EVALUATION OF LOAD FORECAST MODEL PERFORMANCE IN CROATIAN DSO

Ivona Sičaja[a], Ante Previšić[a], Matija Zečević[a], Domagoj Budiša[b]
Končar – Power Plant and Electric Traction Engineering[a],
HEP ODS d.o.o. Elektroslavonija Osijek[b]
Croatia

SUMMARY

During the revitalization of the Remote Control Systems of four Distribution System Operators in Croatia: Elektra Zagreb, Elektroslavonija Osijek, Elektroprimorje Rijeka and Elektrodalmacija Split, the load forecasting subsystems were implemented as an integral part of the DMS system.

Accurate electricity load forecasting presents an important challenge in managing supply and demand of electricity since it cannot be stored and has to be consumed immediately. Electricity consumption forecasting has an important role in the scheduling, capacity and operational planning of the distribution power system. Load forecasting of certain parts or the whole distribution network helps to improve distribution network planning, operation and control which also increases the safety level of the entire distribution system.

Although many forecasting methods were developed, none can be generalized for all load patterns. Accurate results of electricity load models are essential to make important decisions in planning and controlling so it is important to keep models as accurate as possible regarding input variables such as historical loads and meteorological data. This article gives a description of the implemented load forecasting subsystems using an artificial neural network with a feedforward multilayer perceptron and backpropagation as a learning strategy. The emphasis is on the simple and systematic use of input and output data as well as on forecasting scenarios of specific measured points where hourly forecasted results for a week ahead are presented and compared for Croatian Distribution Centers.

KEYWORDS

Short-Term Load Forecasting, Artificial Neural Networks, Load Forecast Model, Parameters Tuning

1. INTRODUCTION

The power sector was traditionally based on vertically integrated utilities including generation, transmission, distribution and retail. Due to remarkable changes in the electric power industry in recent years, the new structural organization is mainly based on liberalized electricity markets that promote competition. The utilization of renewable energy sources in electrical power production, mainly photovoltaic panels, wind turbines and biomass, has rapidly grown in past decades. Current and future power systems with intensive use of distributed renewable generation and the liberalization of the electricity market increase power systems complexity and bring huge challenges to the power industry. Power system planning, control and operation require an adequate use of existing resources to increase system efficiency. Power unit activities' planning has become a more complex process as companies have to take care of various variables of a technical and social character but still produce electrical energy with minimum costs, provide power quality, safety of the power system, etc. Electricity load forecasting is considered one of the critical factors for economical operation of a power system. Accurate load forecasting holds a great saving potential for electric utility corporations. Load forecasting helps an electric utility in making important decisions regarding the purchase of electric energy, dispatching generation units, load switching, security analysis, maintenance scheduling and infrastructure development.

The increase of power system complexity has led to enhanced use of computational intelligence methods because of their quality results in solving diverse power system optimization problems. Load forecasting highly depends on the selection of a mathematical model and on the quality of the input variables. The load forecasting technique used in this article is Artificial Neural Network (ANN). Artificial Neural Networks are relatively crude electronic models based on the neural structure of the brain.

Load forecasting involves the accurate prediction of the electricity load in time scales compatible with operational requirements. Depending on the planning horizon, load forecasting can be divided into three categories: short-term forecasts, medium-term forecasts and long-term forecasts. Short-term forecasts usually span from one hour to one week and are commonly referred as hourly load forecasts. They play an important role in the day-to-day utility operations such as unit commitment, economic dispatch and load management. Medium-term forecasts are necessary for scheduling unit maintenance and energy trading. They usually span from a few weeks to a few months. Long-term electricity forecasts are required to be valid from 5 to 25 years. They are important because of their direct influence on production, transmission and distribution capacities planning [1].

During the revitalization of the Remote Control Systems of the four biggest Distribution System Operators in Croatia: Elektra Zagreb, Elektroslavonija Osijek, Elektroprimorje Rijeka and Elektrodalmacija Split, the load forecasting subsystems were implemented as an integral part of the DMS system (*Distribution Management System)*. The total consumption of the Distribution areas is different depending on the size of Distribution, population and type of customers. Elektra Zagreb covers an area of 2,550 km^2 and is the smallest in size of the four mentioned Distributions but with more than 550 000 customers and peak consumption in 2014 of 665,25 MW it is the biggest Distribution in the country. On the other hand, Elektroslavonija Osijek covers an area of 4,152 km^2 but has around 150 000 customers and peak consumption in 2014 of 163 MW [2]. This paper presents the survey of a neural-network-based short term load profile prediction for Distribution areas. The neural network inputs are load data and meteorological data, while the neural network output is load at a particular moment. Neural network training and verification are performed on load data recorded at each Distribution center and on meteorological data obtained from the Meteorological and Hydrological Service of Croatia, from September 2014 to December 2017. Several models have been surveyed to identify the load pattern and predict the future load.

2. LOAD FORECASTING SYSTEM

2.1. Load forecasting calculation algorithm

The implemented load forecasting system is based on Artificial Neural Networks (ANN). Artificial Neural Networks are computational models inspired by the human brain that are capable of machine learning, pattern recognition and data fitting. They are based on sophisticated mathematical techniques for identification and studies of connecting links (linear and non-linear) between observed variables. By structure, artificial neural networks can be divided into two groups, static (feed-forward) and dynamic (feed-back). Unlike dynamic ones, static neuron models do not contain dynamic elements and their output depends entirely on current values of input signals and model parameters.

A neural network consists of multiple neurons organized in layers - the input and output layer, and also of a number of hidden layers in between, where each hidden layer can contain an arbitrary number of neurons. In this paper, we deal with a static neural network with MultiLayer Perceptron, the so called MLP, with a single hidden layer. Figure 1 shows a static MLP neural network with an input layer with two inputs, two hidden layers with three neurons in each hidden layer and with an output layer with two outputs [3].

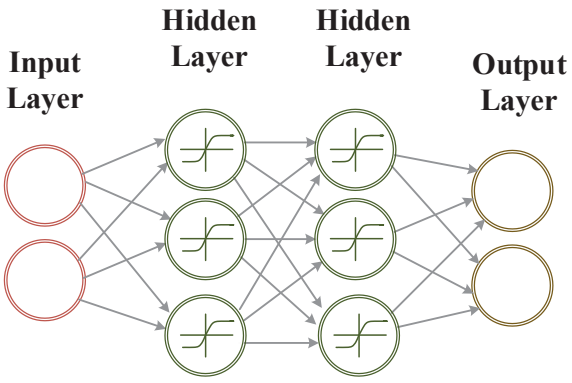

Figure 1 Static MLP Neural Network

Neural networks are tuned to carry out a required mapping of inputs to the outputs using training algorithms. The most commonly used training algorithm for static networks is *error backpropagation*. The learning method can be divided into two categories, unsupervised learning and supervised learning. The *Error backpropagation* method is a supervised learning model where the error between the expected output and the calculated output is computed and minimized by adjusting the weights between two connection layers starting backwards from the output layer to the input layer [4]. In this paper, a backpropagation algorithm uses the learning concept and the historical relationship between the load and temperature for a given period, day type and hour of the day.

2.2. Factors affecting electricity load forecasting

The purpose of neural network learning is to find the model with a load pattern as reliable as possible. A lot of factors are considered to have an impact on load forecasting, but the most important ones are the following [1]:

- **Time factor** – electricity consumption varies as cyclic time dependency on an hour of day basis, day of week basis and time of year basis. The specific load patterns can be presented on characteristic curves of consumptions that present activities during a certain period in time. The load curve changes during the time period depending on the type of customers. The characteristic consumption curve for areas populated mainly

with households and business areas has different forms for weekdays (two peaks in a day) and weekends while the consumption curve for industrial areas has more similar form during time periods.

- **Weather conditions** – the most important weather variables affecting electricity consumption are:
  - Temperature – A huge correlation between electricity consumption and temperature exists during the whole year. As temperatures rise during summer, the increased usage of cooling appliances also increases load consumption. As temperatures fall in the winter season, the more usage of heating appliances also increases load consumption.
  - Humidity - Humidity affects short term load forecasting since it increases the feeling of the severity of the temperature in summer and during rainy seasons. Thus, load consumption increases during a humid summer day.
  - Wind speed
  - Cloud cover
- **Economic factor** – In general, electricity consumption enlarges with population growth, industry development, increase of Gross Domestic Product, reduction of electricity costs, etc.
- **Customer factor** – The characteristic curve of consumption depends on customer classes. Most electric utilities serve different types of customers as residential consumer, commercial consumer and industrial consumer.

2.3. Remote control system configuration

Hardware configuration for the Remote Control Systems installed in the dispatching centers Elektra Zagreb, Elektroslavonija Osijek, Elektroprimorje Rijeka and Elektrodalmacija Split is shown in Figure 2. The configuration of the SCADA/DMS system is based on a server/client model, on a distributed model of hardware and software equipment including a process database.

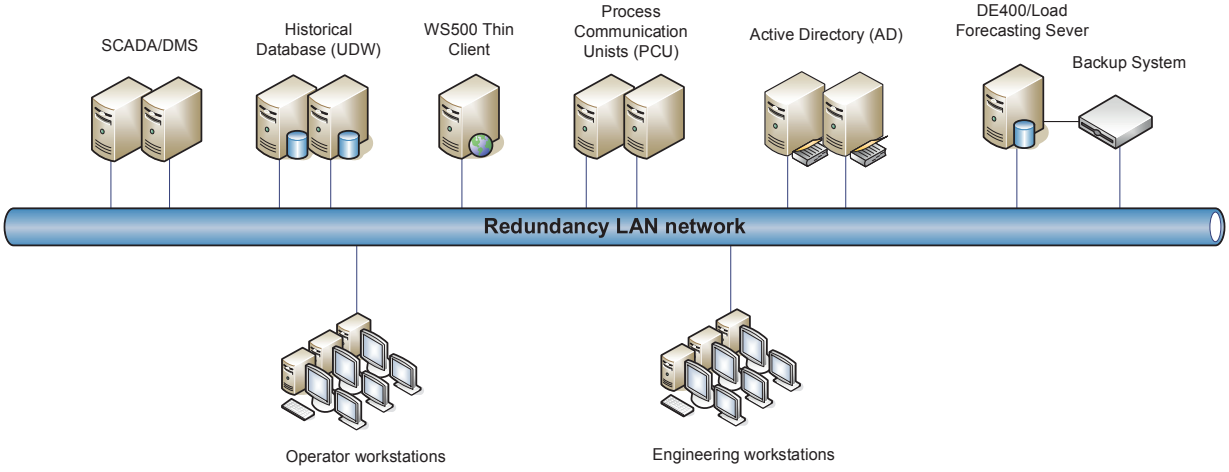

Figure 2 SCADA/DMS Hardware Configuration

Load forecasting system software functions are implemented on the Oracle database on the Load Forecasting Server. The load forecasting system is installed on an individual HYPER-V virtual server on the DE Server (*Data Engineering*), the server for the maintenance and data engineering of the entire SCADA System. The load forecasting system can be accessed remotely by connecting to the Load Forecast Server.

2.4. *Load forecasting system implementation*

The data required for the load forecasting process is automatically transferred from the Historical Database called UDW (*Utility Data Warehouse*) in a defined file format to predefined directories on the Load Forecasting Servers. After the load forecasting process, the file with the forecasted data is automatically sent to the predefined location on the Load Forecasting Server, after which the data is transferred to the SCADA server.

Automatic data exchange between the Load Forecasting Server and SCADA and UDW Servers is done by using the DCI functionality (*Data Communication Interface*) which ensures the transfer of correctly structured data from the Historical Database to the Load Forecasting Server using a FTP protocol (*File Transfer Protocol)* and vice versa, the forecasting process results transfer on the SCADA Server and their insertion in the Historical Database.

In this way all data is available to the operators though the SCADA HMI.

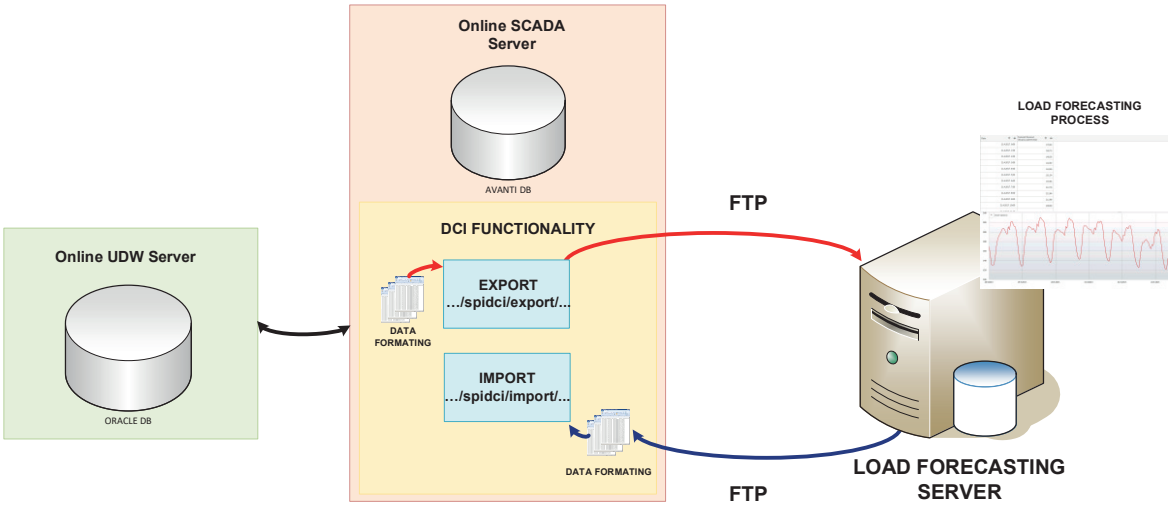

Figure 3 Functional Data Exchange Scheme

2.5. *Load forecasting results control*

The accuracy of output values can be verified with a large number of measures [5]. In this article, MAPE, MAE and RMSD measures are used to verify the neural network performances.

MAPE (*Mean Absolute Percentage Error)* expresses accuracy as percentage and is defined by the formula:

$$M = \frac{100}{n}\sum_{t=1}^{n}\left|\frac{A_t - F_t}{A_t}\right|, \qquad (1)$$

Where A_t is the *Actual value* and F_t is the *Forecast value*. The difference between A_t and F_t is divided by the *Actual value* A_t. The absolute value in this calculation is summed for every forecasted point in time and divided by the number of fitted points *n*.

RMSD (*Root Mean Square Deviation*) is defined as square root of the average square differences between values predicted by a model or an estimator and the values actually observed. It is calculated by:

$$RMSD = \sqrt{\frac{\sum_{t=1}^{T}(F_t - A_t)^2}{n}}, \qquad (2)$$

Where F_t is *Forecasted value* and A_t is *Actual value*. It is computed in *t* moment for *T* different predictions.

MAE (*Mean Absolute Error)* is a measure of average difference between two variables. It is given by:

$$MAE = \frac{\sum_{i=1}^{n}|A_i - F_i|}{n}, \quad (3)$$

Where F_t is *Forecasted value*, A_t is *Actual value* and *n* is number of fitted points.

3. MODEL RESULTS EVALUATION

3.1. Load forecasting model configuration

Each of the four biggest Croatian Distribution Operators has its own Load Forecasting System with several models defined. Each Distribution Operator predicts the total consumption of its distribution area as well as the loads of smaller parts such as forecasting consumption of certain cities or islands. In this article, four models with forecasting of the total consumption of Distributions Elektra Zagreb, Elektroslavonija Osijek, Elektroprimorje Rijeka and Elektrodalmacija Split are studied.

The models are configured to make calculations with meteorological data from the Meteorological and Hydrological Service of Croatia. The data files with future data (seven days ahead) and past data (last 24 hours) are sent to the Load Forecasting Systems once a day at a specified time. Meteorological data for the observed models includes past and future hourly temperatures for Zagreb, Osijek, Rijeka and Split – the centers of distribution areas. In accordance with the available meteorological data for seven days ahead, the load forecasting outputs are values for the same period.

The importing files have a predefined form with the possible time period of the input variable: 15 minutes, 30 minutes, an hour, a day, etc. Input variables used in this article, both meteorological and load variables, are hourly values. To prevent overfitting, load data sets are divided into training and verification data sets. In all observed models, the period from September 2014 until June 2016 is used for neural network training, while the period from July 2016 until the end of 2016 is used for neural network verification.

The days with deviation from usual consumption are also specified in all models. They include all national holidays and significant days such as sport events, cultural events, etc.

Additional parameters related to the complexity of the neural network and the duration of model learning are: Number of Training Passes and Number of Hidden Nodes. Number of Training Passes is the number of passes through the training data for each of the cycles of training. For Back Propagation, the total number of iterations through the data is this number times 50 training cycles. Number of Hidden Layer Nodes is the number of layer nodes in the second layer in which the input data is processed. Increasing the number of nodes in the hidden layer may result in better training and thus better forecast results but it also increases the complexity of the neural network and therefore increases the time required to train the network. These parameters can be changed as many time as necessary to improve output values therefor the parameters are different for all four models. According to some recommendations, number of Hidden Neurons to start model training should be 10 [6].

After getting an output variable, models can be re-trained and corrected as many times as necessary by having the user change the input variables in order to get better output values.

3.2. Comparison of models' Error Statistic

The four models with different input data but same training and verification time period are defined. It is possible to draw a conclusion by checking the models Error Statistic (Table 1) that described forecasting models are reliable (MAPE < 5%). Elektra Zagreb model has the smallest MAPE measure 4.46%, while the Elektroslavonija Osijek model has the smallest

RMSD measure (7) and MAE measure (5). Different MAPE measures indicate that some models could be better, i.e. should be re-trained. MAPE measure for Elektrodalmacija Split model is 5.31% which indicates model re-training in order to get more accurate results.

Models' errors depend on changing input data. Just a little modification of input data such as time period, makes the output data, thus error statistic, different. The operators in each Distribution maintain their own models to have output values as accurate as possible. The accurate output variables are the result of adjusting model's parameters and keeping input data correct.

Table 1 Comparison of four models' Error Statistic

DISTRIBUTION	MAPE	RMSD	MAE
Elektra Zagreb	**4.46%**	**15**	**10**
Elektroslavonija Osijek	**4.91%**	**7**	**5**
Elektrodalmacija Split	**5.31%**	**20**	**15**
Elektroprimorje Rijeka	**4.97 %**	**13**	**10**

3.3. A month result preview

The forecasting values depend on accuracy of the defined model. The less model errors, the output forecast values are more similar to actual ones. As it was concluded from the model error statistic, the output values are reliable. The following figures present the comparison graphs of Actual and Forecast Values in January 2017 for four defined models for four Croatian Distributions. The load forecast graphs follow the load actual graphs in all figures. Due to winter and cold meteorological conditions the consumption in January is higher than in other parts of the year. The biggest residuals between Actual and Forecast Values are when Actual Value differs significantly from the value of the day before or the value from the same day a week ago.

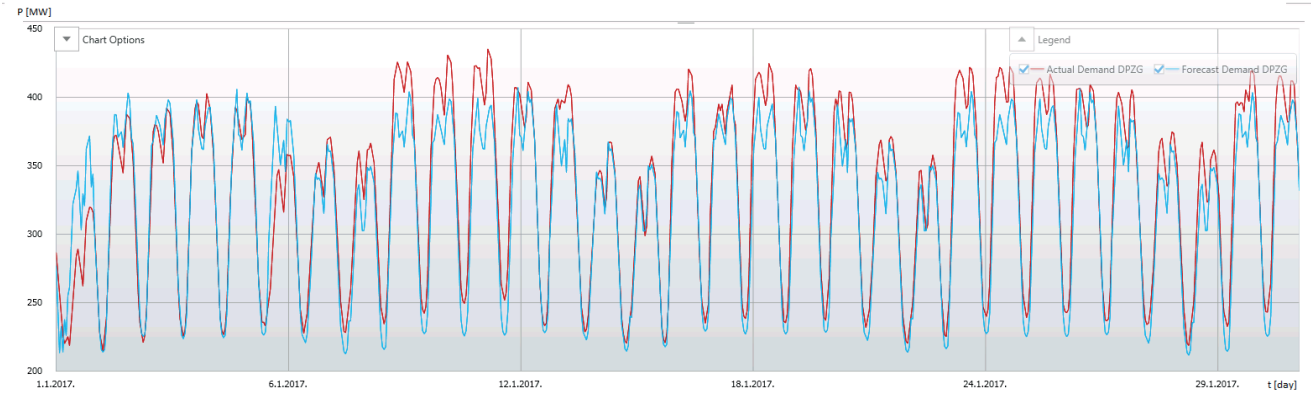

Figure 4 Comparison graph of Actual and Forecast Load Values for Elektra Zagreb Distribution in January 2017

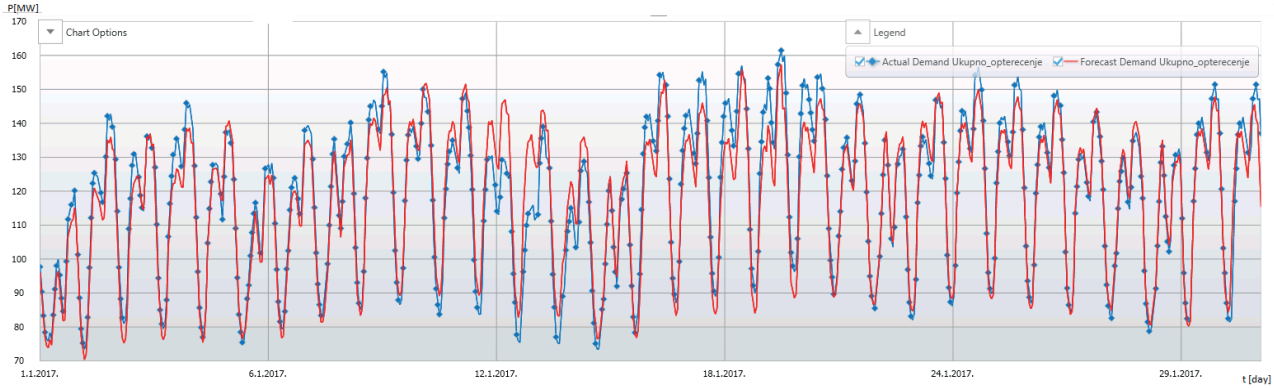

Figure 5 Comparison graph of Actual and Forecast Load Values for Elektroslavonija Osijek Distribution in January 2017

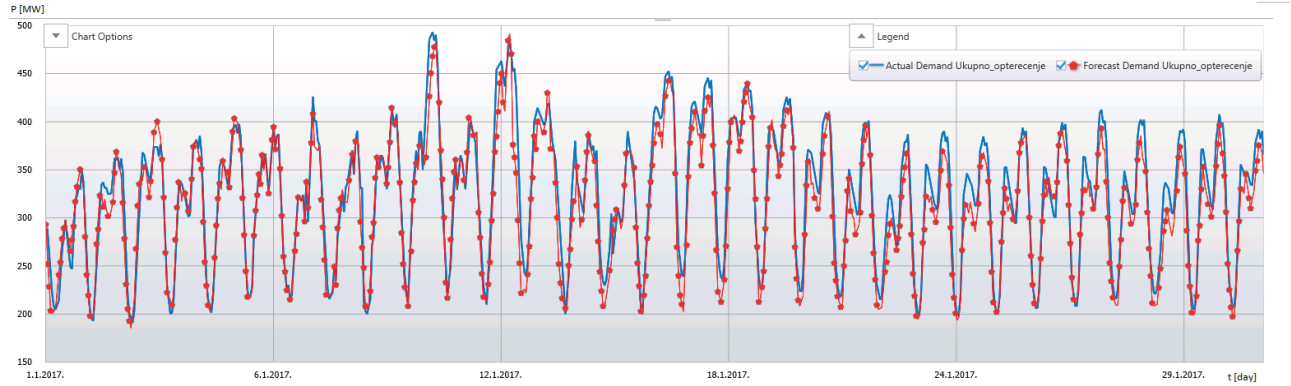

Figure 6 Comparison graph of Actual and Forecast Load Values for Elektrodalmacija Split Distribution in January 2017

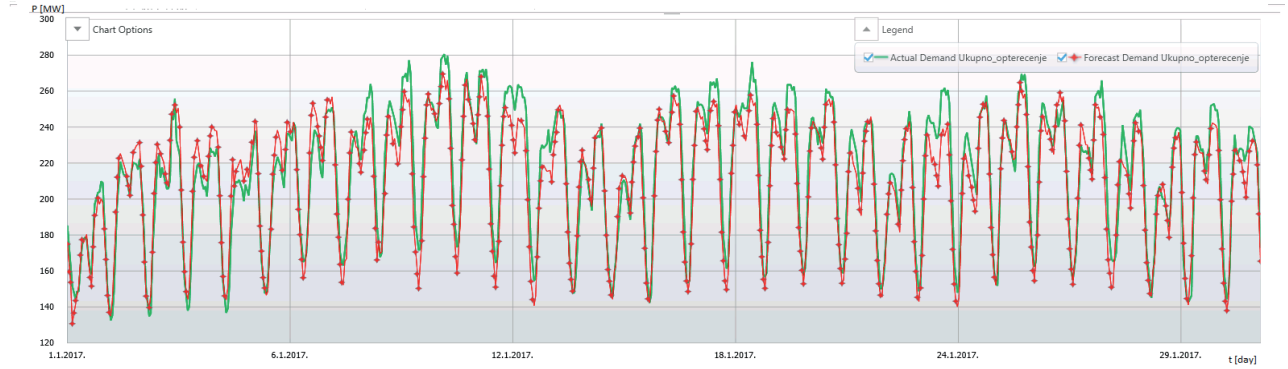

Figure 7 Comparison graph of Actual and Forecast Load Values for Elektroprimorje Rijeka Distribution in January 2017

3.4. Updated model for Elektroslavonija Osijek Distribution

The models have to be maintained regularly and input data has to be updated on a regular basis in order to keep output values accurate. Due to changes in each Distribution regarding population, economic and customers' factors, models have to be re-trained after a certain amount of time.

The Elektroslavonija Osijek Distribution is specific because of the significant increase of renewable energy sources installed in the network. The renewable sources contain biomass and photovoltaic panels. The total installed power in biomass and biogas sources is 30 MW where the number of biogas units is 13 and number of biomass units is 3. The number of installed photovoltaic panels is 393 and the total installed power is 25 MW. These changes, as well as other social and economic changes, bring huge challenges to operators in order to plan the supply and demand of electricity consumption.

The consumption of Elektroslavonija Osijek is predicted for the period from August 15th until August 31st 2017 with two models, with the existing one (model used in the previous case with input data until December 31st 2016) and a new model that contains updated input data

until July 31st 2017. Figure 8 shows comparison of Actual Value (light blue) and two Forecast Values (from two models). The model with updated input values (dark blue graph) has more accurate output values for August 2017 than the model with the input data until December 31st (yellow graph).

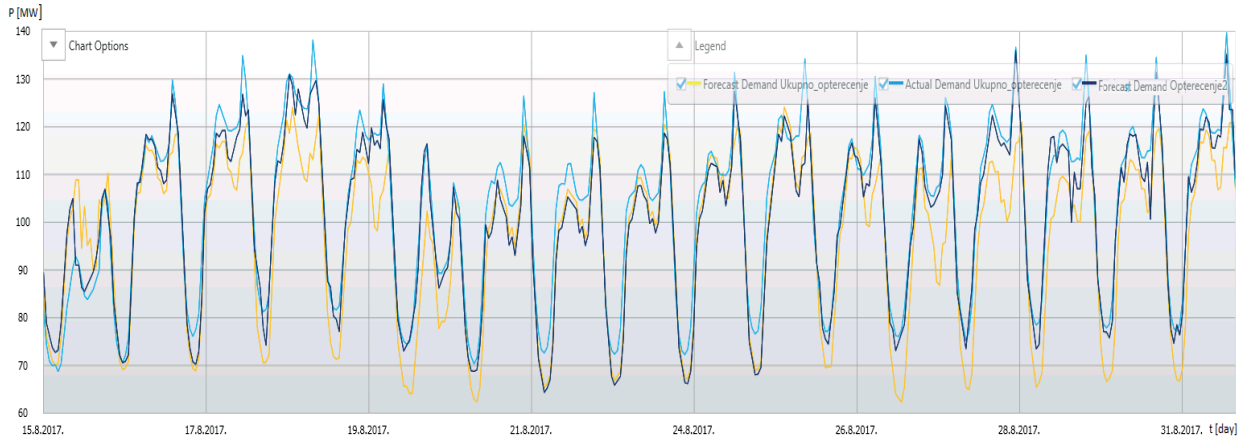

Figure 8 Comparison graph of Actual and Forecast Load Values from two models for Elektroslavonija Osijek Distribution for part of August 2017

4. CONCLUSION

The article describes the principles of the load forecasting systems implemented within four Distribution System Operators in Croatia: Elektra Zagreb, Elektroslavonija Osijek, Elektroprimorje Rijeka and Elektrodalmacija Split. Four neural network models for short-term prediction of active electrical energy consumption are observed. Neural network inputs are the total consumption of observed Distributions and the meteorological data for the period from September 2014 until December 2016. It is shown that trained neural networks have a very good performance and are reliable in predicting future consumption. Residuals between actual and forecast values are alleviated by neural network tuning with which the neural network is able to adapt to nonlinearities. By MAPE measure, forecasting model for Elektra Zagreb is the most accurate of four observed models. In order to improve model, results it is important to improve the quality of input variables and optimize the complexity of the model. To keep forecasting model correct after certain period of time, it is necessary to update input variables, regularly maintain and re-train the model.

REFERENCES

[1] N.Phuangpornpitak, W.Promme: *A Study of Load Demand Forecasting Models in Electric Power System Operations and Planning,* GMSARN International Journal 10 (2016)

[2] HEP - Operator distribucijskog sustava d.o.o.: 2014. *Godišnje izvješće*, Zagreb, Croatia, 2015

[3] M. Gulin, M. Vašak, G. Banjac, T. Tomiša: *Load Forecast of a University Building for Application in Microgrid Power Flow Optimization*, IEEE International Energy Conference (ENERGYCON 2014), Dubrovnik, Croatia, May 2014

[4] I. Petrović, M. Baotić, N.Perić: *Inteligentni sustavi upravljanja: Neuronske mreže, evolucijski i genetički algoritmi*, FER, Zagreb, Croatia, 2011.

[5] G.E.Nasr, E.A.Badr, M.R.Younes: *Neural Networks in Forecasting Electrical Energy Consumption*, Byblos, Lebanon, 2001.

[6] *Nostradamus User Guide,* Network Manager, Ventyx an ABB Company, 2014

Journal of Energy

VOLUME 67 Number 2 | 2018 Special Issue

journal homepage: http://journalofenergy.com/

Temperature rise and DC current capability tests of star-point reactor used in HVDC transmission

[a]Dalibor Filipović-Grčić, [c*]Božidar Filipović-Grčić, [b]Igor Žiger, [b]Danijel Krajtner, [a]Danijel Brezak, [a]Rajko Gardijan

[a]Končar - Electrical Engineering Institute Inc., Zagreb, Croatia

[b]Končar - Instrument Transformers Inc., Zagreb, Croatia

[c]University of Zagreb, Faculty of Electrical Engineering and Computing, Croatia

SUMMARY

Star-point reactors are grounding devices installed in HVDC stations between the converter transformer secondary side and AC side of converter arms to provide a reference to ground. Such reactors are used as high-impedance grounding on the converter side of power transformers, providing high impedance path for the fundamental harmonic (i.e. 50 or 60 Hz) and a low impedance path for DC current, eliminating DC current flowing through the transformer windings. Temperature rise and DC current capability tests of 420 kV star-point reactor are presented in this paper. The purpose of temperature rise test is to verify that temperatures that can damage the insulation of star-point reactor will not be reached with the specified service conditions. The temperature rise test was carried out according to the requirements of the IEC 61869-3 standard and client's request which included simultaneous application of fundamental, 3rd harmonic voltage and DC excitation. The inclusion of 3rd harmonic excitation of an amplitude up to 15% simulates voltage harmonic distortion which may appear in the power system at the location of star-point reactor installation. Prior to temperature rise test, DC current capability test was performed. The goal of this test is to determine the value of DC current at which the saturation point is reached. DC current is injected through star-point reactor while AC voltage is applied. Two different cases are considered regarding AC voltage: test with fundamental voltage harmonic and test with fundamental voltage harmonic with superimposed third voltage harmonic. Test circuit is proposed which is suitable for generation of complex voltages composed of fundamental harmonic and superimposed third harmonic with amplitudes up to 15% of the applied fundamental harmonic. The proposed test circuit was also used during the temperature rise test and it is applicable for testing of HV equipment with rated voltage up to 420 kV.

KEYWORDS

Temperature rise test, star-point reactor, DC current capability test, HVDC transmission.

1. INTRODUCTION

HVDC transmission enables economic power delivery across long distances, as well as interconnections between systems of different frequencies or networks that cannot be synchronized. HVDC transmission can be also used in cases when direct connection between two AC systems with the same frequency or a new connection within a meshed grid may be impossible because of system instability, too high short-circuit levels or undesirable power flow scenarios. Furthermore, HVDC grids are a very attractive solution for interconnection of off-shore wind power plants to add an additional level of redundancy, flexibility and efficiency to the expansive power system [1].

With the increasing number of converter stations being built, the requirements on high voltage apparatus also change. One of such requirements is the simultaneous AC and DC loading of high voltage apparatus. While there are several types of units which could be subject to simultaneous AC and DC loading, the focus of this paper is placed on earthing reactors, also known as star-point reactors. These special grounding devices are installed between the converter transformer secondary side and AC side of converter arms to provide a reference to ground in the converter station [2]. These units are mostly used in HVDC stations with modular multilevel converters (Fig. 1) and they consist of three star-connected inductors with their neutral connected to the ground [3].

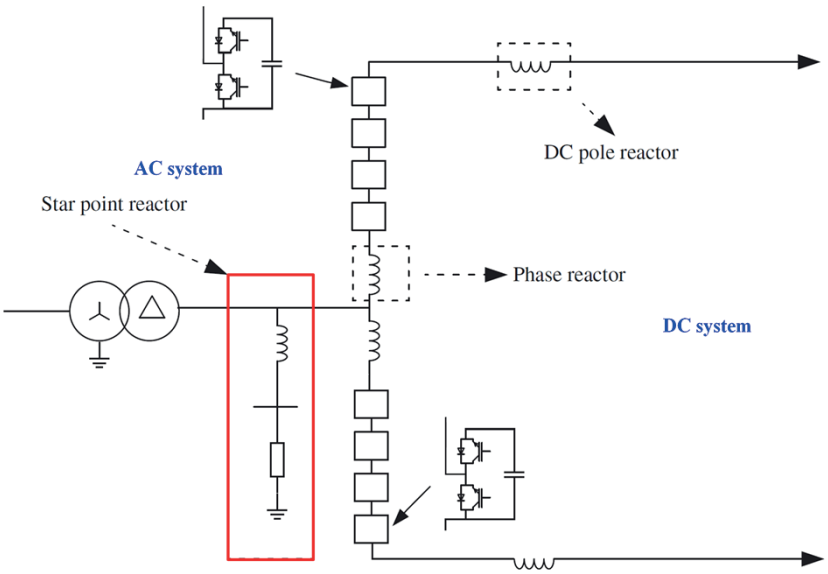

Figure 1. Star-point reactor connected between the converter transformer and the valves

When it comes to wind-power plant application, due to the space limitations at the offshore platform, normally the star-point reactor is installed at the onshore converter station. Such reactors are used as high-impedance grounding on the converter side of power transformers, providing high impedance path for the fundamental harmonic (i.e. 50 or 60 Hz) and a low impedance path for DC current, eliminating DC current flowing through the transformer windings. The predominant effect that DC current has on the operational characteristics of a power transformer is half cycle saturation [4], [5]. This leads to increased harmonic distortion, increased reactive power losses, overheating and elevated acoustic noise emissions. The DC current flowing through the star-point reactor may also cause saturation and consequently the above stated negative effects.

Star-point reactor is a device which is similar to inductive voltage transformer but without the low voltage winding. Therefore, for testing of star-point reactors standard for inductive voltage transformers is the most suitable [6]. However, requirements in available standards are

not completely appropriate for star-point reactors, which are a novel product concept. Therefore, several special tests that demonstrate the specialities of star-point reactors need to be introduced. These tests reflect the application modes of such units, as well as realistic conditions in the power network, which are not considered in [6]. DC current capability test is performed to check the conditions which can drive reactor's core into saturation [7]. Temperature rise tests on inductive voltage transformers are normally performed with power frequency voltage, but for star-point reactor the client's request was to superimpose third harmonic voltage up to 15% of the applied fundamental harmonic voltage. These requirements cannot be fulfilled with standard test equipment normally found in HV laboratories. Additional test circuit is proposed for generating third harmonic voltage equipped with blocking and passing filters and compensation.

2. CHARACTERISTICS OF 420 kV OPEN-CORE STAR-POINT REACTOR

Star-point reactor data are given in Table I and electrical scheme is shown in Fig. 2, where A is top end terminal, MT is measuring terminal and N is ending of the primary winding.

Table I. Star-point reactor data

Rated voltage	420/√3 kV
Continuous 3rd harmonic voltage	37.6 kV
Rated resistance at 75 °C	> 7500 Ω
Maximum DC current	80 mA
Maximum simultaneous current	125 mA

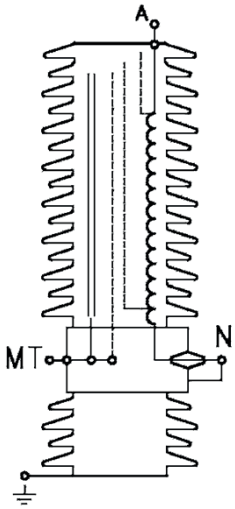

Figure 2. Electrical scheme of star-point reactor

Magnetic characteristic of 420 kV star-point reactor with open-core is measured according to [8]. An indirect method is needed to get the magnetic characteristic since the linked flux cannot be measured directly. Calculation of the magnetic characteristic is possible from measurements made of the instantaneous values of the current and voltage when an AC voltage of sufficient magnitude to cause saturation is applied for at least one cycle. If a measurement of the characteristic is requested for currents above the maximum service current, a method shall be used that does not overload the reactor, for instance the DC method which is applied in this paper. The magnetic characteristic for currents well above nominal current can then be evaluated. By charging the reactor with a DC current (higher than nominal peak current) the magnetic linked flux will increase following the magnetisation curve (switch 1 and 3 are closed in Figure 3). The reactor should be charged as quickly as possible in order not to introduce a resistance change caused by temperature rise. The reactor is then short-circuited and the decaying current $i(t)$ is recorded (switch 2 closes and switch 1 and 3 open). From this decaying current, the magnetic characteristic can be determined by using the following expressions derived from the circuit shown in Fig. 3:

$$U_L + U_R = 0;\ U_L = -\frac{d\psi(t)}{dt};\ U_R = R \cdot i(t), \tag{1}$$

Dalibor Filipović-Grčić, Božidar Filipović-Grčić, Igor Žiger, Danijel Krajtner, Danijel Brezak, Rajko Gardijan, Temperature rise and DC current capability tests of star-point reactor used in HVDC transmission, Journal of Energy, vol. 67 Number 2 (2018), Special Issue, p. 63–72

$$\frac{d\psi(t)}{dt} = R \cdot i(t), \tag{2}$$

$$\psi(t) = \int_0^T R \cdot i(t)dt, \tag{3}$$

where U_L is voltage drop across inductance L, U_R is voltage drop across R which is the known ohmic resistance of the whole circuit (winding + connecting leads + current shunt) and T is time sufficient for current and flux to drop to negligible value. The total linked flux change $\psi(t)$ is determined from expression (3).

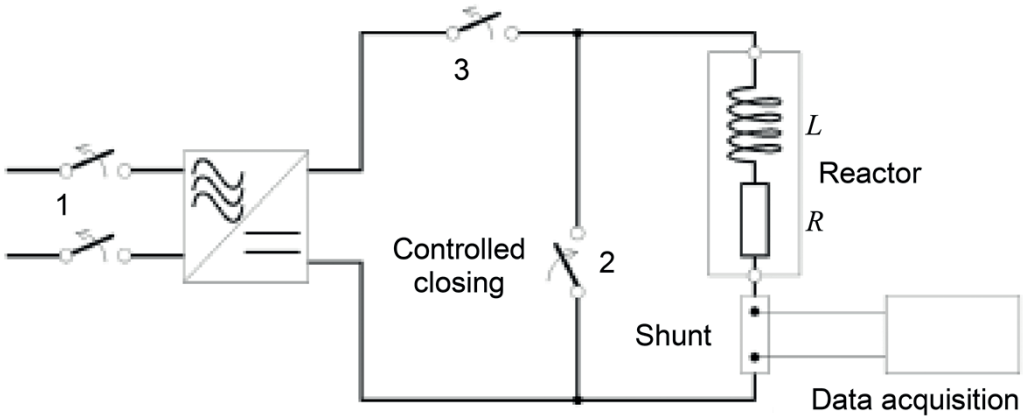

Figure 3. Circuit for measurement the magnetic characteristic according to [8]

Finally, the magnetic characteristic of star-point reactor derived from the measurements is shown in Fig. 4.

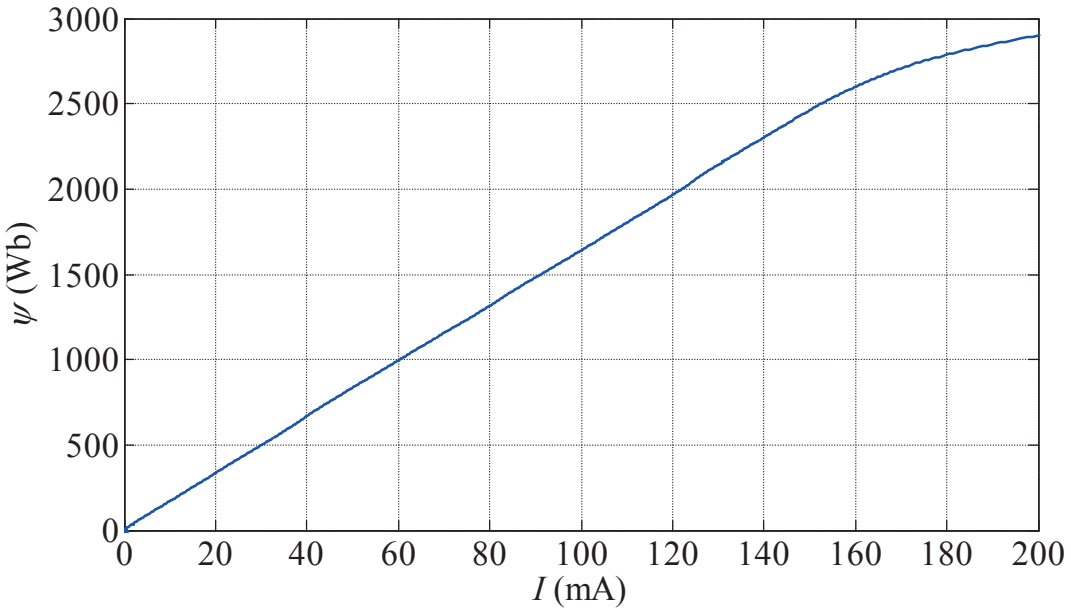

Figure 4. Measured magnetic characteristic of 420 kV open-core star-point reactor

Prior to temperature rise test, DC current capability of star-point reactor with respect to saturation was checked.

3. DC CURRENT CAPABILITY TEST

The goal of DC current capability test is to determine the value of DC current at which the saturation point is reached. In this test, DC current is injected through star-point reactor while

AC voltage is applied. Two different cases are considered regarding AC voltage: test with fundamental voltage harmonic (50 Hz) and test with fundamental voltage harmonic with superimposed third voltage harmonic (150 Hz), which simulates voltage harmonic distortion which may appear in the power system at the location of star-point reactor installation.

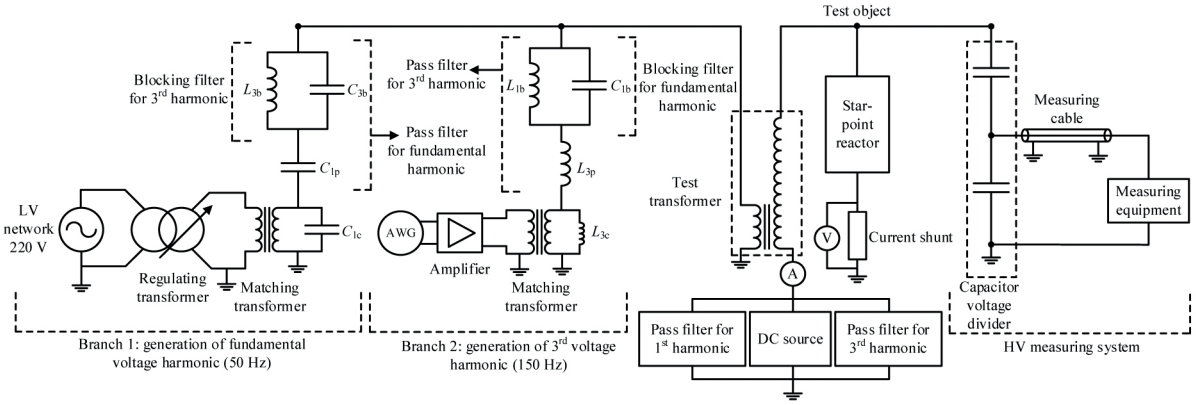

Figure 5. Test circuit for DC current capability test

Proposed test circuit for performing DC current capability test is shown in Fig. 5. Fundamental frequency voltage is generated directly from low voltage network (220 V) through regulating transformer and matching transformer (branch 1). In this branch, a blocking filter (L_{3b}, C_{3b}) for 3rd harmonic and a pass filter (L_{3b}, C_{3b}, C_{1p}) for fundamental harmonic are connected. Compensation capacitance C_{1c} for fundamental harmonic is connected in parallel with matching transformer. 3rd voltage harmonic is generated from arbitrary waveform generator (AWG) signal which is amplified by low frequency amplifier and afterwards stepped up by the matching transformer (branch 2). In this branch, a blocking filter (L_{1b}, C_{1b}) for fundamental harmonic and a pass filter (L_{1b}, C_{1b}, L_{3p}) for 3rd harmonic are connected. Compensation inductance L_{3c} for 3rd harmonic is connected in parallel with matching transformer. One of the main benefits of the test circuit is that it can be easily adapted for injection of higher harmonics (e.g. the 3rd harmonic) of a significant amplitude (5-15% of the applied fundamental voltage), which is a very common requirement for inductive voltage transformers and star-point reactors [9]. The test circuit shown in Fig. 5 is suitable for testing of HV equipment with rated voltage up to 420 kV. Test arrangement in HV laboratory during the DC current capability test is shown in Fig. 6.

3.1. Test with fundamental voltage harmonic and injected DC current

In this test, a 50 Hz voltage U_p=420/√3=242.5 kV is applied on the star-point reactor, while DC current is gradually increased to determine the saturation point. Below the saturation point, as DC current increases, AC component of current does not change since applied AC voltage is constant. Above saturation point, AC current trough the reactor increases significantly. Measurement results show that the star-point reactor starts to exhibit saturation when the applied DC current is around 112 mA. Current-voltage waveforms recorded at star-point reactor for operating points without and with saturation are shown in Figs. 7 and 8. Influence of AC primary voltage increase on reactor saturation is investigated. During this test, constant DC current of 80 mA was injected through reactor according to client's request. This value of DC current is equal to maximum DC current which is expected at the site of star-point reactor installation in the HVDC substation. Current-voltage waveforms recorded at star-point reactor for primary voltage U_p=241.3 kV and U_p=265.6 kV are shown in Figs. 9 and 10, respectively.

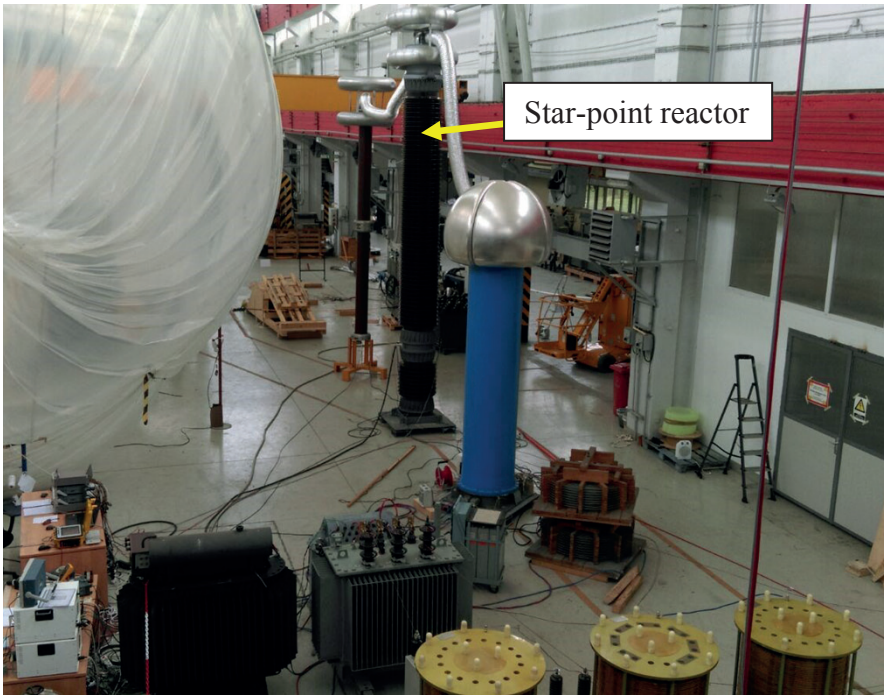

Figure 6. Test arrangement in HV laboratory during the DC current capability test

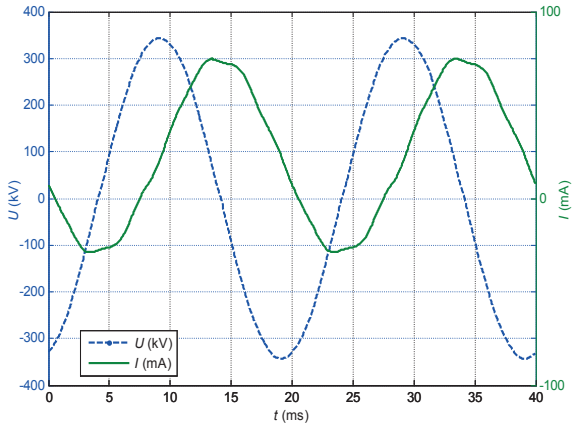

Figure 7. *U-I* waveforms in the region without saturation (I_{DC}=22.0 mA)

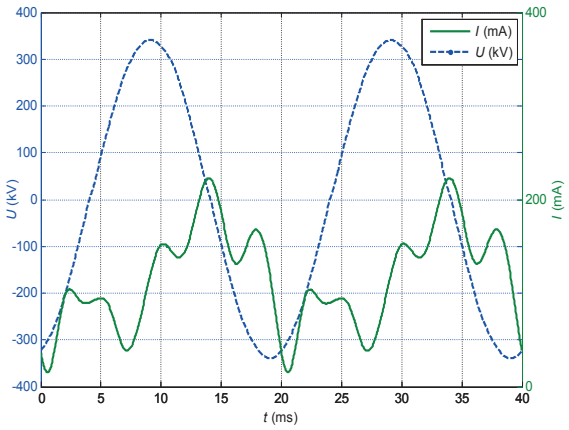

Figure 8. *U-I* waveforms in the saturation region (I_{DC}=120.4 mA)

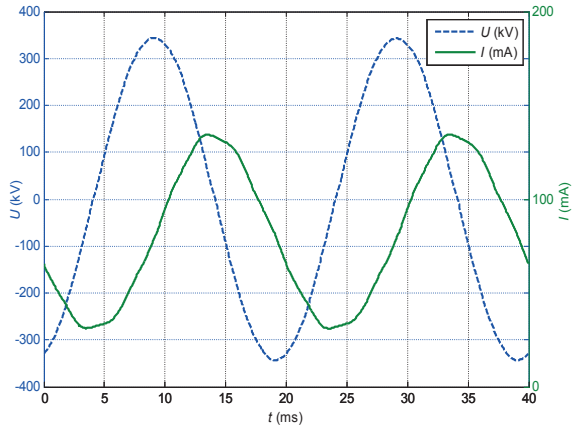

Figure 9. *U-I* waveforms for U_p=241.3 kV (I_{DC}=80 mA)

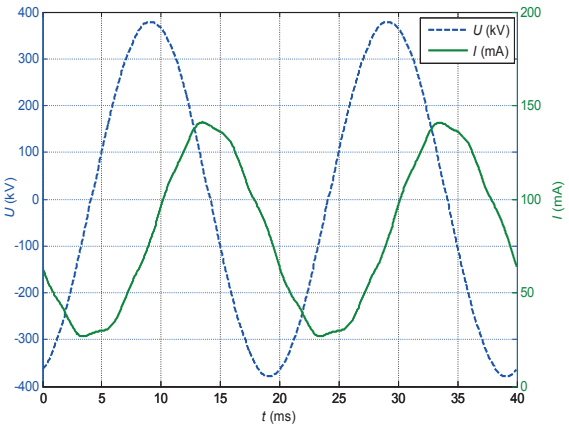

Figure 10. *U-I* waveforms for U_p=265.6 kV (I_{DC}=80 mA)

Tests results show that there was no notable change of ratio between the applied primary voltage U_p and current through shunt reactor. This indicates that AC primary voltage increase did not cause saturation of star-point reactor.

3.2. Test with fundamental voltage harmonic, superimposed third voltage harmonic and injected DC current

The test was carried out at rated primary 50 Hz voltage U_p=242.5 kV, with superimposed 37.7 kV of the 3rd harmonic (150 Hz), corresponding to 15.5% of rated voltage, while DC current is gradually increased up to 80 mA. Current-voltage waveforms for I_{DC}=0 mA and I_{DC}=80 mA are shown in Figs. 11 and 12, respectively.

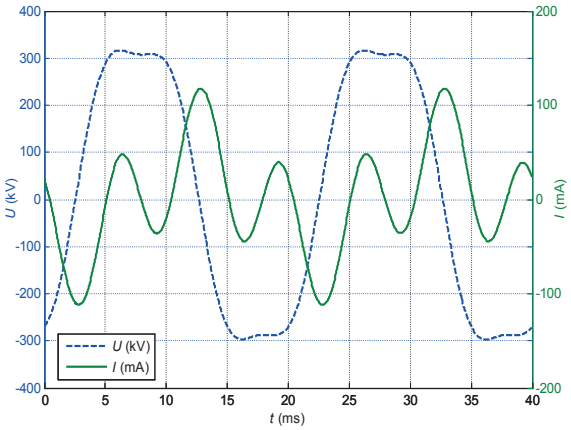

Figure 11. *U-I* waveforms for I_{DC}=0 mA

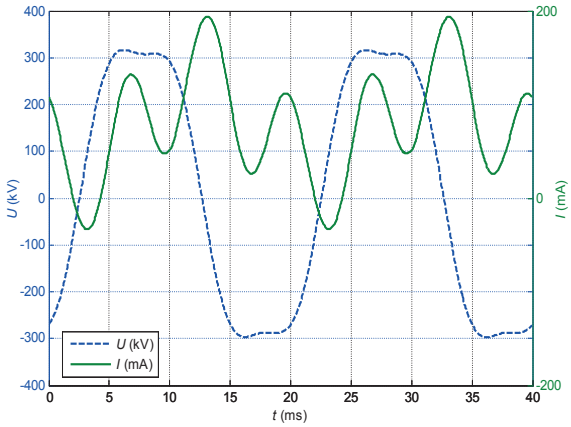

Figure 12. *U-I* waveforms for I_{DC}=80 mA

From the test results there was no notable change of AC current through the reactor. Saturation point has not been reached at 80 mA of DC current. Influence of AC 50 Hz primary voltage increase on reactor saturation is investigated. During the test, constant DC current of 80 mA was injected through reactor. Current-voltage waveforms recorded at star-point reactor for primary voltage U_p=248.6 kV and U_p=260.1 kV are shown in Figs. 13 and 14, respectively.

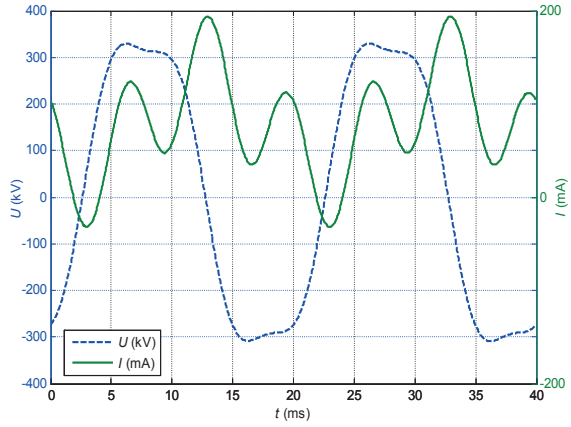

Figure 13. *U-I* waveforms for U_p=248.6 kV (I_{DC}=80 mA)

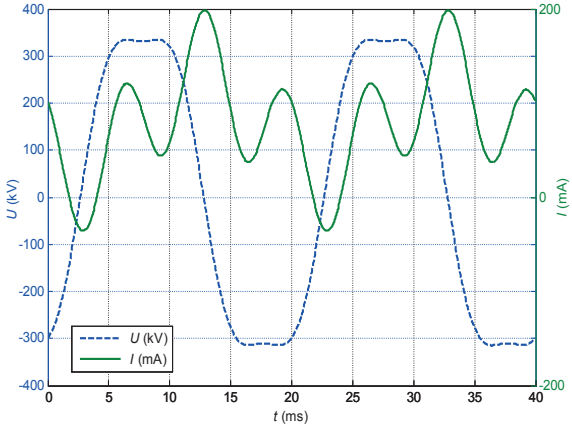

Figure 14. *U-I* waveforms for U_p=260.1 kV (I_{DC}=80 mA)

Tests results show that there was no notable change of ratio between the applied 50 Hz primary voltage U_p and current through shunt reactor. This indicates that primary voltage increase did not cause saturation of star-point reactor.

4. TEMPERATURE RISE TEST

The purpose of this test is to verify that temperatures that can damage the insulation will not be reached with the specified service conditions. The temperature rise test was carried out according to the requirements of [6] and client's request. For this test, star-point reactor was mounted vertically in a manner representative of the mounting in service. Temperature rise tests are normally performed with power frequency voltage, but the client request was to superimpose third harmonic voltage up to 15% of the applied fundamental harmonic voltage. These requirements cannot be fulfilled with standard test equipment normally found in HV laboratories. Therefore, an additional circuit for generating third harmonic voltage needs to be used along with blocking and passing filters and compensation. The test was carried out at rated primary 50 Hz voltage 242.5 kV, with superimposed 37.6 kV of the 3rd harmonic (150 Hz) and DC current 80 mA. For the temperature rise test, the same test setup is used as for the DC current capability test (Fig. 5).

Additional measuring equipment for temperature measurement and winding resistance measurement was used during the temperature rise test. The temperature rise of winding is measured by the increase in resistance (*U-I* method). Flange temperature and top oil temperature are measured with cuprum-constantan thermocouples. Thermocouple layout during the temperature rise test is shown in Fig. 15.

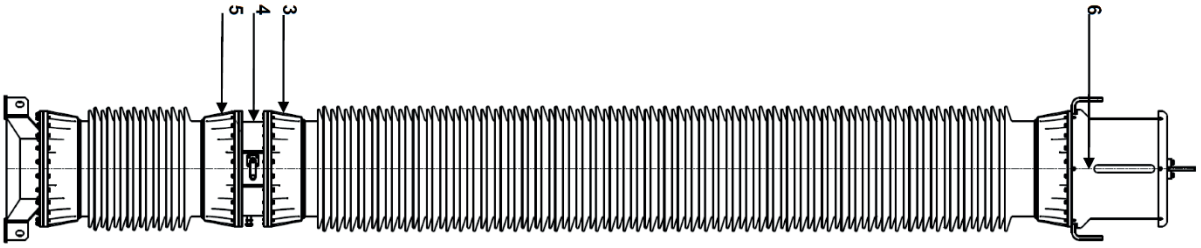

Figure 15. Thermocouple layout during the temperature rise test

Six thermocouples are used during the temperature rise test. Thermocouples 1 and 2 are used for measurement of ambient temperature, thermocouples 3-5 for measurement of flange temperature and thermocouple 6 for measurement of top oil temperature. Ambient temperature is measured with two thermocouples placed in oil containers (volume 0.5 litre). It is considered that a star-point reactor reached steady-state temperature when the rate of temperature rise does not exceed 1 K/h. The temperature rises of windings, magnetic circuits and any other parts of reactor shall not exceed values given in Table II [10], when operating under specified rated conditions. The temperature rise of the windings is limited by the lowest class of insulation either of the winding itself or of the surrounding medium in which it is embedded.

Table II. Limits of temperature rise for various parts, materials and dielectrics of star-point reactors [10]

Parts of star-point reactor	**Temperature rise limit (K)**
top oil	50
top oil, hermetically sealed	**55**
winding average	60
winding average, hermetically sealed	**65**
other metallic parts in contact with oil	as for winding

Results of temperature rise test are shown in Table III, where T_a represents average ambient temperature, T_f average flange temperature, T_o top oil temperature, R_w winding resistance and T_w winding temperature.

Table III. Results of temperature rise test

	T_a	T_f	T_o	R_w	T_w
Initial state (cold)	23.9°C	23.9°C	23.9°C	7450 Ω	23.9°C
4 hours before steady-state	25.7°C	33.7°C	42.9°C	7689 Ω	32.2°C
2 hours before steady-state	26.3°C	34.5°C	43.4°C	7701 Ω	32.6°C
Steady state	26.7°C	35.0°C	43.9°C	7715 Ω	33.1°C
Temperature rise	-	8.3 K	17.2 K	-	6.4 K

Temperature rise is less than 65 K for winding average temperature rise and 55 K for oil temperature rise, as shown in Table II. According to the test results, star-point reactor successfully passed the temperature rise test.

5. CONCLUSION

With the increasing number of HVDC converter stations being built, the requirements on high voltage apparatus also change. One of such requirements is the simultaneous AC and DC loading of high voltage apparatus. Although the applicable international standards for testing such apparatus are subject to constant further development, they do not cover all specific requests from the utilities based on different conditions in the power network. This leads to an increase in the number of special tests which are partly covered or are not covered at all by the available international standards.

In this paper, temperature rise and DC current capability tests of 420 kV star-point reactor with open core used in HVDC transmission are presented. Prior to performing these tests, a magnetic characteristic of reactor was measured by applying DC current charging/discharging method. Temperature rise tests are normally performed with power frequency voltage, but for star-point reactor the client's request was to superimpose third harmonic voltage up to 15% of the applied fundamental harmonic voltage to consider the voltage harmonic distortion which may appear in the power system at the location of star-point reactor installation. This test cannot be performed with standard test equipment normally found in HV laboratories. Therefore, a new test circuit is proposed for generating third harmonic voltage equipped with blocking and passing filters and compensation. Test circuit is suitable for testing of HV equipment with rated voltage up to 420 kV. DC current capability test is performed to determine the value of the DC current at which the saturation point is reached. In this test, DC current is injected through star-point reactor while AC voltage is applied. Two different cases are considered regarding AC voltage: test with fundamental voltage harmonic and test with fundamental voltage harmonic with superimposed third voltage harmonic. Influence of AC primary voltage increase on reactor saturation is investigated. For performing the DC current capability test, the same test circuit is used as for the temperature rise test.

Currently more than 200 HVDC systems are operating around the world and many new HVDC projects, both overhead line and cable projects, are being planned. HVDC applications are increasing steadily to meet increasing load demands or to interconnect renewable generation resources, such as wind and solar, to the main transmission network because of technical and economic advantages. Power electronics is a key enabling technology for both renewable energy generation and HVDC transmission, but also has important impacts on grid stability, high voltage apparatus and power quality because of its fast control and sensitivity to faults and other abnormal conditions in the grid. In the future it is to be expected that the number of special tests in high-voltage laboratories, such as those described in the paper, will increase due to the growing number of HVDC stations and the increasing demands on the reliability of the high voltage apparatus required by the utilities.

REFERENCES

[1] A. J. Beddard, "Factors Affecting the Reliability of VSC-HVDC for the Connection of Offshore Windfarms", PhD thesis, University of Manchester, School of Electrical and Electronic Engineering, 2014.

[2] K. Sharifabadi, L. Harnefors, H.-P. Nee, S. Norrga, R. Teodorescu, "Design, Control, and Application of Modular Multilevel Converters for HVDC Transmission Systems", Wiley-IEEE Press; 1st edition, October 2016.

[3] H. Wang, G. Tang, Z. He, J. Yang, "Efficient Grounding for Modular Multilevel HVDC Converters (MMC) on the AC Side", IEEE Transactions on Power Delivery, vol. 29, no. 3, pp. 1262-1272, June 2014.

[4] A. K. Zeimer, "The Effect of DC Current on Power Transformers" University of Southern Queensland, Faculty of Engineering and Surveying, October 2000.

[5] W. Xu, T. G. Martinich, J. H. Sawada, Y. Mansour, "Harmonics from SVC transformer saturation with direct current offset", IEEE Transactions on Power Delivery, vol. 9, no. 3, pp. 1502-1509, July 1994.

[6] IEC 61869-3, "Instrument transformers - Part 3: Additional requirements for inductive voltage transformers", 2011.

[7] I. Žiger, D. Krajtner, D. Filipović-Grčić, "DC current capability of high voltage apparatus based on the open-core concept", in Press, Electric Power Systems Research, 2017 (doi: 10.1016/j.epsr.2017.10.017).

[8] IEC 60076-6, "Power transformers - Part 6: Reactors", 2007.

[9] D. Filipović-Grčić, B. Filipović-Grčić, D. Krajtner, "Frequency response and harmonic distortion testing of inductive voltage transformer used for power quality measurements", Procedia Engineering, volume 202, pp. 159-167, 2017.

[10] IEC 61869-1, "Instrument transformers - Part 1: General requirements", 2007.

Journal of Energy
VOLUME 67 Number 2 | 2018 Special Issue
journal homepage: http://journalofenergy.com/

Advanced prevention against icing on high voltage power lines

B. NEMETH[1], V. LOVRENČIĆ[2], M. JARC[2], A. IVEC[2], M. KOVAČ[3], N. GUBELJAK[4], G. GOCSEI[1], U. KRISPER[5]
[1] Budapest University of Technology and Economics, Hungary;
[2] C&G d.o.o. Ljubljana, Slovenia; [3] OTLM d.o.o. Ljubljana, Slovenia;
[4] Universtiy of Maribor, Faculty of Mechanical Engineering, Slovenia;
[5] Elektro Ljubljana d.d., Slovenia

SUMMARY

Historical meteorological data indicates, that our weather is becoming more and more extreme. For the electrical utility operators (Distribution System Operators - DSOs and Transmission System Operators - TSOs), these changes arise in new operation challenges that need to be addressed. For example, frequent icing phenomenon affects all the components of the power line by a significant mechanical overload: it endangers the conductors, the insulators and the towers, as well. The result is often fatal and beside serious failures, it effects on operators' decisions. These not only endanger the reliability of electrical grids by the loss of a power line for weeks or even months, but in general, the safety in the surroundings of the power line. As technology advances, we will be able to collected, analyses and predict very large databases in the field of meteorology and electrical engineering. The ability of processing mentioned data, combined with know-how results in the capacity to operate power lines at their thermal limits during different ambient parameters. This technology called Dynamic Line Rating (DLR) – is not only a great way to increase the transmission capacity of a given line, but can also be effectively used to prevent, or even solve icing-related issues. Higher currents result in higher Joule-heats, that consequently heat the conductors. If limits can be reached or approached, icing can be prevented. If prevention is not possible, detection and removal of ice layer is necessary. The proper handling of this icing issues, requires advanced algorithms (expert systems) and reliable measuring equipment. The combination and synchronization between algorithms, weather service and measuring equipment is the key of the successful operation. An EU H2020 financed project called FLEXITRANSTORE has just been launched to develop a cross-country co-operation, with objective to improve anti-icing and de-icing solutions. To establish and analyse different solutions, the project includes several universities, TSOs and DSOs. To solve mentioned icing issues Budapest University of Technology and Economics' (BME) developed an advanced neural-network based algorithm which use OTLM system. It is planned to install and demonstrate the capabilities of this new technology on the DSOs grid (Electro Ljubljana - ELJ). Besides the introduction of DLR and icing, this paper also focuses on the preparation/organisation of co-operation between different companies and universities.

KEYWORDS

icing, de-icing, dynamic line rating, Flexitranstore, BME, C&G, OTLM, ELJ

INTRODUCTION OF PROJECT FLEXITRANSTORE

21.7 M Euro project »Flexitranstore« has begun on the 1st of November 2017 and will lasts for 4 years. 27 project partners with 8 demonstrations in 6 countries will provide new results in several topics including Dynamic Line Rating (DLR).

The project itself aims to contribute to the evolution towards a pan-European transmission network with high flexibility and high interconnection levels. This will facilitate the transformation of the current energy production mix by hosting an increasing share of renewable energy sources. Novel smart grid technologies, control and storage methods and new market approaches will be developed, installed, demonstrated and tested introducing flexibility to the European power system [1].

Increasing the reliability of both the distribution and the transmission grid is essential, especially in cases of unpredictable or even extreme weather conditions. During the project, a novel Dynamic Line Rating (DLR) model is going to be developed and tested. DLR enables existing power lines to be used in the same way as lines with higher rated temperature of the conductors. A de-icing algorithm to be developed will integrate the advantages of several already established DLR systems with some additional parameters in an effort to increase accuracy. Given a more precise DLR algorithm the state of the conductors during the de-icing process can be followed online. During normal operational conditions DLR constitutes an effective way to increase the transfer capabilities of a power line. In case of extreme weather conditions de-icing can prevent serious failures.

The main objectives are to demonstrate sensor technology for power system operators to effectively handle and prevent sudden and often fatal failures, especially during icing weather conditions, to increase system security and reliability by reducing icing phenomena and to facilitate cross-border power exchanges by the implementation of the described systems [2].

INCREASING TRANSMISSION CAPABILITIES – DYNAMIC LINE RATING

Today's energy consumption and energy demand is increasing. That is particularly true in case of electric power consumption. Although the transmission lines should operate at their designed voltage and ampacity, due to the increased demands, some of the lines are already operating on elevated temperatures. To resolve that issue, the capacity of the transmission network should be increased. Dynamic Line Rating is one of the most cost effective way to increase the transmission capacity of the already existing network. DLR is an operating method, which makes it possible to utilise better the network, based on real-time data and calculations.

The DLR system is based on different types of sensors, weather stations and weather forecast which provide the essential data for the system. Line monitoring sensors are complex electrical equipment which has to function reliably and properly on the conductor or near to the conductor. Therefore, these sensors have to be tested and fitted to operate in high voltage environment [3].

Having higher ampacity rates over a power line due to DLR, increased thermal stress occurs not only on the conductors, but on insulators, and on other pieces of equipment as well. Increased ampacity resulting in increased temperature of conductors brings about an increase in sag, thus electrical clearance might be violated with higher probability [4].

During DLR system implementation the first step is critical span analysis. In this phase of work all of the spans of the selected transmission line shall be examined by different aspects through calculations and simulations. Therefore, critical spans can be identified which firstly violate the regulations related to clearance, especially when the conductor operates near the designed maximal temperature or exceed this temperature even for a short period of time.

The longitudinal section of the whole overhead line has to be investigated, and critical spans shall be selected by the following criteria:

- Highest level differences between towers,

- Longest spans,
- Obstacles and terrain under the span.

The length of the span is a critical factor, because longer spans have higher sag in case of elevated temperatures. Level difference of the towers is also crucial, because in case of larger level differences the permitted sag is smaller than in case of smaller ones. Furthermore, obstacles and terrain under the span shall also be inspected.

These objects may violate clearance, because they may change after the construction of the line, too. As the result, design documentation may not take these effects into consideration (e.g. the growth of the vegetation or terrain changes due to landscaping). Figure 1 shows a part of an elevation profile of a transmission line, which is based on the above-mentioned three criteria.

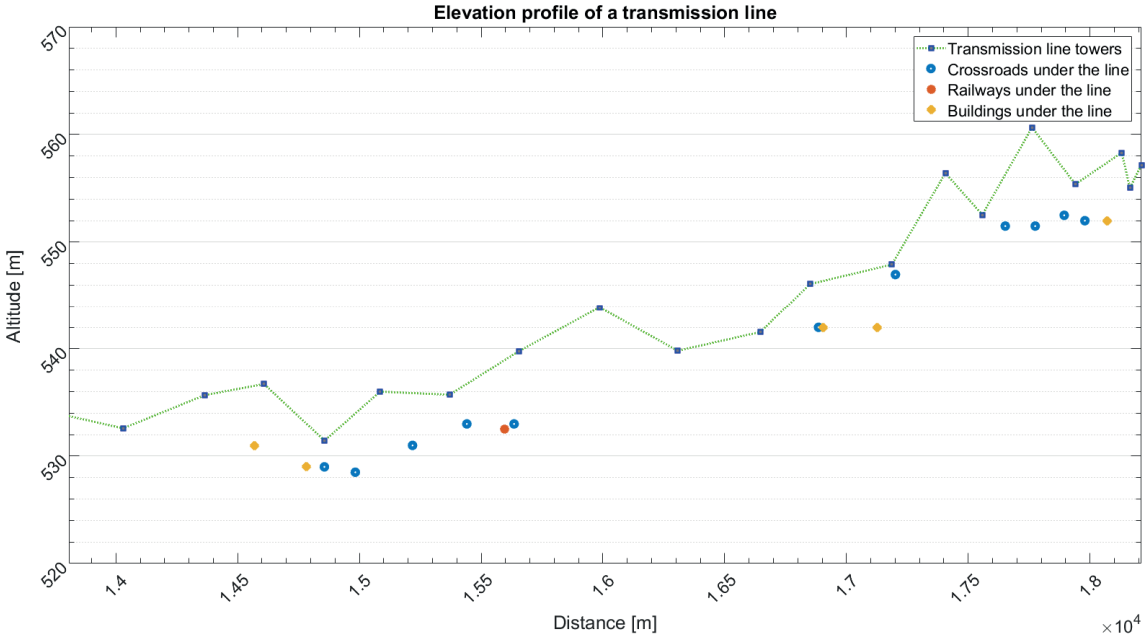

Figure 1 – Elevation profile of a transmission line (example)

To ensure that clearance regulations are not violated, critical spans shall be locally examined, and the sag of the line shall be calculated for higher temperatures than the designed to know which the thermal limit is, when the sag reach the clearance limit. In case of DLR, operating temperature might exceed the designed temperature for short time – e.g. during the use of short-time emergency rating – and the clearance regulations should be comply under all operating conditions. The transmission line sag calculations are usually carried out by modelling the sag as a parabola as it is shown in Figure 2.

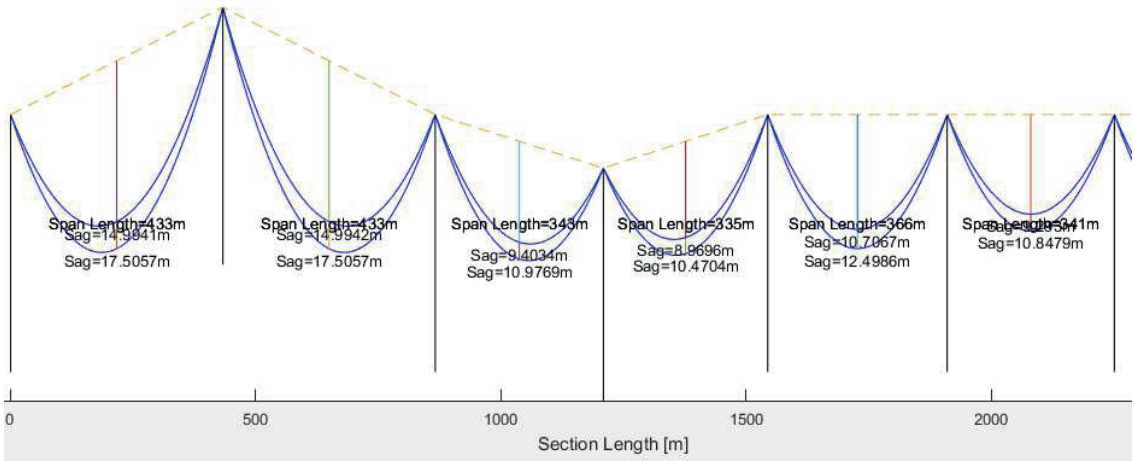

Figure 2 – Sag simulations for different conductor temperatures

BME'S WHITE-BOX AND BLACK-BOX MODELS FOR CALCULATION

Preliminary studies of wind

As several studies have shown in the past, the main cooling factor is the wind during the DLR calculations (both speed and direction).

It is common that a given direction characterizes the behaviour of the wind. This direction correlates with the strength of the wind, so the higher the wind speed is, the direction becomes closer to the dominant wind direction. Most of the studies agree that the wind speed above 5 m/s is worth to calculate with.

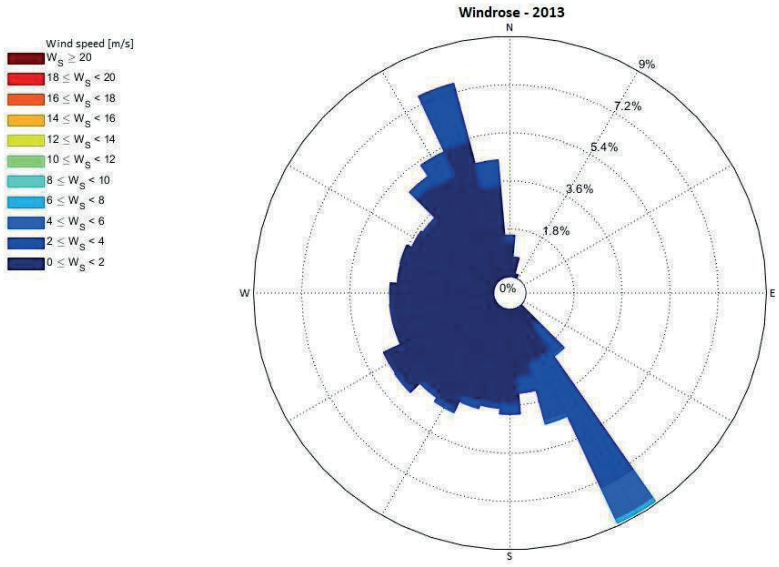

Figure 3 – Windrose (example)

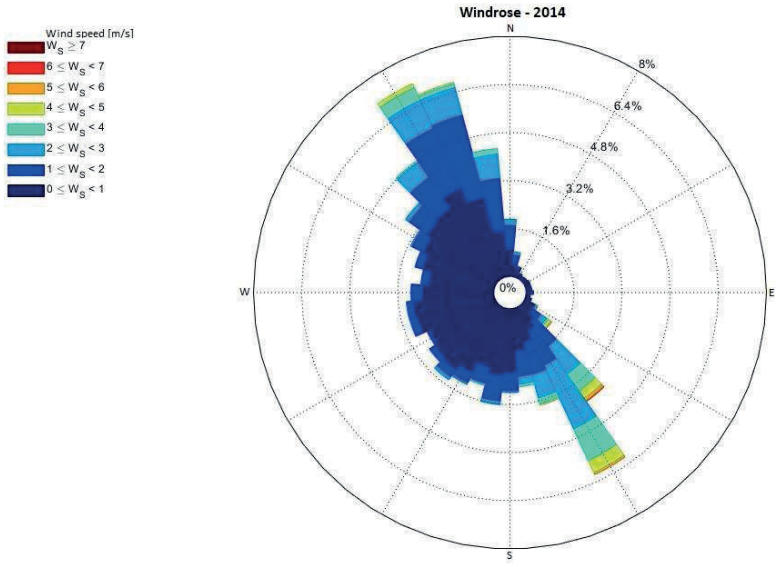

Figure 4 – Windrose (example)

Figure 4 and Figure 5 shows the windroses based on real meteorological data between 2013 and 2014. The diagrams justify the claim, that there is no characteristic win direction in case of low wind speeds – while wind speed ≤ 5m/s – thus the direction of the wind is fully stochastic. In case of higher wind speeds – while wins speed > 5 m/s – there is major direction which was south-southeast and north-northeast in this study. This study showed the wind direction cannot be accurately predicted in case of low wind speeds.

BME's extended white box model

In case of so-called »white-box« models, results of the calculations are based on equations taking the inputs as variables into consideration. An extended white box model was developed in the Budapest University of Technology and Economics (BME) based on the experiences gained during the analysis of archive weather data and the physical equations of the calculation methods. BME's extended white box model unites the international standards with the following new approaches:

- Takes into account the cooling effect of the precipitation
- Considering wind effect in different OHL sections
- Improved weather forecast processing

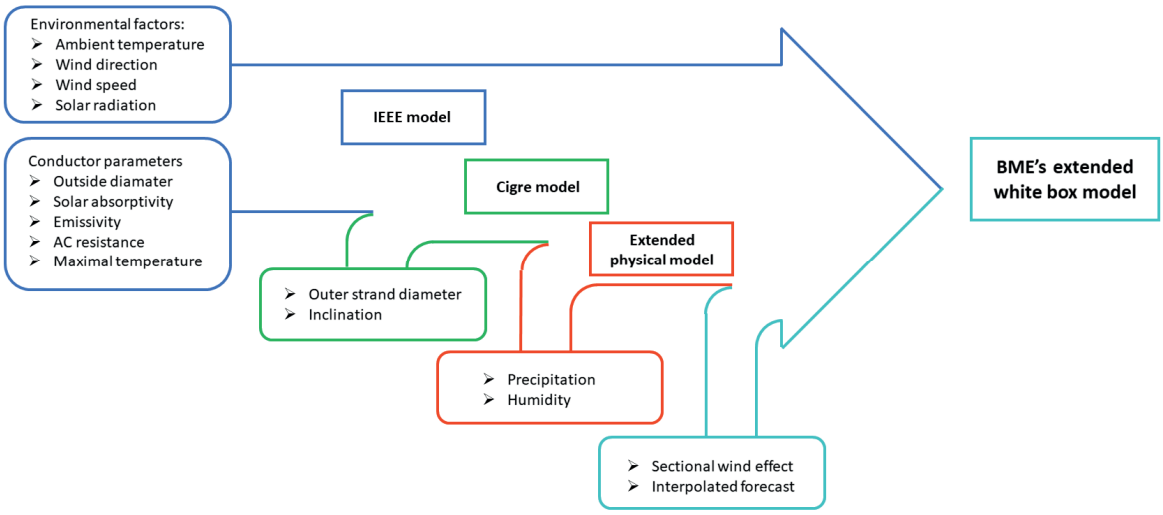

Figure 5 - Schema of BME's extended white box model

The extended physical model takes into consideration the cooling effect of the precipitation on the line, which is grant higher transmission capacity in case of rainy weather conditions. The stochastic behavior of the wind was corrected with the consideration of the wind in different OHL sections, thus the local thermal overloads of the conductor was eliminated. The improved weather forecast processing module increases the time resolution of the weather forecast with various interpolation methods.

BME's black box model

Currently there are two well-known algorithms to determine the ampacity of a given power line by the white-box model: CIGRE [5] and IEEE [6] methods. In general, CIGRE model takes more environmental factors into account than IEEE. In terms of »black-box« models, no equations are used. In the algorithm of BME, a novel approach has been developed and introduced based on the use of soft-computing methods (neural networks). Figure 6 shows the applicability of the neural network for DLR calculations:

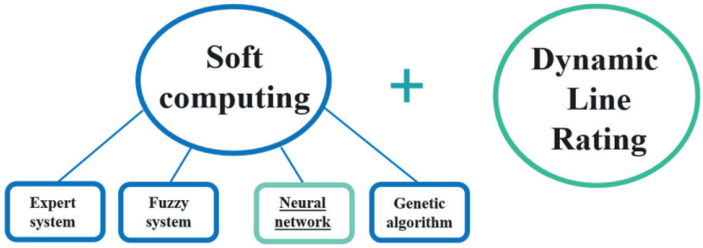

Figure 6 – Intelligent agents and DLR

The DLR model of the CIGRE and IEEE standards are empirical ones which means that there are some simplifications (cooling effect of the precipitation) in both of them. Moreover, there are special circumstances when these models provide different limit values for the current (e.g. when the wind speed is above 5 m/s). Due to this fact, it may be worthwhile investing new models based on different approaches. The examinations

of the soft computing methods have shown that the use of neural network could be promising, because these kinds of networks are able to learn and handle complex data-sets. In BME's model, there are 2 main steps for the determination of the maximum current value: the calculation of the temperature of the line and the determination of the DLR value itself.

For the calculation of the temperature of the conductor, a neural network is applied. There are 4 inputs of the network, such as ambient temperature, wind speed, solar radiation, and the real-time current, while the output of the model is the temperature of the conductor. Running the simulations have shown, that a 4-layer, forward cascade neural network has the lowest error, where the number of the neurons are 4 in the input, 32 in the hidden and 1 in the output layer as it shown in Figure 7. Figure 8 illustrates the validation of the used neural network.

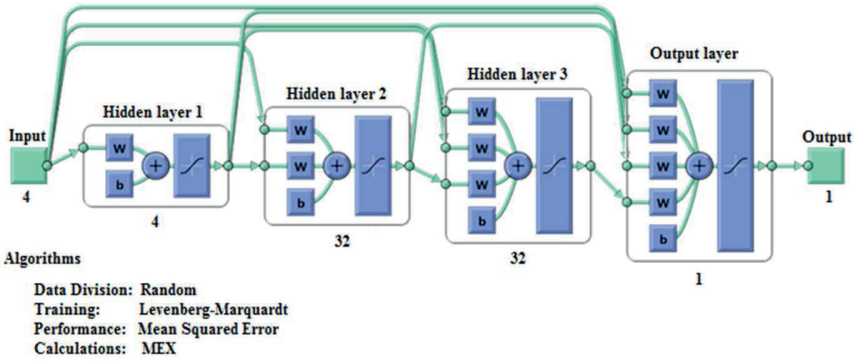

Figure 7 – The structure of the chosen neural network

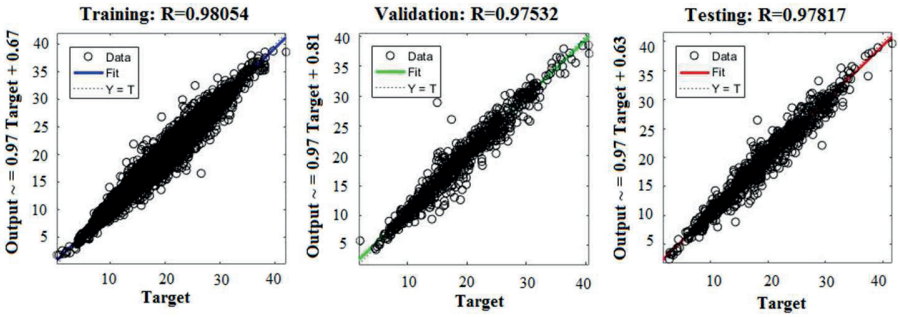

Figure 8 – The training, validation and test of the neural network

The average error of the network is about 2-3 °C, which is shown in Figure 9. This error is acceptable, because the average deviation of most sensors is ±2°C.

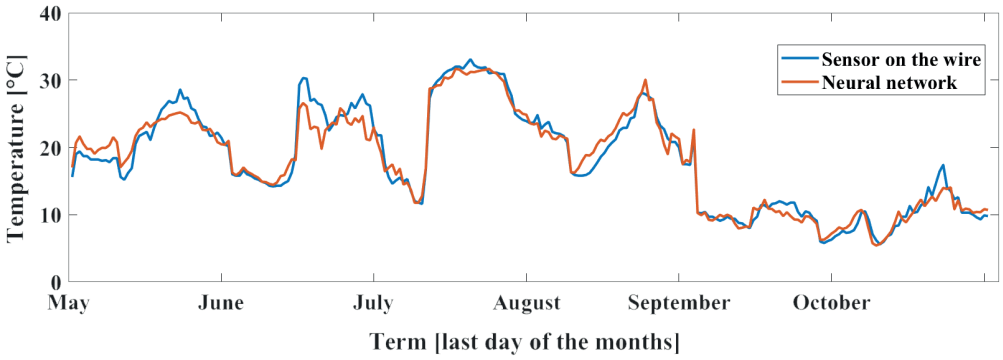

Figure 9 – The temperature of the wire as a function of time

As the line temperature is available, the DLR value can be calculated from a heat equation by determining the extra heat gained from the increased current of the grid as it shown in Figure 10. By using this calculation method, it is important to not exceed the temperature limit of the conductor.

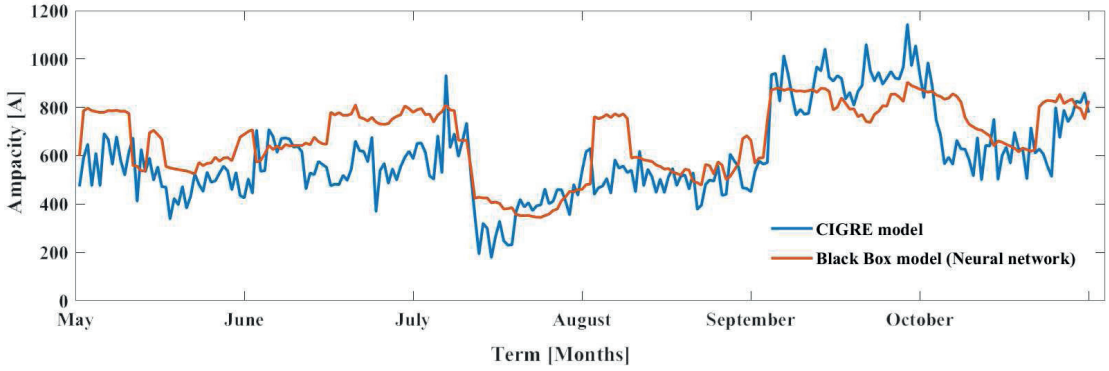

Figure 10 – DLR value of the last days of the 6 months as a function of time

The biggest advantage of the black box model is that temperature sensor for the validation of the results is installed on the line, while all the environmental parameters can be taken into account.

SPECIAL APPLICATIONS OF DLR: ANTI-ICING AND DE-ICING

Atmospheric icing may cause serious damage in infrastructures including power grid equipment, such as overhead line towers and power lines themselves. The increased mechanical load due to the ice accretion may even cause the power lines to collapse, which is not only dangerous to the environment, but may compromise the power grid's stability, as well.

The process of ice accretion can be separated to two main groups: dry growth and wet growth icing. During the first type, there is no precipitation. The humidity of air freezes onto the bare conductor in a more or less consistent thickness. The ambient temperature range – when this phenomenon may occur – is really wide. When the humidity is high enough, and the wind speed is significant, as well, hard rime develops from around 0 □ to -8 □. When temperature is between -8 □ to -20 □ and of course, there is sufficient humidity, soft rime sticks to the surface.

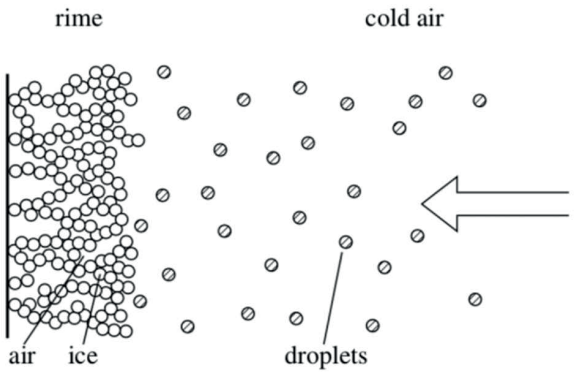

Figure 11 – Dry growth [5]

As for the wet growth, the ice accreting by supercooled water droplets hitting the conductor's surface (called freezing rain) or from wet snow sticking to the conductor. In both cases, the temperature is around 0 □. These two types may inflict notable mechanical load in a short period of time.

B. Nemeth, V. Lovrenčić, M. Jarc, A. Ivec, M. Kovač, N. Gubeljak, G. Gocsei, U. Krisper, Advanced prevention against icing on high voltage power lines, Journal of Energy, vol. 67 Number 2 (2018), Special Issue, p. 73–85

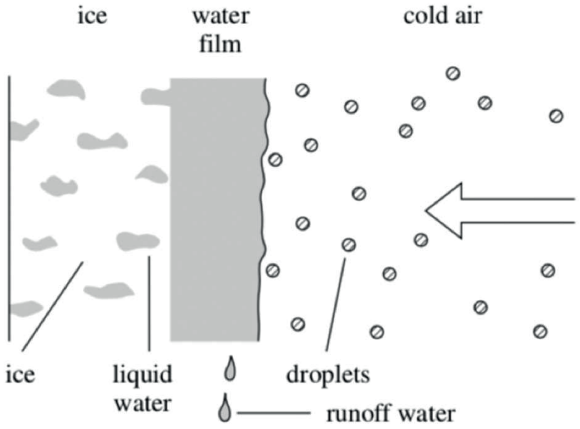

Figure 12 – Wet growth [5]

DLR is an effective technique not only for ampacity calculation, but to use increased and controlled currents for anti-icing and de-icing purposes, as well. In order to prevent or at least predict events with serious consequences, several models [6], [7] were created or updated to calculate ice growth properly, especially on cylindrical shape because of the application. The icing process has a lot of external influences which are hard to describe and even a small inaccuracy during modelling, measuring, or calculating may cause completely different results in prediction [5]. If the accreted ice's weight is high enough to cause damage, then some de-icing methods need to be performed on the power line. There are several techniques [8] for this application, but with improper implementation, the melting attempt itself can endanger the stability of the power grid.

In order to prevent mentioned icing the mathematical model has been developed for sag and horizontal force calculation. The model was developed as a computer application. Model includes installation conditions and conductor characteristics and determines the interdependence between conductor sag and horizontal force for actual conductor temperatures. The computer application is an integral part of OTLM software. The catenary represents a starting condition for monitoring conductor behaviour on the span between two towers. Temperature of conductor, ambient conditions and the electrical line current cause changes in conductor length and consequently a change in catenary geometry. The developed mathematical model includes mechanical and physical characteristics of the conductor, conductor weight and sag size for the calculation of internal forces. Based on optical-laser sag measurements, a calibration curve was developed between the sag/angle/temperature/tensile force in the OHL conductor, which applies to normal working conditions or operational load [8]. This enables us to estimate the change in catenary form in a wider temperature range.

The measurement of conductor catenary on different conductor temperatures and ambient temperature shows an excellent correlation between measured sags in the field and the sags that were determined with a mathematical model "OTLM-SAG". It confirms that the data can be used as an alarm when the critical sag are reached. The described application offers the user real-time monitoring and it helps a safe operation of the chosen OHL.

Combining measurements of conductor geometry and sag at several conductor temperatures with software is using for calibration of the sag and angle function. Ensuring conformity is crucial for the implementation of the function ICE-ALARM, since a continued growth of discrepancy between the measured and calculated angle in ambient conditions is a sign of glaze ice on the conductor.

The model as the computer application takes into account the geometry of the catenary curve after the conductor mounting, depending on the temperature of the conductor, where a laser measurement of the geometry of the catenary curve was made. The sag and thus the geometry of the catenary's conductor change according to the tensile force relationship by changing the meteorological conditions and the temperature of the conductor.

The mathematical model re-calculates the new geometry of the catenary and the tensile force depending on the changes in temperature, while the measured angle of the inclination of the conductor at the position of OTLM

device serves as the control value. The model is based on the independent treatment of the catenary curve of the conductor from the place of clamping on the bracket and/or insulator to the lowest point and/or place of the maximum sag for each side.

The parameters of the catenary curve at the temperature of the wet growth represent the initial state of the activation of the ICE-ALARM computer algorithm.

If favourable conditions for the formation of ice appear during the continuous monitoring of the conductor condition and condition on the route in the surroundings of the meteorological station then it is possible to estimate the amount of additional loading and the ice thickness on the basis of the change in the angle of inclination and by knowing the tension-deformation behaviour of the conductor at increased loading.

Figure 13 shows the change in the angle in accordance with the model and the angle measured by the inclinometer. White circles present actual average angles as a function of average temperature of conductor measured in the time interval of 30 s.

Red circles present the expected behaviour of the conductor and/or a change in the angle due to the build-up of the ice on the conductor.

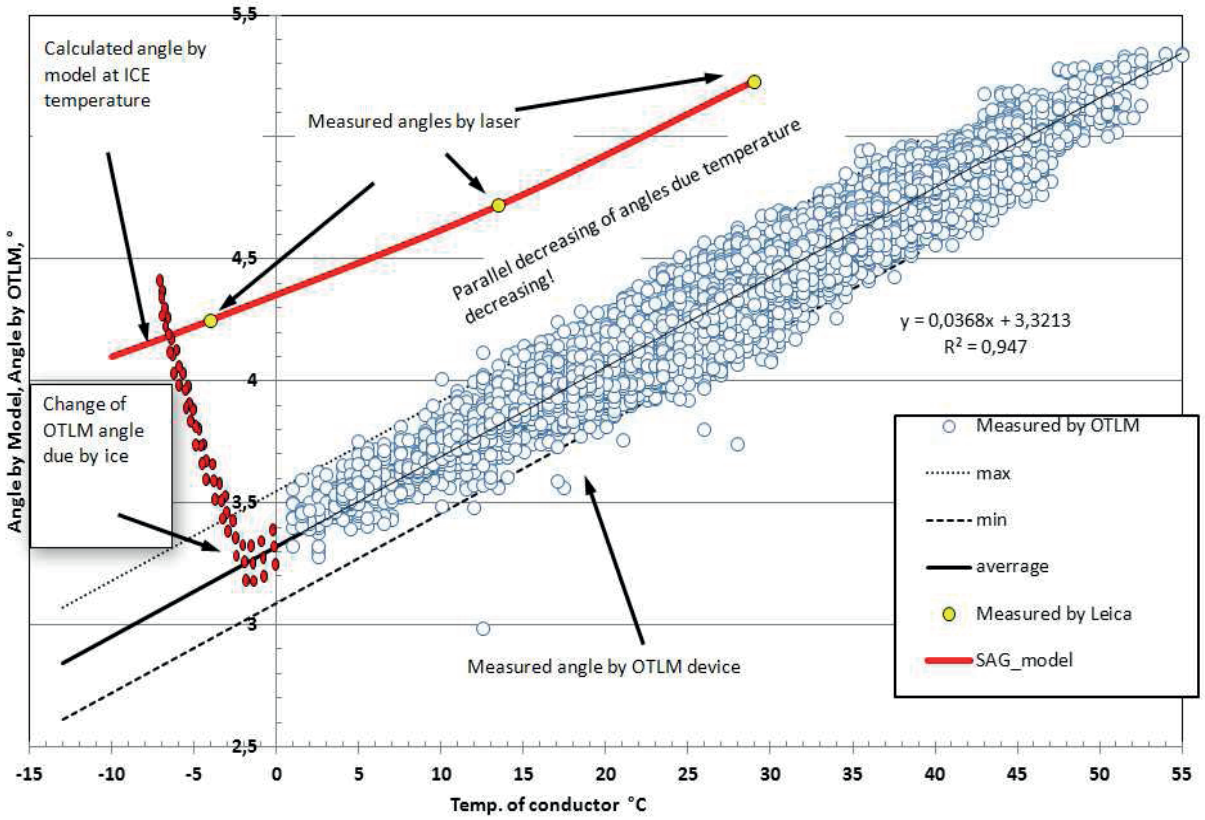

Figure 13 – Change in an angle at the OTLM device position depending on temperature

B. Nemeth, V. Lovrenčić, M. Jarc, A. Ivec, M. Kovač, N. Gubeljak, G. Gocsei, U. Krisper, Advanced prevention against icing on high voltage power lines, Journal of Energy, vol. 67 Number 2 (2018), Special Issue, p. 73–85

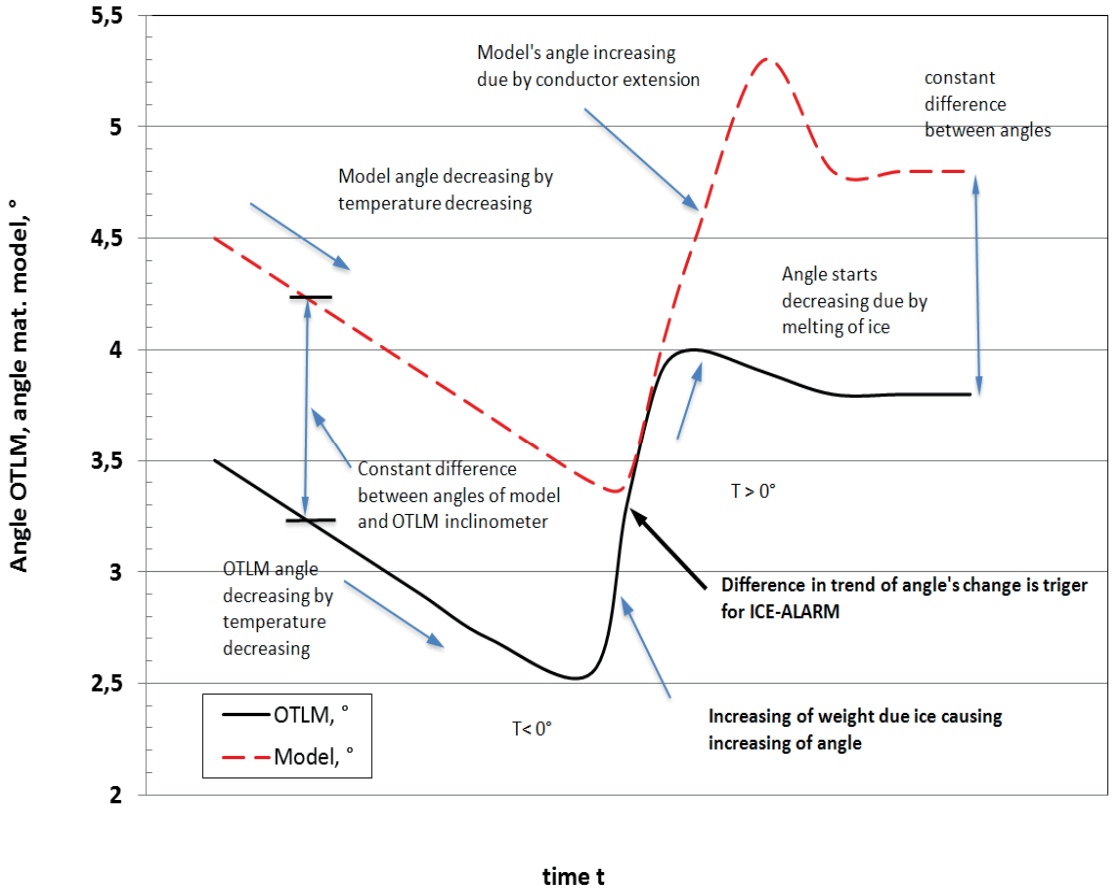

Figure 14 – Change in an angle of inclination during the activation of ICE-ALARM and melting of ice

The continuous line in Figure 13 represents the angle of inclination depending on temperature according to the mathematical model. At the temperature of the freezing rain – 4 °C the angle is the same, as shown in Figure 13. If an angle significantly increases in the meteorologically favourable conditions and the temperature inversion and if the calculated angle significantly differs from the angle measured by inclinometer, the application informs the operator that ice has built up on the conductor.

Figure 14 shows the expected change in the angle at the position of the OTLM device according to the model and the angle measured through the time interval during the detection of ice build-up on the conductor. The reliability of the ice build-up measurement depends on the accuracy of angle measurement of +/- 0.25° and causes a time lag during the beginning of ice build-up and the beginning of the ICE-ALARM activation.

The application is activated only after the measured change in angle of inclination is larger than the statistical error of an angle measurement. ICE-ALARM warns the operator that an increase in the current is required. The larger current gradually increases the temperature of the conductor, but the ice can still build up, elongating the conductor and consequently increasing the angle of inclination. Based on the characteristic of the elastic and constant elongation of the Al-Fe (ACSR) 240/40 conductor recorded in the laboratory, it is possible to determine and monitor the elongation [9]. The model (red hatched line in Figure 14) monitors the elongation of the conductor and re-calculates the change in the angle, accordingly. At the moment, when the ice thickness begins to decrease (the highest value on the continuous line in Figure 14), the angle measured by the inclinometer in the OTLM device also starts reducing. When all of the ice has melted, a new geometry of the catenary curve and/or a new sag of the conductor and new initial position before the new build-up of the ice are obtained, as it has been simulated by a laboratory testing of the conductor.

Parameters of the catenary curve were monitored in the adequately long time period and under various weather conditions and currents in order to develop a mathematical model in form of the mathematical algorithm that determines the expected geometry of the catenary curve and the conductor angle of inclination at the position of

the OTLM device, as determined DLR concept. When discrepancy between the measured and the expected angle of inclination outside the tolerance interval of deviations is observed, the algorithm for the re-calculation of the change in the catenary curve is started due to the additional ice load causing an elongation of the conductor on the span. The elongation corresponds to the additional tensile force calculated in accordance with the model. Tensile testing of the conductor was necessary to determine the dependence of the tensile force to the elongation.

Figure 15 presents the relations between the total angle of inclination, additional tensile strain in the conductor and ice thickness. The angle to ice thickness dependence is linear, while the increase in horizontal (shear) strength up to the destruction force of 86.4 kN is exponential.

Figure 15 shows also an increase in the force during the ice build-up depending on the g factor and the angle on the location of the OTLM device. The initial value of the force equals the initial tensile strain in Figure 15, and amounts to 15.25 kN on one side and to 15.24 kN on the other one, at the initial angle of 4.25° at the position of the OTLM device. The increase is possible only up to critical fracture strength of the tensile force of the conductor, which amounts to 86.4 kN. In case of the presented span it corresponds to the gravity factor of 9.2·g and an increase in the angle by 4.56° and/or to 8.24°, as shown in Figure 15.

Figure 15 presents the relations between the total angle of inclination, additional tensile strain in the conductor and ice thickness. The angle to ice thickness dependence is linear, as evident in Figure 15, while the increase in horizontal (shear) strength up to the destruction force of 86.4 kN is exponential.

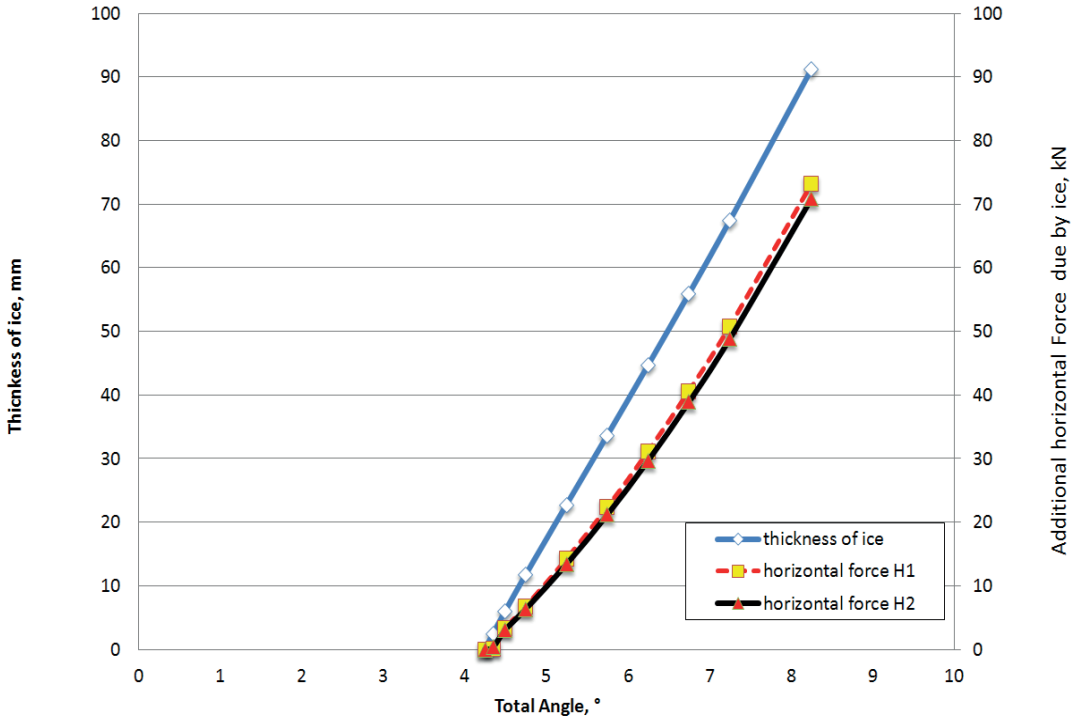

Figure 15 – The relation between ice thickness, the angle of inclination and horizontal forces

CONCLUSIONS

DLR is a novel, effective and promising technique not only to increase transmission capabilities, but in some cases (like extreme weather conditions), precise control of ampacity allows its use for anti-icing and de-icing purposes.

The development of the ICE-ALARM application is based on the existing computer algorithm in the OTLM device. The developed computer algorithm is based on the mathematical model for a re-calculation of the sag and tensile strains in the conductor. It takes into account the actually measured form of the catenary curve of the conductor on the presented span at the conductor temperature measured by OTLM as the initial state. Based

on the knowledge about the change in the sag of the catenary curve and the tensile forces dependence on the temperature of the conductor and monitored weather conditions, it is possible to determine the moment of activation the ICE-ALARM application

In the framework of project Flexitranstore, there is a great opportunity for the development of these applications through the test of several DRL sensors from different manufacturers. From the results, not only the precision of sensors, but efficiency of the algorithms will be seen clearly.

ACKNOWLEDGMENT

This project has received funding from the European Union's Horizon 2020 research and innovation programme under grant agreement No 774407.


SUPPORTED BY THE ÚNKP-17-2-II NEW NATIONAL EXCELLENCE PROGRAM OF THE MINISTRY OF HUMAN CAPACITIES

REFERENCES

[1] http://www.flexitranstore.eu/The-project, (date of visit: 24 April 2018)
[2] http://www.flexitranstore.eu/Demo-3, (date of visit: 24 April 2018)
[3] T. Viola, B. Németh, G. Göcsei "Applicability of DLR sensors in high voltage systems" (6th International Youth Conference on Energy (IYCE), Budapest, Hungary, 2017)
[4] D. Balangó, B. Németh, G. Göcsei "Predicting conductor sag of power lines in a new model of Dynamic Line Rating" (IEEE Electrical Insulation Conference (EIC), Seattle, WA, USA, 2015)
[5] Cigre 601 WG B2.43 – Guide for thermal ratin calculations of overhead lines, 2014
[6] IEEE Standard for Calcating the Current Temperature of Bare Overhead Conductors, Transmission and distribution comittee of the IEEE Power Engineering Society, IEEE Std 738-2006
[7] C. Volat, M. Farzaneh, A. Leblond "De-icing/Anti-icing Techniques for Power Lines: Current Methods and Future Direction" (IWAIS XI, Montréal, June 2005)
[8] Maurice Huneault, Christian Langheit, Josée Caron: Combined Models for Glaze Ice Accretion and De-Icing of Current-Carrying Electrical Conductors, IEEE Tractions on power delivery, Vol. 20, No. 2, April 2005
[9] Pierre McComber , Jacques Druez , Jean Laflamme, A comparison of selected models for estimating cable icing, Atmospheric Research Vol. 36 No. 207-220, 1995
[10] L. Makkonen "Models for the growth of rime, glaze, icicles and wet snow on structures "Phil. Trans. R. Soc. Lond. Phil. Trans. R. Soc. Lond. A (2000) 358, 2913–2939, 2000)
[11] V. Lovrenčić, N. Gubeljak, B. Banić, A. Ivec, D. Kozjek, M. Jarc "On-line monitoring for direct determination of horizontal forces vs. temperature and incline angle of transmission conductor" (11th Symposium on power system management HRO-CIGRE, Opatija, Croatia, November 2014)
[12] N. Gubeljak, B. Banič, V. Lovrenčić, M. Kovač, S. Nikolovski "Preventing transmission line damage caused by with smart on-line conductor monitoring" (Proceedings of 2016 International Conference on Smart Systems and Technologies, (SST), Osijek, Croatia, October 12-14, 2016)

Journal of Energy
VOLUME 67 Number 2 | 2018 Special Issue
journal homepage: http://journalofenergy.com/

REGIONALY IMPORTANT SINCRO.GRID SMART GRID PROJECT

S. JAMSEK*
ELES
SLOVENIA

S. TOT
ELES
SLOVENIA

M. LASIC
HOPS
CROATIA

I. PERISA
HEP ODS
CROATIA

M. MIKLAVCIC
SODO
SLOVENIA

SUMMARY

Regional transmission and distribution challenges has evolved and changed a lot in recent years. Four contradictory influences increasingly affected the operations of Slovenian and Croatian electricity systems. Regional electricity systems experienced increasing support of RES integration to meet the EU targets, a lower electricity consumption due to the economic crisis, a growing lack of centralized electricity production for electric system support and the high interconnectivity between the neighboring control zones. TSOs and DSOs observed growing network overvoltage issues as well as a decrease in secondary reserve capacities. Such situation starts to impact national and regional renewable integration targets affecting the security of supply at European level. SINCRO.GRID joint investment project addressed the above-mentioned issues in a sustainable manner. Such cross-border systemic approach will bring synergetic benefits. It will enable an acceptable level of security of operation for at least the next ten years hosting levels of RES in line with the trends foreseen to reach the 2030 targets safely. The project is going to integrate new active elements in the transmission and distribution grids. It leans on the following main pillars: deployment of six compensation devices, deployment of advanced dynamic thermal rating (DTR) systems, deployment of electricity storage systems, integration of distributed renewable generation (DG) and deployment of a virtual cross-border control center (VCBCC). A key aspect of the SINCRO.GRID project lies in the synergy brought by the simultaneous innovative deployment of a portfolio of mature technology-based solutions bring high benefits and positive externalities for the region and European Union.

KEYWORDS

Regional Impact – Innovation - Project – Investment - Smart Grid - Compensation Devices - Electricity Storage - Virtual - Cross-border - Control Center - Dynamic Thermal Rating - Distributed - Renewable Generation - Overvoltage - Secondary Reserve.

1 INTRODUCTION

Regional transmission and distribution challenges has evolved and changed a lot in recent years. SINCRO.GRID is a project proposal of four promotors from two neighboring countries as an answer to these challenges and network issues using a systemic approach. Storyline [1] of the project describes the origin and its impact addressing different stakeholders. The outline of project storyline is presented in this paper. Comprehensive information is given about its main components as well as description of project benefits and costs. The project achieved PCI status in 2015 and obtained European co-funding on the second call for proposals in 2016 (CEF-Energy-2016-2). An important project success factor is achievement of positive externalities along three lines: macro-regional security of supply, solidarity with other countries and technological innovation with replication potential.

2 ORIGIN AND IMPACT OF THE PROJECT

Primary tasks of Transmission System Operators (TSO) are enabling security of operation, facilitation of regional markets and integration of renewable energy sources (RES). Thus, development of grid infrastructure, supporting technologies and mechanisms are key elements for proper and timely integration of additional RES. All abovementioned results in network development plans, market and grid connection activities. In addition, TSOs also address network-ageing issues and weather related risks with technical solutions that keep the electric system secure at acceptable costs.

In recent years, the Slovenian and Croatian electricity systems have been increasingly challenged by four contradictory influences affecting the operations of both electricity systems:

1. Support of RES integration to meet the EU targets,
2. A lower electricity consumption due to the economic crisis,
3. A growing lack of centralized electricity production for electric system support,
4. The high interconnectivity between the neighboring control zones.

Consequently, the Slovenian and Croatian TSOs and DSOs observe growing network overvoltage issues as well as a decrease in secondary reserve capacities in the recent years. Security of supply is therefore at stake and has already had an impact on national and regional RES integration targets.

The Slovenian and Croatian TSOs and DSOs started separately addressing these issues in 2014. Classical engineering approaches to address them were taken into account in the two existing TYNDPs. The implementation of technical measures within each control zone was studied first, with a common conclusion that:

- Uncoordinated actions taken in one of the two control zones would significantly impact the other since these two control zones are highly interconnected;
- A progressive deployment of technological solutions would be less efficient since the same issues would resurface soon, leading to repeated investments in order to keep the security of operation above the bottom line;
- In the long run, uncoordinated approach would never lead to a satisfactory level of security of operation while allowing for hosting higher levels of RES integration and maintaining a sufficient level of ancillary services in both electricity systems.

Therefore, joint actions would create synergies and solve the problem in a sustainable way.

The TSOs and DSOs therefore agreed to work together to address all the pending issues and designed a joint cross-border systemic approach to bring enduring solutions to all of the four above issues at once. They end up with the SINCRO.GRID investment project: it is an innovative system integration of several mature technology components where synergies among all the proposed solutions are searched to maximize the investment impact onto both electric systems and create further regional benefits. SINCRO.GRID project will deliver an increased and acceptable level of security of operation for at least the next ten years, with no additional requirements for repeated investments to maintain the acceptable security level and at the same time the possibility to host increasing amount of RES integration to reach the 2030 targets in an integrated and competitive market.

The SINCRO.GRID project integrates new active elements in the transmission and distribution grids, which are managed via a virtual cross-border control center involving advanced data management, common system optimization and generation/consumption forecasting, thanks to an increased cross-border cooperation between TSOs and DSOs.

A key aspect of the SINCRO.GRID project lies in the synergy brought by the simultaneous deployment of a portfolio of mature technology-based solutions: jointly, they bring high benefits and positive externalities. Those synergies are illustrated below by Figure 1 while the VCBCC allows for orchestrating the whole portfolio of solutions.

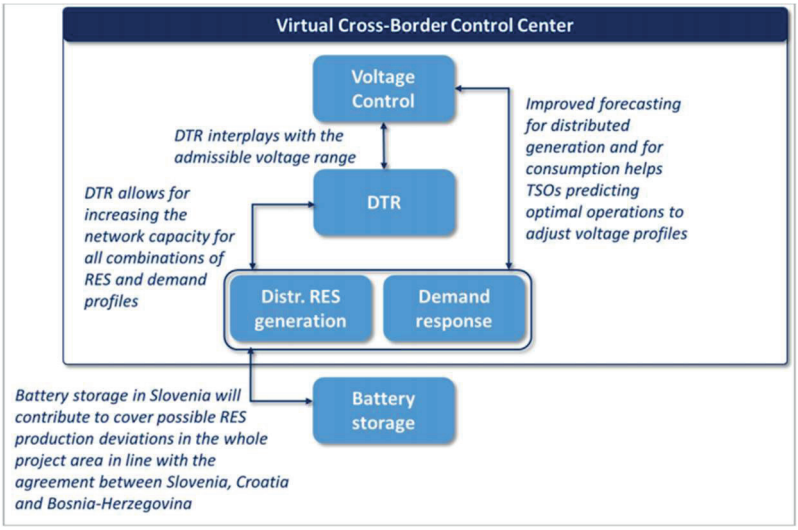

Figure 1: SINCRO.GRID synergies

Bringing these components jointly into play is technically challenging: experience gained can be knowledge-transferred to others DSOs and TSOs.

National regulatory authorities (NRA) of Slovenia and Croatia have examined the SINCRO.GRID project: a strong support was given by the two NRAs, however, cannot commit to full project cost recovery by network tariffs. Firstly, the economic conditions in Slovenia and Croatia do not allow for making network users support the full project costs. Economic simulations show that the transmission tariff in Slovenia would increase up to 9%, which would be unbearable for users connected to the transmission network. Second, full inclusion of the project by NRAs would render it necessary to defer or cancel other projects, which have been included in the national TYNDPs, causing other potential system security issues coming from network ageing or weather-related issues not any more addressed by the reshuffled portfolio of foreseen investments. For example, project Koper-Izola-Lucija internal line and various transformer upgrades in Slovenia, 110 kV Adriatic undersea cable projects connecting islands of Krk and Brac with mainland and revitalization of various aged overhead lines (220 kV OHL Zakucac-Bilice, 110 kV OHL Matulji-Lovran-Plomin, etc.) in Croatia would need to be deferred. As this would cause consumer security of supply issues investment deferrement is not viable. Thus, the current technical, economic and regulatory framework in Slovenia and Croatia allows for covering at most 50% of the TSOs' eligible investment costs.

The project cost-benefit analysis (CBA) [2] shows that on top of the benefits brought to the project promoters (already taken into account in the financial net present value FNPV), other positive externalities are brought by the project along three lines:

1. Macro-regional security of supply: the connection of new RES-based electricity generation as well as provision of ancillary services is provided in a securely manner and has an impact on a wider regional level. This increased regional security of supply improves the security of supply at European level since the area is hosting major transit flows from East (Bulgaria / Romania / Ukraine) to West (Italy / Switzerland / France / Germany). Overall, this project improves the EU Internal Electricity Market by increasing potential for transits arising from regional electricity sources (RES and other) without new interconnectors. This would improve the liquidity and resilience of the energy system and would allow full use of the region's energy efficiency and renewable energy potential.

2. Solidarity with other countries: mostly all neighboring countries of Slovenia and Croatia (e.g. Hungary, Austria, Italy, etc.) will directly benefit from the improved security of operation in Slovenia and Croatia. In particular, Bosnia and Herzegovina will draw directly upon the available sources to activate power reserves in the Slovenia-Croatia-Bosnia control block more efficiently. This will be more and more relevant when unpredictable production from renewable energy sources makes it more difficult to ensure a safe and reliable operation of interconnected electric power systems.
3. Technological innovation with replication potential: at a time where one of the next Horizon2020 call for proposal invites research and innovation activities about "Tools and technologies for coordination and integration of the European energy system", SINCRO.GRID delivers five synergetic technology building blocks which meet some of the Horizon2020 research and innovation specifications. Here lies the potential for replication, where the first TSOs for the deployed solutions are the other regional TSOs, which will learn from this systemic approach in view of preparing the possible implementation of similar technology building blocks.

The SINCRO.GRID project promoters applied for CEF funding, proposing an innovative systemic approach integrating several innovative, yet mature, technologies to solve short term security of supply issues impacting Slovenia and Croatia. This will in turn progressively allow the connection of new RES-based electricity generation in these Member States and the SEE region. Co-funding was awarded on the second call for proposals in 2016 (CEF-Energy-2016-2).

3 MAIN COMPONENTS OF THE PROJECT

The concept of different technological solutions put together into the smart grid project solution SINCRO.GRID is shown on Figure 2.

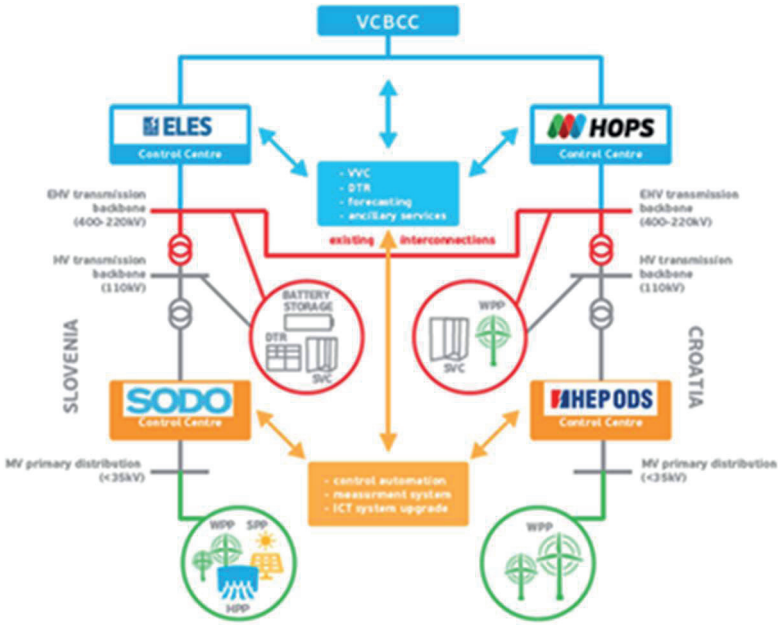

Figure 2: The SINCRO.GRID Project structure

The main components of the project are:

- The deployment of compensation devices to address overvoltage and voltage instability issues within the transmission grid. Multiple reactive power compensation devices will be implemented throughout Slovenia and Croatia (3 locations in Slovenia and 3 locations in Croatia) to tackle the rising problem of voltage control. Common approach and joint cross-border coordinated operation of these devices will bring positive effects to electric power systems of Slovenia and Croatia and neighboring systems as well.

- The deployment of advanced dynamic thermal rating (DTR) systems in both the Slovenian and Croatian transmission grid, tailored to operation under alpine weather conditions and rough terrain. Methods and software are being developed to deal with the highest possible power flows of the lines, considering all weather situations. DTR system uses different heterogeneous subsystems from different vendors, and the results of the calculations are aggregated and are shown in the network control center by means of a visualization platform.
- The deployment of electricity storage systems. Batteries with a capacity of 10 MW will be installed in Slovenia to support the solidarity agreement among Slovenia, Croatia and Bosnia-Herzegovina regarding the secondary active power control.
- The integration of distributed renewable generation (DG). In Slovenia, 2 MW of DG sources with the ability to accumulate primary energy (small hydro, biogas) are integrated into the virtual power plant for the same purpose as for the above batteries. An advanced, short-term forecasting tool for demand and DG generation is established at DSO and TSO levels.
- The deployment of a virtual cross-border control center (VCBCC) for renewable energy sources (RES). It will consist of dedicated IT infrastructure and software to be used by system operators for the efficient and coordinated management of RES. The equipment and operation of the virtual center will be distributed between the existing control systems of system operators (TSOs and DSOs). Advanced algorithms for VVC optimization, secondary reserve, advanced real time operation of the grid using dynamic thermal rating, and a communication platform of the demand side will be established.
- Common Platform for the purpose of efficient data exchange between TSO and DSO to increase possible introduction of demand response into tertiary reserve.
- Establishing efficient ICT infrastructure that will enable data exchange between control centers and on-field equipment.

4 THE PROJECT IMPACT

Quantifiable benefits expected from the SINCRO.GRID project are the following [2]:

- Reduction of GHG emissions,
- Avoided cost of purchasing capacity for secondary reserve,
- Avoided generation capacity investment for spinning reserve,
- Deferred transmission investment,
- Financial benefits due to increased cross border capacity,
- Societal benefits due to increased cross border capacity,
- Reduced cost of equipment breakdowns,
- Reduced electricity technical losses,
- Value of service,
- Decreased amortization value due to longer lifespan of equipment, and
- Decreased cost of purchasing reactive power from generation units.

The quantification and monetization of these benefits leads to a total of 345 M€ of quantifiable benefits, spread amongst Slovenia, Croatia and some neighboring countries. A sensitivity analysis on some key parameters shows high robustness of the project to changes in some specific variables: within our estimations, the total amount of benefits would lie between 202 M€ and 545 M€.

The SINCRO.GRID investment value amounts to 88.6 million Euros in detail elaborated in project Business Plan [3]. Since the project is on European Project of Common Interest (PCI) list, project promotors were eligible to apply for European funding from CEF instrument. The application for Action was submitted in November 2016 and after successful assessment 40.5 million Euro from CEF fund were granted to it. The Action received the highest score among 22 gas, electricity and smart grid projects, which applied for grant on second CEF call in 2016.

5 CONCLUSION

Large-scale Smart Grid projects are a challenge for European utilities. It is not easy to meet the PCI requirements and even harder task is a preparation of successful CEF application. European Commission recognized the SINCRO.GRID project as model application and invited project team to promote PCI application preparation for potential Smart Grid project promotors for the third PCI list in 2017. The next challenge is successful project implementation in the next five years. Soundness of the project structure and excellent project team are a good starting point.

REFERENCES

[1] ELES, HOPS, SODO, HEP-ODS: SINCRO.GRID Project Storyline, 2016.

[2] EIMV: Cost Benefit Analysis of SINCRO.GRID Project, 2016.

[3] ELES, HOPS, SODO, HEP-ODS: SINCRO.GRID A Project of Common Interest Business Plan, 2016.

ENERGIJA